

# Methods for protein crystal delivery: Exploring new techniques for encapsulation and controlled release

Dissertation

zur Erlangung des Doktorgrades der Naturwissenschaften (Dr. rer. nat.)  
der Julius-Maximilians-Universität Würzburg



vorgelegt von

**Sebastian Puhl**

aus Erlangen

Würzburg 2015



Eingereicht am: \_\_\_\_\_

Bei der Fakultät für Chemie und Pharmazie

1. Gutachter: Prof. Dr. Dr. Lorenz Meinel
2. Gutachter: Prof. Dr. Oliver Germershaus

der Dissertation

1. Prüfer: \_\_\_\_\_
2. Prüfer: \_\_\_\_\_
3. Prüfer: \_\_\_\_\_

des öffentlichen Promotionskolloquiums

Tag des öffentlichen Promotionskolloquiums: \_\_\_\_\_

Doktorurkunde ausgehändigt am: \_\_\_\_\_



Die vorliegende Arbeit wurde in der Zeit von April 2011 bis Juli 2015 am  
Institut für Pharmazie und Lebensmittelchemie

der Bayerischen Julius-Maximilians-Universität Würzburg

unter Anleitung von

**Prof. Dr. Dr. Lorenz Meinel**

und

**Prof. Dr. Oliver Germershaus**

angefertigt.



# Table of Contents

|          |  |    |
|----------|--|----|
| <b>1</b> | <b>Summary</b> .....   | 1  |
| 1.1      | Zusammenfassung .....  | 3  |
| <b>1</b> | <b>Recent Advances in Crystalline and Amorphous Particulate Protein Formulations for Controlled Delivery</b> .....                             | 8  |
| 1.2      | Introduction .....   | 10 |
| 1.3      | Particle production methods .....  | 11 |
| 1.3.1    | Batch crystallization .....  | 12 |
| 1.3.2    | Protein particles .....  | 14 |
| 1.4      | Stability of protein crystals .....  | 15 |
| 1.5      | Protein Crystal Delivery .....   | 16 |
| 1.5.1    | Protein crystal delivery without further processing .....  | 17 |
| 1.5.2    | Protein crystals delivery after further processing .....   | 18 |
| 1.6      | Delivery systems employing non-crystalline protein particles .....   | 20 |
| 1.6.1    | Non-crystalline protein particles for delivery without further processing .....  | 21 |
| 1.6.2    | Non-crystalline protein particles for protein delivery with further processing, i.e. encapsulation .....                                       | 22 |
| 1.7      | Conclusion and outlook .....   | 23 |
| 1.8      | References .....   | 25 |
| <b>2</b> | <b>Controlled Protein Delivery from Electrospun Non-Wovens: Novel Combination of Protein Crystals and a Biodegradable Release Matrix</b> ..... | 32 |
| 2.1      | Introduction .....   | 34 |
| 2.2      | Experimental section .....   | 35 |
| 2.2.1    | Materials .....  | 35 |
| 2.2.2    | Lysozyme Crystallization and Crystal Size Determination .....  | 36 |
| 2.2.3    | FITC Labeling of Lysozyme .....  | 36 |
| 2.2.4    | PCL Electrospinning .....  | 37 |
| 2.2.5    | In Vitro Release .....   | 39 |
| 2.2.6    | Relative Bioactivity of Lysozyme .....   | 40 |
| 2.2.7    | Morphology and Fiber Diameter .....  | 40 |
| 2.2.8    | Wettability of the Non-Wovens .....  | 41 |
| 2.2.9    | Statistical Analysis .....   | 41 |
| 2.3      | Results .....  | 42 |
| 2.3.1    | Morphology of Lysozyme Crystals and Non-Wovens .....   | 42 |
| 2.3.2    | Effect of Scaffold Composition on Lysozyme Release, Relative Bioactivity, and Sorption of Release Buffer .....                                 | 46 |

|          |  |           |
|----------|--|-----------|
| 2.4      | Discussion .....   | 51        |
| 2.5      | Conclusion .....   | 54        |
| 2.6      | References .....   | 55        |
| <b>3</b> | <b>Protein release from electrospun nonwovens: Improving the release characteristics through rational combination of polyester blend matrices with polidocanol .....</b> | <b>60</b> |
| 3.1      | Introduction .....   | 62        |
| 3.2      | Materials and Methods .....  | 63        |
| 3.2.1    | Lysozyme crystallization and crystal size determination.....   | 63        |
| 3.2.2    | PCL electrospinning.....   | 64        |
| 3.2.3    | Morphology and fiber diameter .....  | 65        |
| 3.2.4    | Wettability and sorption rate of the nonwovens.....  | 65        |
| 3.2.5    | Swelling of polymer blends .....   | 66        |
| 3.2.6    | Differential scanning calorimetry .....  | 67        |
| 3.2.7    | In vitro release .....   | 67        |
| 3.2.8    | Relative bioactivity of lysozyme .....   | 68        |
| 3.2.9    | Statistical analysis.....  | 68        |
| 3.3      | Results.....   | 69        |
| 3.3.1    | Morphology of nonwovens.....   | 69        |
| 3.3.2    | Differential scanning calorimetry .....  | 72        |
| 3.3.3    | Contact angle, sorption rate and swelling behavior .....   | 72        |
| 3.3.4    | Polidocanol release .....  | 74        |
| 3.3.5    | Lysozyme release .....   | 75        |
| 3.3.6    | Bioactivity.....   | 77        |
| 3.4      | Discussion .....   | 78        |
| 3.5      | Conclusion .....   | 83        |
| 3.6      | References .....   | 84        |
| <b>4</b> | <b>Silk fibroin coating of protein crystals for controlled delivery .....</b>  | <b>88</b> |
| 4.1      | Introduction .....   | 90        |
| 4.2      | Materials and Methods .....  | 92        |
| 4.2.1    | Preparation of Lysozyme Crystals and Optimization of Crystallization by Design of Experiments .....  | 92        |
| 4.2.2    | Silk fibroin extraction .....  | 93        |
| 4.2.3    | Labeling of lysozyme with FITC and silk fibroin with Rhodamine-X .....   | 93        |
| 4.2.4    | Coating of protein crystals with silk fibroin and purification.....  | 94        |
| 4.2.5    | Microscopic characterization .....   | 95        |



|       |  |     |
|-------|--|-----|
| 4.2.6 | Release studies .....  | 96  |
| 4.2.7 | Relative Bioactivity.....  | 96  |
| 4.2.8 | FTIR .....   | 97  |
| 4.3   | Results.....   | 97  |
| 4.3.1 | Controlled crystal formation of lysozyme .....   | 97  |
| 4.3.2 | SEM and light microscope pictures .....  | 100 |
| 4.3.3 | CLSM analysis.....   | 102 |
| 4.3.4 | FTIR analysis.....   | 103 |
| 4.3.5 | Lysozyme in vitro release and bioactivity .....  | 103 |
| 4.4   | Discussion.....  | 105 |
| 4.5   | Conclusion.....  | 108 |
| 5     | Conclusion and outlook.....  | 114 |
| 6     | Abbreviations.....   | 119 |
| 7     | Publications.....  | 120 |
| 8     | Curriculum vitae .....   | 121 |
| 9     | Acknowledgments.....   | 122 |
| 10    | Documentation of authorship.....   | 124 |
| 11    | Erklärung zu den Eigenanteilen des Doktoranden sowie der weiteren Doktoranden als Koautoren an Publikationen und Zweitpublikationsrechten bei einer kumulativen Dissertation |     |

# 1 Summary

More and more newly registered drugs are proteins. Although many of them suffer from instabilities in aqueous media, the most common way of protein drug administration still is the injection of a solution. Numerous protein drugs require frequent administration, but suitable controlled release systems for proteins are rare. Chapter 1 presents current advances in the field of controlled delivery of particulate protein formulations. While the main focus lies on batch crystallized proteins, amorphous particulate proteins are also discussed in this work. The reason is that, on the one hand precipitated protein particles hold some of the advantages of crystalline proteins and on the other hand the physical state of the protein may simply be unknown for many drug delivery systems or semi-crystalline particles have been used. Crystallization and precipitations methods as well as controlled delivery methods with and without encapsulation in a polymeric delivery system are summarized and critically discussed.

In chapter 2 a novel way of protein crystal encapsulation by electrospinning is introduced. Electrospinning of proteins has been shown to be challenging via the use of organic solvents, frequently resulting in protein unfolding or aggregation. Encapsulation of protein crystals represents an attractive but largely unexplored alternative to established protein encapsulation techniques because of increased thermodynamic stability and improved solvent resistance of the crystalline state. We herein explore the electrospinning of protein crystal suspensions and establish basic design principles for this novel type of protein delivery system. Poly- $\epsilon$ -caprolactone (PCL) is an excellent polymer for electrospinning and matrix-controlled drug delivery combining optimal processability and good biocompatibility. PCL was deployed as a matrix, and lysozyme was used as a crystallizing model protein. By rational combination of lysozyme crystals with a diameter of 0.7 or 2.1  $\mu\text{m}$  and a PCL fiber diameter between 1.6 and 10  $\mu\text{m}$ , release within the first 24 h could be varied between approximately 10 and 100%. Lysozyme loading of PCL microfibers between 0.5 and 5% was achieved without affecting

processability. While relative release was unaffected by loading percentage, the amount of lysozyme released could be tailored. PCL was blended with poly(ethylene glycol) and poly(lactic-co-glycolic acid) to further modify the release rate. Under optimized conditions, an almost constant lysozyme release over 11 weeks was achieved.

Chapter 3 takes on the findings made in chapter 2 and further modifies the properties of the nonwovens as protein crystal delivery system. Nonwoven scaffolds consisting of poly-ε-caprolactone (PCL), poly(lactic-co-glycolic acid) (PLGA) and polidocanol (PD), and loaded with lysozyme crystals were prepared by electrospinning. The composition of the matrix was varied and the effect of PD content in binary mixtures, and of PD and PLGA content in ternary mixtures regarding processability, fiber morphology, water sorption, swelling and drug release was studied. Binary PCL/PD blend nonwovens showed a PD-dependent increase in swelling of up to 30% and of lysozyme burst release of up to 45% associated with changes of the fiber morphology. Furthermore, addition of free PD to the release medium resulted in a significant increase of lysozyme burst release from pure PCL nonwovens from approximately 2% to 35%. Using ternary PCL/PD/PLGA blends, matrix degradation could be significantly improved over PCL/PD blends, resulting in a biphasic release of lysozyme with constant release over 9 weeks, followed by constant release with a reduced rate over additional 4 weeks. Based on these results, protein release from PCL scaffolds is improved by blending with PD due to improved lysozyme desorption from the polymer surface and PD-dependent matrix swelling.

Chapter 4 gives deeper insight on lysozyme batch crystallization and shows the influences of the temperature on the precipitation excipients. Yet up to now protein crystallization in a pharmaceutical useful scale displays a challenge with crystal size and purity being important but difficult to control parameters. Some of these influences are being discussed here and a detailed description of crystallization methods and the achieved crystals are demonstrated.

Therapeutic use of such protein crystals may require further modification of the protein release rate through encapsulation. Silk fibroin (SF) harvested from the cocoons of *Bombyx mori* is a well-established protein suitable for encapsulation of small molecules as well as proteins for controlled drug delivery. This novel polymer was deployed for as carrier for the model drug crystals. Lysozyme again was used as a crystallizable protein and the effect of process- as well as formulation parameters of batch crystallization on crystal size were investigated using statistical design of experiments. Lysozyme crystal size depended on temperature and sodium chloride and poly(ethylenglycol) concentration of precipitant solution. Under optimized conditions, lysozyme crystals in a size range of approximately 0.3 to 10  $\mu\text{m}$  were obtained. Furthermore, a solid-in-oil-in-water process for encapsulation of lysozyme crystals into SF was developed. Using this process, coating of protein crystals with another protein was achieved for the first time. Encapsulation resulted in a significant reduction of dissolution rate of lysozyme crystals, leading to prolonged release over up to 24 hours.

### **1.1 Zusammenfassung**

Immer mehr neu zugelassene Arzneimittel sind Proteine. Obwohl viele von ihnen in wässrigen Milieus sehr instabil sind, werden die meisten Proteine immer noch als Parenteralia formuliert. Kontrollierte Freisetzungssysteme sind selten, und das obwohl zahlreiche Proteine regelmäßig verabreicht werden müssen. Kapitel 1 befasst sich mit den aktuellen Fortschritten im Bereich der kontrollierten Darreichungsformen für Proteinpartikel. Das Hauptaugenmerk liegt klar auf den „batch“ kristallisierten Proteinen, aber auch allgemeine ‚amorphe‘ Proteinpartikel werden diskutiert. Das liegt daran, dass zum einen präzipitierte Proteinpartikel ebenfalls einige Vorteile der Proteinkristalle haben und zum anderen wurde in einigen Fällen der physikalische Zustand der Proteine nicht bestimmt oder es wurden zumindest semi-kristalline Proteinpartikel verwendet. In diesem Kapitel werden Kristallisations- und Präzipitationsmethoden sowie kontrollierte Freisetzungssysteme mit und ohne vorherige Einbettung in ein Polymersystem zusammengefasst und kritisch diskutiert.

Kapitel 2 stellt eine neue Methode der Proteinkristalleinbettung durch Electrospinning vor. Electrospinning von Proteinen hat sich aufgrund des häufigen Einsatzes von organischen Lösemitteln als schwierig heraus gestellt und führt häufig zum Entfalten oder Denaturieren des Proteins. Aufgrund höherer thermodynamischer Stabilität und verbesserter Kompatibilität mit organischen Lösemitteln haben sich Proteinkristalle hier als attraktive wenngleich bisher ziemlich unbeachtete Alternative heraus gestellt. In diesem Kapitel wird das Electrospinning von Proteinkristallsuspensionen erforscht und grundlegende Bedingungen für diese neuartige Art der Proteinverkapselung etabliert. Poly- $\epsilon$ -caprolacton (PCL) eignet sich hervorragend für das Electrospinning und zeichnet sich durch matrixkontrollierte Freisetzung, einfache Handhabbarkeit sowie gute Biokompatibilität aus. PCL wurde als Matrix und Lysozym als Modelprotein eingesetzt. Mittels Kombination zweier Lysozymkristalldurchmesser, 0,7 oder 2,1  $\mu\text{m}$ , und der Variation des PCL-Fadendurchmessers zwischen 1,6 und 10  $\mu\text{m}$  konnte die Initialfreisetzung innerhalb der ersten 24 Stunden zwischen ca. 10 und 100 % modifiziert werden. Die Beladung der PCL Mikrofäden mit Lysozym zwischen 0,5 und 5 % konnte ohne Beeinträchtigung des Herstellungsprozesses erreicht werden. Hierdurch konnte die gesamt freigesetzte Menge an Lysozym variiert werden, während die relative freigesetzte Menge konstant blieb. Um weitere Modifikationen an der Freisetzungsrates vorzunehmen, wurden Poly(ethylen glycol) und Poly(lactic-co-glycolic acid) (PLGA) dem PCL beigemischt. Dadurch konnte unter optimierten Bedingungen eine Freisetzungsdauer von über 11 Wochen erreicht werden.

Kapitel 3 greift die Entdeckungen des zweiten Kapitels auf und nimmt weitere Modifikationen an den Fasermatten vor. Die mit Proteinkristallen beladenen Fasermatten wurden wieder durch Electrospinning hergestellt und bestehen aus PCL, PLGA und Polidocanol (PD). Die Zusammensetzung der Matrix wurde variiert und die Auswirkungen des PD-Gehalts in binären Mischung, sowie des PD- und PLGA-Gehalts in ternären Mischsystemen auf die

Verarbeitbarkeit, Fadenmorphologie, Wassersorption, Quellung und Wirkstofffreisetzung untersucht. Binäre Fasermatten aus einer Mischung aus PCL/PD zeigten PD-abhängige Zunahme der Quellung von bis zu 30 % und eine Zunahme der Initialfreisetzung von bis 45 %. Dieser Anstiege werden einer Veränderung der Fasermorphologie zugeschrieben. Das Hinzufügen von freiem PD zum Freisetzungsmedium von reinen PCL Fasermatten führte zu einer Zunahme der Initialfreisetzung von ca. 2 % auf etwa 35 %. Durch den Einsatz von ternären Mischsystem, bestehend aus PCL/PD/PLGA, kam es zu einem signifikant erhöhten Matrixabbau gegenüber den PCL/PD Mischungen. Das führte wiederum zu einem zweiphasigen Freisetzungverhalten, das durch eine konstante Freisetzungsrates innerhalb von 9 Wochen, sowie eine anschließende langsamere, ebenfalls konstante Freisetzung über weitere 4 Wochen gekennzeichnet war. Aufgrund dieser Ergebnisse kann gesagt werden, dass die Proteinfreisetzung aus PCL Matrices durch das Hinzufügen von PD aufgrund von verbesserter Lysozymdesorption vom Polymer sowie PD-abhängiger Matrixquellung verbessert werden konnte.

Kapitel 4 bringt tiefere Erkenntnisse bezüglich der Lysozym Batchkristallisation und zeigt den Einfluss der Temperatur auf die verwendeten Fällungsreagenzien. Bis heute stellt die Kristallisation von Proteinen in einem pharmazeutisch sinnvollen Maßstab eine Herausforderung dar, wobei die Kristallgröße und die Reinheit wichtige und dennoch schwer kontrollierbare Parameter sind. Einige dieser Einflüsse werden hier näher beleuchtet und Kristallisationsmethoden sowie die erhaltenen Kristalle näher beschrieben.

Lysozym wurde erneut als kristallisierbares Protein eingesetzt und die Einflüsse der Prozess- sowie Formulierungsparameter der Batch-Kristallisation mit Hilfe von statistischen Experimentendesigns (Design of Experiment, DoE) untersucht. Die Kristallgröße wurde durch die Temperatur sowie die Natriumchlorid- und Poly(ethylenglycol)konzentration der Fällungslösung bestimmt. Unter kontrollierten Bedingungen konnten Kristallgrößen in einem

Bereich zwischen ca. 0.3 bis 10  $\mu\text{m}$  erreicht werden. Darüber hinaus wurde ein „solid-in-oil-in-water“ (Feststoff-in-Öl-in-Wasser) Verfahren entwickelt mit dem Lysozymkristalle in Seidenfibroin eingebettet werden konnten. Mit Hilfe dieses Verfahrens wurden erstmals Proteinkristalle mit einem anderen Protein überzogen. Diese Einbettung brachte eine signifikante Auflösungsverzögerung mit einer verlängerten Freisetzung über 24 Stunden.

## Summary



# **1 Recent Advances in Crystalline and Amorphous Particulate Protein Formulations for Controlled Delivery**

The chapter is unpublished.

## **Abstract**

Solid controlled release systems for biologics are rare as compared to liquid forms. This review presents current advances in the field of controlled delivery of particulate protein formulations. While the main focus lies on batch crystallized proteins, amorphous particulate proteins are also discussed in this work. Considering that precipitated protein particles may comprise some of the advantages of crystalline proteins makes them as suitable for encapsulation and controlled release. However in many studies the physical state of the protein simply has not been determined for many drug delivery systems or semi-crystalline particles have been used. Crystallization and precipitations methods as well as controlled delivery methods with and without encapsulation in a polymeric delivery system are summarized and critically discussed.

## 1.2 Introduction

With more and more new drugs being biologics, the pharmaceutical delivery of these proteins to the human body is of special interest for the formulation scientist. Despite many advances in this field controlled protein delivery remains a challenge. The oral route mostly yields very poor bioavailability because of low absorption and harsh conditions in the gastro-intestinal tract threatening the stability of macromolecules, although lately there was some progress [1–3]. At the moment parenteral application is still the most favored route of administration. However, parenteral formulations require several points to be taken into account including sterility, tonicity as well as an optimally physiological pH. To meet these requirements and still deliver functionally uncompromised proteins, more requirements are added to the formulation list. In aqueous solution most proteins are prone to degradation, with stability mostly suffering from unfavorable buffer pH and ionic strength [4]. Moreover, if proteins are administered as a solution by subcutaneous injection, protein concentration is a critical parameter, especially with high doses. Apart from the rising risk of aggregation, the increasing viscosity affects the ability to be injected into the human body [5]. Because of fast degradation within the human body parenteral administration of therapeutic proteins often demands frequent application. Naturally, controlled drug release would be beneficial at this point. Encapsulating proteins in a controlled drug delivery system for parenteral application may circumvent these problems and stabilize the macromolecule. It may protect the protein from exterior influences like moisture, salts or harmful pH. However, processes needed for this encapsulation again inherit risks for the protein and long term release over days or even months of macromolecules requires adequate stability within the drug delivery system [6,7]. Protein crystals have proven to evade many of these issues: they are densely packed, have a reduced outer surface and are thermodynamically more stable than their amorphous counterparts [8]. Because of delayed dissolution they often allow controlled release without further encapsulation in a polymeric system, although at the moment this is limited to about 48 hours. As long as the protein crystal does not dissolve, processing is

simplified: Viscosity does not rise as massively, making higher drug loading possible [9]. Interactions in aqueous or organic media is reduced and the protein is better able to withstand elevated temperatures [10]. Despite these advantages the crystallization of proteins with and without subsequent encapsulation for controlled delivery is still in its infancy. Previous reviews on this topic mainly have dealt with general suitability [11] as well as the upscaling and characterization of protein crystals [10].

In this review we present the latest developments in the crystallization of pharmaceutically active proteins as well as give an update on the progress in delivery and encapsulation methods of amorphous protein precipitates and protein crystals.

### **1.3 Particle production methods**

Finding optimal conditions for protein crystallization and precipitation can be tedious and translation of crystallization conditions among molecules is typically unsuccessful rendering this 'art' rather empirical. The biologics have to be transferred into a thermodynamically unstable supersaturated state which returns to equilibrium by development of a crystalline or amorphous phase. For crystallization it is the goal to increase the interactions between two protein molecules so that a well ordered arrangement takes place while nonspecific aggregation is avoided [12]. In general the native conformation is maintained during and often preserved effectively after crystallization (see chapter 2.3.). There is a broad knowledge about protein crystallization with the aim of purification or structure determination [13] but less with the focus on manufacturing larger batches. For the latter, only a few large and flawless crystals are required. However in order to be able to produce protein drugs in a pharmaceutical useful scale, batch crystallization methods appear to be the most suitable solution (chapter 2.1.). The formation of protein particles is a wide field with countless methods published, and only a selection is presented in chapter 2.2.

### 1.3.1 Batch crystallization

Batch crystallization is the production of uniform crystals in a large scale, preferably with a high yield [14]. In general the strategy is to quickly reach a high level of supersaturation of the protein so that many crystallization nuclei are formed simultaneously followed by a growth phase, whereby all nuclei grow in parallel and to the same size (**Fig. 1A**). This process is often initiated by a liquid-liquid phase separation between the protein and the solvent, followed by a first nucleation within the protein droplets [15]. According to the classical nucleation theory more nuclei are formed if the free energy cost ( $\Delta G$ ) is largely negative, i.e. the system reaches a lower free enthalpy level than before. With the free enthalpy  $\Delta G$  being related to the chemical potential by  $\mu = (\partial G / \partial n)_{p,T}$  systems spontaneously ‘escape’ to lower chemical potentials as this leads to a reduction of the free enthalpy if other parameters, particularly the pressure  $p$  and the temperature  $T$  are held constant. Thereby, supersaturated solutions are thermodynamically instable as the chemical potentials in the supersaturated state are higher as compared to the solid aggregate state – hence, these systems tend to aggregate with crystals frequently forming the lowest free enthalpy state. Accordingly, dissolved proteins in a supersaturated state spontaneously aggregate and, thereby form nuclei on which further protein will deposit. The speed and extend at which supersaturation is reached strongly affects nuclei size and size distribution [16], but if the if the degree of supersaturation is pushed too high precipitation takes place [14]. Commonly, supersaturation is reached by admixing a solution containing high concentrations of precipitating agents or by a rapid temperature drop. For the crystallization of individual proteins, different buffers and precipitating agents like salts, glycol, alcohols or poly(ethyleneglycol)s are required [17,18]. Decreasing the solvation of the protein is the primary goal for crystallization. For example, “salting out” a protein by the addition of

kosmotropes (e.g. sodium, lithium, fluoride, sulfate or phosphate) has proven to be effective for crystallization [12].

The subsequent growth phase may endure a few seconds or up to several days [19]. Similar as for all the other methods (e.g. sitting drop, hanging drop etc.) an individual screening and optimization process is required. For systematic screening, methods may be based on experimental designs, after determination of the factors with the greatest influence on crystallization. Protein concentration, type of precipitant, ionic strength, pH and temperature are important parameters for protein crystallization. Moreover late-time crystal growth, known as Ostwald ripening, favors the creation of larger crystals, if the solution is not being stabilized [20–22].

Methods to explore batch crystallization conditions are to start with water vapor diffusion experiments and transfer the experiences for the scale up to micro-batch and up to larger batch crystallization [23,24]. A two or more dimensional phase diagram can be produced narrowing down the optimal conditions for crystal growth (**Fig. 1B** [25]). Hereby the interactions and influences of two or more parameters on the solubility of the protein are described.

Insulin is probably one of the most prominent examples of protein crystallization but batch crystallization is still under investigation and optimization. Nanev et al. introduced a method for insulin batch crystallization [26]. Various sizes between 18 and 57  $\mu\text{m}$  with narrow size distributions could be achieved by high supersaturation of the protein solution. Insulin was dissolved in a citrate buffer at pH 7 in the presence of  $\text{ZnCl}_2$  and acetone and the solution was preheated to 50 °C. Nucleation was initiated by a rapid temperature drop. Parameters for the crystal size were the insulin concentration, the crystal growth time and the growth temperature. Crystallizing proteins by complexation with metal ions like Zn or other ionic molecules (e.g. protamine, ionic liquids) has not only proven to be effective but also to delay dissolution, offering the possibility to serve as a delivery system without further processing [27–31].

Recent advances in crystallization of pharmaceutically active drugs have been made in the field of monoclonal antibodies: trastuzumab, rituximab, infliximab [9] and anti-hTNF-alpha have successfully been crystallized [32,33]. Another pharmaceutically active protein with reported methods for batch crystallization is human growth hormone (hGH) [34].

Apart from the advantages as drug delivery systems, batch crystallization of recombinant proteins and antibodies can be applied with regards to optimized NMR characterization or downstream processing. Such methods represent a cost-effective alternative to X-ray diffraction or Protein A or ion exchange chromatography, respectively, even though mostly in experimental scale so far [35,36].

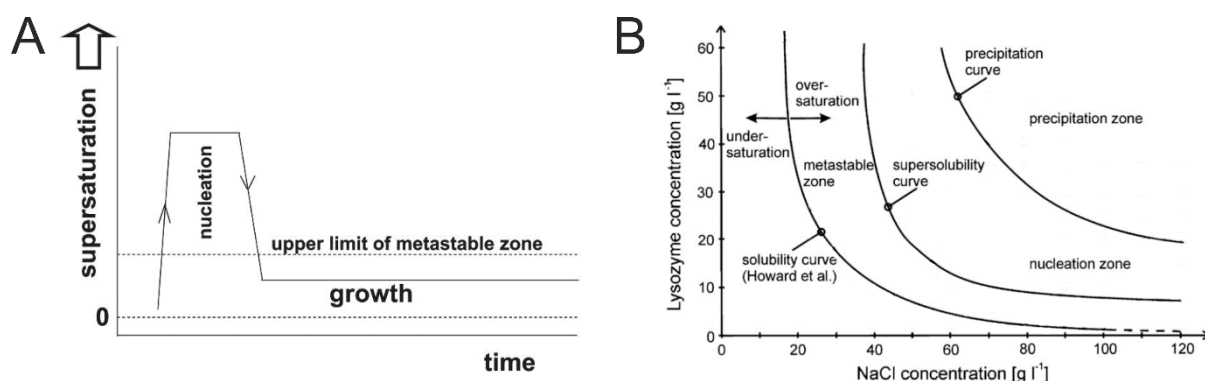


**Figure 1:** (A) Theoretical depiction of time-wise nucleation with subsequent crystal growth. Reproduced with permission from [26]  
 (B) Phase diagram of lysozyme crystallization, with permission slightly modified from [23]. For crystallization the aim is to surpass the supersolubility curve but to stay in the nucleation zone to avoid precipitation.

### 1.3.2 Protein particles

The production of amorphous protein particles gives the experimenter many possibilities. Mild and bioactivity preserving processes include freeze drying, spray-drying, spray-freeze-drying and the precipitation in supercritical fluids. Freeze drying of a protein/PEG blend solution and subsequent removal of PEG from the matrix has proven to yield precipitated protein particles with homogenous size distribution [37]. Spray-drying of proteins has been established as a

suitable method for protein particle production, e.g. recombinant human anti-IgE and recombinant human deoxyribonuclease could be spray dried with and without addition of excipients and yielded in stable particles [38]. Spray-freeze drying represents an extended way of spray drying and offers the production of protein particles without the threat of degradation by heat. The sprayed protein particles are collected in liquid nitrogen and are subsequently transferred to a freeze dryer [39,40]. Genentech and Alkermes developed a product consisting of recombinant human growth hormone microparticles that were encapsulated in PLGA in amorphous form (Nutropin Depot). Particles of rhGH were suspended in a solution of PLGA and spray-freeze-dried into liquid nitrogen.

Supercritical antisolvent precipitation technique (SAS) was demonstrated to provide protein particles by spraying solutions of various proteins dissolved in DMSO into a concurrently flowing supercritical CO<sub>2</sub> [41]. The supercritical CO<sub>2</sub> acts as a solvent for the DMSO but as a non-solvent for proteins (e.g. insulin, trypsin and lysozyme) and thus precipitates them. After evaporation of the solvents, the protein particles can be collected. Advantages are the low temperatures as well as the low toxicity of all excipients.

Further methods of protein precipitation are summarized in chapter 5.

#### **1.4 Stability of protein crystals**

Studies on the stability of protein crystals have been performed and have been discussed before [8]. For insulin it was found that the dried amorphous form possess higher stability, while suspended in aqueous media the insulin crystals were found to be more stable [42]. However, several other examples revealed an increased overall stability of crystalline proteins. Shenoy et al. compared the crystalline and amorphous forms (with and without stabilization agents like sucrose and trehalose) of glucose oxidase and lipase and found increased stability of the protein crystals [8]. Elkordy et al. obtained similar results for lysozyme [43].



The cause of the stabilizing effect of the crystalline state can be derived from the Hofmeister series. Effect of salts on stability of proteins in relation to the Hofmeister series has been investigated by Broering et al. [44]. With increasing concentration of kosmotropes, proteins are increasingly excluded from (aqueous) solvents, reducing potential risk of degradation. As mentioned above, kosmotropes are often used as excipients for protein crystallization suggesting a relationship between the stabilizing effects of the kosmotropic ions and the desolvatisation during crystallization. Collins evaluated the stabilizing effects of kosmotropes on proteins and underlined the relationship between the stabilizing effect and their capacity to crystallize proteins [12]. Protein stabilization and crystallization are both initiated by an exclusion of protein surface from the solvent forcing the protein to diminish its outer surface to a minimum. The structure having minimum surface usually represents the native state. This process can be continued until higher interactions between the protein molecules lead to a well-ordered combination of more and more molecules to finally yield a crystal lattice in which all protein molecules are bound in their native state.

Frequently, organic solvents are used to encapsulate proteins in organic polymers. To prevent the crystals from dissolving during encapsulation, the solubility of proteins in all used solvents needs to be considered. The integrity of undissolved protein crystals is likely to be maintained despite the contact with otherwise harmful solvents. Chin et al. have shown that solubility of lysozyme, a protein with high aqueous solubility, greatly depends on logP of the respective solvent and thus can be estimated for other solvents [45]. A certain aqueous layer is still required though to maintain the native conformational state of the protein, leading to a common connotation that proteins should only be dried to a certain (maximally preserving) extent [46].

### **1.5 Protein Crystal Delivery**

There are basically two possibilities for the controlled delivery of protein crystals: with and without further encapsulation. Since some protein crystals already possess a delayed dissolution

pattern the need for further encapsulation is not always given. E.g. insulin crystals formed by complexation with zinc or protamine have proven to sustain release after subcutaneous application [47,48]. Additionally, encapsulated proteins have the benefit of protection from humidity, pH and light.

### 1.5.1 Protein crystal delivery without further processing

Brader et al. developed an insulin co-crystal composed of human insulin and octanoyl modified insulin [49]. The modification with octanoyl was achieved by covalent conjugation to LysB29 of human insulin. Thereby, hydrophobicity was increased without loss of bioactivity. Co-crystallization of unmodified and modified insulin at different ratios yielded insulin crystals with overall prolonged dissolution behavior (**Fig. 2**).

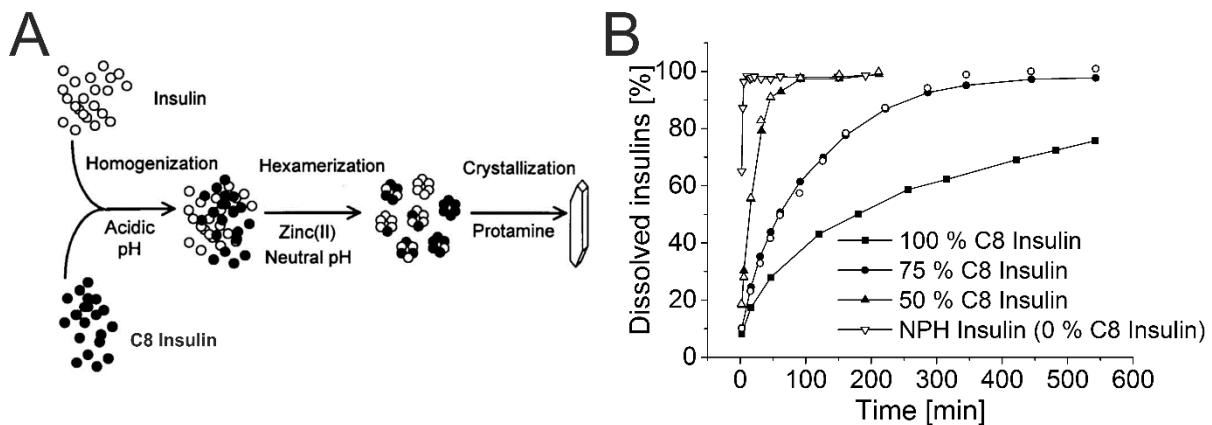


**Figure .3:** (A) Schematic drawing of co-crystallization of insulin with octanoyl (C8) modified insulin. (B) Dissolution rate of insulin crystals with different ratios of C8 insulin. Open symbols represent unmodified insulin, filled symbols C8 insulin. Reproduced with permission from [49]

Other proteins like recombinant human interferon (rhIFN)  $\alpha$ -2b crystals chelated with Zn ions showed decreased dissolution rates [50]. Crystals were produced by hanging drop vapor diffusion method in the presence of zinc acetate and sodium acetate. Several morphologies were examined, achieved by varying pH, ionic strength and the addition of further precipitants like PEG of different molecular weight. Biological activity was retained and dissolution of rhIFN in vitro was characterized by an initial burst over 8 hours followed by a release up to 48 h.

Shi et al. developed a method for batch crystallization of rhIFN [29]. They formed a semi-crystalline structure by molecular self-assembly of the protein and the polycationic protamine sulfate in the presence of zinc acetate. Spherical, monodisperse semi-crystals were obtained with adjustable ratios of protamine in the semi-crystal. Dissolution depended on the relative amount of protamine in the particles while higher ratios showed the longest release of up to one week. In vivo experiments proved the delayed dissolution and extended blood levels up to seven days for the highest protamine ratio were detected.

### **1.5.2 Protein crystals delivery after further processing**

Human growth hormone (hGH) crystals were obtained by batch crystallization using two different approaches. Admixing sodium acetate and PEG 6000 and incubating over 12-16 hours at 33 °C produced circular crystals with yields over 90 %. In contrast, crystallization of hGH with zinc and acetone as precipitating agents for 21-24 hours at 15 °C resulted in hexagonal crystals (yield > 50 %). Crystals were coated either with the positively charged poly(arginine) or protamine simply by overnight incubation in the crystallization medium. Protein structure and activity could be completely retained. After coating of crystals in vitro dissolution was significantly prolonged. However no differences between the two coating materials were observed. In vivo tests of poly(arginine) coated hGH crystals in monkeys revealed elevated serum levels of hGH for about 7 days and an increased induction of IGF-1 serum levels compared to soluble hGH [34].

Crystallized lysozyme was encapsulated by Puhl et al. into nonwovens by dispersing the crystals in an organic poly(caprolactone) (PCL) solution followed by electrospinning of the suspension (**Fig. 3A**). Electrospun nonwovens are advantageous with regards to the immensely increased and well controllable surface as well as the flexibility to generate various macroscopic shapes and morphologies optimally adapted to the site of application. Crystals withstood the entire encapsulation process and were found to be located discretely within the fibers of the

nonwovens (**Fig. 3B**). Loading was adjustable between 0.25 and 5 % m/m. It was shown that release depended on the size of the crystals and diameter of nonwoven fibers as well as the polymer compositions of the fibers. Burst release was controlled within broad margins by varying the crystals size and the fiber diameter (**Fig. 3C**). It was found that higher ratios of fiber diameter to crystal size resulted in reduced burst release. Moreover the addition of polidocanol to the polymer matrix prior to electrospinning increased the overall release, altering the release mechanism. Release rate modification was achieved by the addition of PLGA for controlled release over several days (**Fig. 3D**) [51,52]

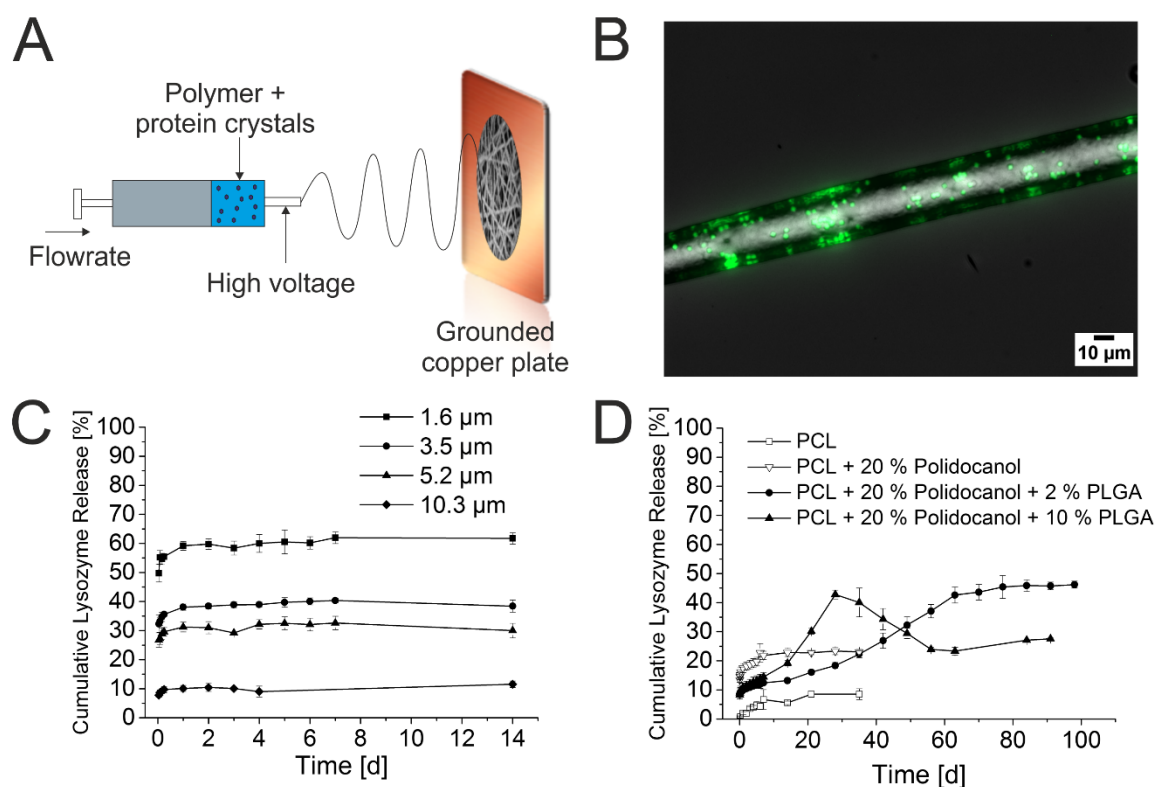


**Figure 3:** (A) Schematic depiction of encapsulation of protein crystals by electrospinning (B) Micrograph of distribution of FITC labeled lysozyme crystals incorporated within a PCL fiber with a loading of 5 % m/m (C) Cumulative lysozyme release from electrospun nonwovens with different fiber diameters while keeping lysozyme crystal size constant (2.1 µm) (D) Cumulative lysozyme release from electrospun nonwovens with different polymer compositions Reproduced with permission from [51,52].

Crystalline recombinant human insulin was encapsulated in PLGA microspheres with a solvent extraction method by dispersing the insulin crystals in a DCM solution in which PLGA was

dissolved. By dispersing this solution in an aqueous solution with 5 % PVA a solid-in-oil-in-water (S/O/W) suspension was formed. After DCM evaporation, insulin loaded PLGA microspheres could be collected (**Fig. 4A**). Loading was adjustable between 2.5 and 10 % and encapsulation efficiency ranged between  $99 \pm 10$  % and  $78 \pm 1$  %, at 2.5 and 10% loading, respectively (**Fig. 4B**). The release rate increased with higher loading and exhaustive release was reached after 2-3 weeks. [53].

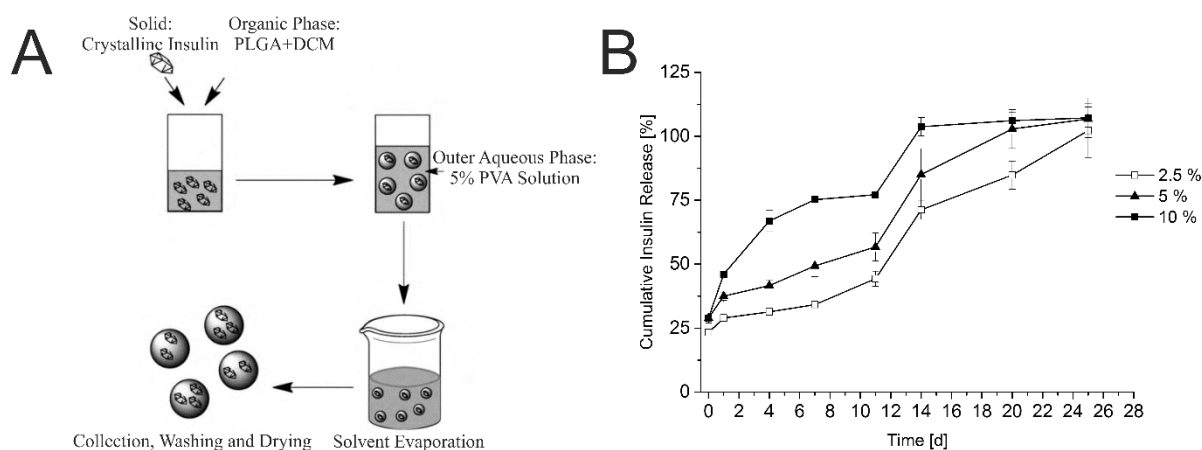


**Figure 4:** (A) Encapsulation of insulin crystals into PLGA microcapsules by solvent evaporation from an S/O/W system (B) Cumulative insulin release from PLGA microspheres with different loading % m/m. Reproduced with permission from [53]

### 1.6 Delivery systems employing non-crystalline protein particles

Particulate protein delivery is a very broad field and it is often difficult to identify the physical state of protein particles (i.e. amorphous or crystalline). The following chapter was included because particulate proteins inherit some of the advantages of crystalline proteins (e.g. dense packaging and reduced surface) or an impact of the physical state difference on delivery is small. Methods of delivery and encapsulation can most likely be transferred to crystalline proteins. Differences may be given in increased dissolution and decreased thermodynamic stability. General approaches for production of amorphous protein particles will be discussed in chapter 2.2. Significant research and development efforts in this field were focused on insulin delivery through inhalation. Exubera®, a spray dried insulin formulation for pulmonary application, was the first marketed product but has been taken off the market due to insufficient

acceptance by patients and doctors and disappointing sales figures [54]. MannKind Corporation is the only company at the moment pursuing inhaled insulin delivery further. In June 2014, MannKind was able to get its fast acting inhalable insulin (Afrezza®) approved by the FDA [55]. Major improvements of inhaler technology resulting in significantly smaller inhaler design than Exubera in conjunction with its, high efficacy and rapid onset of action is hoped to result in a commercially viable product [56].

However, the production and application of spray-dried protein particles is a topic of its own though and does not necessarily comprise the purpose of protein delivery as a particulate system. For further information the reader is referred to [57]. Herein we discuss spray-dried protein particles only in cases where obtained particles were intended for application to the human body and not only prepared for stabilizing reasons.

### **1.6.1 Non-crystalline protein particles for delivery without further processing**

Under normal conditions, amorphous protein particles dissolve rapidly and therefore do not allow sustained release. Protein particle production without further processing are mainly applied when pulmonary application is intended.

Recombinant human insulin particles suitable for pulmonary application were produced by precipitation of insulin and subsequent spray-drying of the resulting suspensions. [58]. First, protein particles of different sizes were produced by the addition of various amounts of methanol to an aqueous insulin solution under stirring. Subsequently, either suspensions of these particles or a particle free protein solution were spray-dried to yield a free-flowing powder with particle sizes of approx. 1-5  $\mu\text{m}$ . The largest precipitates kept their original size after spray-drying while smaller particles agglomerated during spray-drying. The aerodynamic behavior was investigated with a New Generation Impactor (NGI) and all preparations were found to be superior compared to Exubera®. While all insulin particles from the spray-dried suspensions

had no significant difference in aerodynamic behavior the spray-dried solution had the smallest fine particle fraction, which is considered to reach the lung.

### **1.6.2 Non-crystalline protein particles for protein delivery with further processing, i.e. encapsulation**

Human growth hormone (hGH) particles were produced by lyophilization of buffered protein solution with addition of zinc acetate [59]. Zinc was added to reduce the solubility of hGH. The lyophilisate was densified, followed by regrounding to a powder. After sieving through a 212  $\mu\text{m}$  screen, protein particles with defined size were obtained. Both, the precipitation with Zn and the densification, already reduced the dissolution rate effectively. Untreated hGH particles dissolved without delay while it took 20 min for complete dissolution of the densified particles. Complexation with Zn delayed the dissolution for over 100 min. For encapsulation PLGA was dissolved in either 1-methyl-2-pyrrolidone, triacetin, ethyl benzoate or benzyl benzoate and the protein particles were immersed therein. Injection of these suspensions in aqueous medium produced PLGA gels which served as a protein particle depot. Release was tested in vivo and serum hGH levels were measured. After a first burst the release lasted up to 28 days.

Lyophilized recombinant human growth hormone powder was encapsulated in PLGA by the S/O/W method. PLGA was dissolved in dichloromethane and the protein powder was dispersed therein. Injection in water/poly(vinylalcohol) generated an S/O/W emulsion from which DCM was evaporated under stirring until particles were obtained. Particles larger than 74  $\mu\text{m}$  were removed and a powder suitable for s.c. injection was obtained. In vitro it took 16 days for complete protein release (**Fig. 5A**). In vivo release behavior of different formulations with ammonium acetate and ZnO as well as different PLGA types was investigated. Elevated serum hGH concentrations over approx. 16 days were observed for all formulations (**Fig. 5B**) [60].

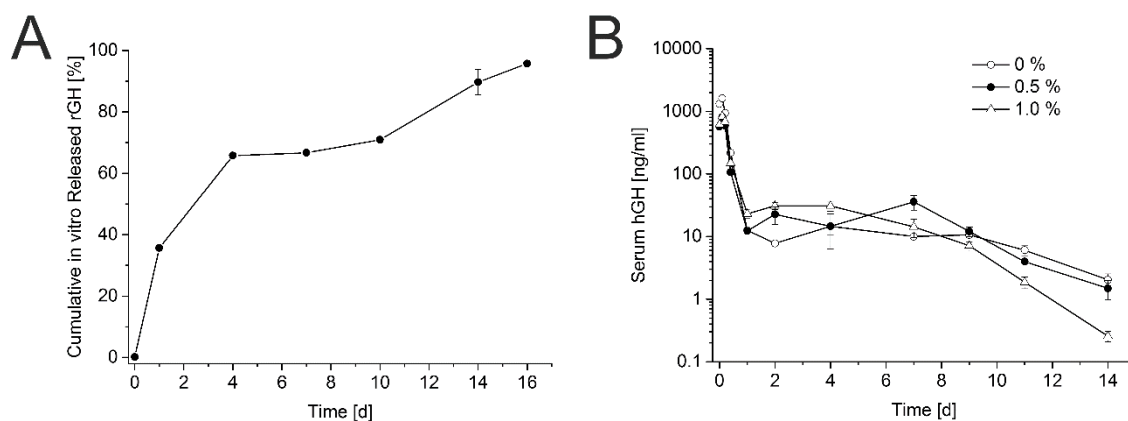


**Figure 5:** (A) Cumulative rGH release from PLGA microspheres with 7 % protein loading. hGH was precipitated with 0.5 % m/m zinc oxide. (B) Serum hGH levels in immunosuppressed rats after a single s.c. injection of hGH loaded PLGA microspheres with different amounts of zinc oxide. Reproduced with permission from [60]

Hen egg lysozyme particles were incorporated in an in situ forming biodegradable microparticle system (ISM) [61]. The protein was dissolved together with PLGA either in pure dimethylsulfoxide (DMSO) or DMSO and the addition of ethyl acetate and water. Ethyl acetate precipitated lysozyme and thus in dependence of the solvent composition either dissolved or homogeneously precipitated lysozyme was incorporated. These solutions/suspensions were emulsified into sesame oil. After injection into aqueous medium a homogeneous microparticle system was produced. Protein was released over approx. two weeks and bioactivity was almost completely retained while the precipitated lysozyme showed slightly greater activity compared to the unprecipitated protein.

## 1.7 Conclusion and outlook

Administering proteins in the crystalline or particulate state represents a versatile and suitable mode of protein delivery. However finding the right crystallization method usually displays an expensive and time consuming process and probably not every protein can be crystallized. This investment may pay off though, considering the benefits of storage and processing stability. In most cases the crystalline state surpasses the amorphous particulate state in terms of



thermodynamic and physical stability. Moreover, crosslinking or crystallization with excipients like protamine may further increase stability and reduced energy within the crystal lattice may reduce dissolution rates offering delivery without further encapsulation.

If crystalline protein cannot be obtained, amorphous particulate protein represents an alternative. Thereby high loading and reduced surface area in contact with potentially harmful surroundings can also be achieved.

Producing particulate protein for delivery, both crystalline and amorphous, is still a rather unnoticed field. With growing expertise on protein crystallization methods as well as protein stability itself, delivery is coming more and more into the focus of the formulation scientists and protein crystallization is slowly moving away from the sole purpose of purification and structure analysis. While momentarily the limits caused by the costs and efforts to be invested often prevail the benefits, this may change with increasing knowledge in protein batch crystallization and thus decreasing hurdles for the exploration of new crystallization protocols. As soon as uniform crystals or precipitated powder is obtained, well established encapsulation methods can be applied. S/O/W solvent deposition, electrostatically driven coating and electrospinning have proven to be applicable with similar methods as for small molecules. Release rates are well controllable although an exhaustive release is not always given for larger macromolecules because their diffusion through polymer matrices is slow. Bioactivity and in vivo experiments underline the compatibility of crystalline and particulate protein formulations for controlled delivery.

Finally another major point has to be considered: the rational reason why one would seek a long term stabilized protein formulation with complex release mechanisms. A conventionally designed protein formulation is very well capable to maintain the protein's integrity over a sufficient timespan. Either protein solutions with the addition of stabilizing agents or lyophilized protein powders, that are reconstituted in premixed buffers prior to application, mostly offer effective stabilization. Besides that in vitro stability and in vivo half-life differ

from protein to protein. The nature of monoclonal antibodies mostly grants them a long circulation in the human body even without controlled release mechanisms. Peptide hormones on the other hand often need frequent administration, sometimes even several times a day (e.g. insulin). For tissue engineering growth hormones benefit from a site directed and controlled release. Consequently for the former group the development of a drug delivery system is far less useful while for the latter patients would feel a real improvement for their treatment.

## 1.8 References

- [1] J.H. Hamman, G.M. Enslin, A.F. Kotzé, Oral Delivery of Peptide Drugs, *BioDrugs*. 19 (2005) 165–177.
- [2] E.-S. Khafagy, M. Morishita, Y. Onuki, K. Takayama, Current challenges in non-invasive insulin delivery systems: a comparative review., *Adv. Drug Deliv. Rev.* 59 (2007) 1521–46. doi:10.1016/j.addr.2007.08.019.
- [3] K. Park, I.C. Kwon, K. Park, Oral protein delivery: Current status and future prospect, *React. Funct. Polym.* 71 (2011) 280–287.
- [4] R. Jaenicke, Protein stability and molecular adaptation to extreme conditions, 728 (1991).
- [5] S.J. Shire, Z. Shahrokh, J. Liu, Challenges in the development of high protein concentration formulations., *J. Pharm. Sci.* 93 (2004) 1390–402. doi:10.1002/jps.20079.
- [6] K. Fu, a M. Klibanov, R. Langer, Protein stability in controlled-release systems., *Nat. Biotechnol.* 18 (2000) 24–5. doi:10.1038/71875.
- [7] G. Zhu, S.R. Mallery, S.P. Schwendeman, Stabilization of proteins encapsulated in injectable poly (lactide- co-glycolide), *Nat. Biotechnol.* 18 (2000) 52–7. doi:10.1038/71916.
- [8] B. Shenoy, Y. Wang, W. Shan, A.L. Margolin, Stability of crystalline proteins., *Biotechnol. Bioeng.* 73 (2001) 358–69. <http://www.ncbi.nlm.nih.gov/pubmed/11320506>.
- [9] M.X. Yang, B. Shenoy, M. Disttler, R. Patel, M. McGrath, S. Pechenov, et al., Crystalline monoclonal antibodies for subcutaneous delivery., *Proc. Natl. Acad. Sci. U. S. A.* 100 (2003) 6934–9. doi:10.1073/pnas.1131899100.

- [10] S.K. Basu, C.P. Govardhan, C.W. Jung, A.L. Margolin, Protein crystals for the delivery of biopharmaceuticals., *Expert Opin. Biol. Ther.* 4 (2004) 301–17. doi:10.1517/14712598.4.3.301.
- [11] A. Jen, H.P. Merkle, Diamonds in the rough: protein crystals from a formulation perspective., *Pharm. Res.* 18 (2001) 1483–8. <http://www.ncbi.nlm.nih.gov/pubmed/11758753>.
- [12] K.D. Collins, Ions from the Hofmeister series and osmolytes: effects on proteins in solution and in the crystallization process., *Methods.* 34 (2004) 300–11. doi:10.1016/j.ymeth.2004.03.021.
- [13] N.E. Chayen, E. Saridakis, Protein crystallization: from purified protein to diffraction-quality crystal., *Nat. Methods.* 5 (2008) 147–53. doi:10.1038/nmeth.f.203.
- [14] A. Ducruix, R. Giegé, *Crystallization of Nucleic Acids and Proteins - A Practical Approach*, Second Edi, Oxford University Press, 1999.
- [15] C. Haas, J. Drenth, Understanding protein crystallization on the basis of the phase diagram, *J. Cryst. Growth.* 196 (1999) 388–394. doi:10.1016/S0022-0248(98)00831-8.
- [16] M. V Saikumar, C.E. Glatz, M.A. Larson, Lysozyme crystal growth and nucleation kinetics, 187 (1998) 277–288.
- [17] A.A. Shukla, M.R. Etzel, S. Gadam, Bulk protein crystallization - Principles and methods, in: *Process Scale Biosep. Biopharm. Ind.*, Taylor & Francis Group, 2007: pp. 159–176.
- [18] A. McPherson, Current approaches to macromolecular crystallization., *Eur. J. Biochem.* 189 (1990) 1–23. <http://www.ncbi.nlm.nih.gov/pubmed/2185018>.
- [19] J.C. Falkner, A.M. Al-somali, J.A. Jamison, J. Zhang, S.L. Adrianse, R.L. Simpson, et al., Generation of Size-Controlled , Submicrometer Protein Crystals, *Chem. Mater.* 13 (2005) 2679–2686.
- [20] I.M. Lifshitz, V. V. Slyozov, The kinetics of precipitation from supersaturated solid solutions, *J. Phys. Chem. Solids.* 19 (1961) 35–50.
- [21] P.W. Voorhees, The Theory of Ostwald Ripening, *J. Stat. Physic.* 38 (1985) 231–252.
- [22] C. Sagui, M. Grant, Theory of nucleation and growth during phase separation, *Phys. Rev. E.* 59 (1999) 4175–4187. doi:10.1103/PhysRevE.59.4175.
- [23] D. Hekmat, D. Hebel, H. Schmid, D. Weuster-Botz, Crystallization of lysozyme: From vapor diffusion experiments to batch crystallization in agitated ml-scale vessels, *Process Biochem.* 42 (2007) 1649–1654. doi:10.1016/j.procbio.2007.10.001.
- [24] D. Hebel, S. Huber, B. Stanislawski, D. Hekmat, Stirred batch crystallization of a therapeutic antibody fragment., *J. Biotechnol.* 166 (2013) 206–11. doi:10.1016/j.jbiotec.2013.05.010.

- [25] N. Asherie, Protein crystallization and phase diagrams., *Methods*. 34 (2004) 266–72. doi:10.1016/j.ymeth.2004.03.028.
- [26] C.N. Nanev, V.D. Tonchev, F. V. Hodzhaoglu, Protocol for growing insulin crystals of uniform size, *J. Cryst. Growth*. 375 (2013) 10–15. doi:10.1016/j.jcrysgro.2013.04.010.
- [27] J. a. Garlitz, C. a. Summers, R. a. Flowers, G.E.O. Borgstahl, Ethylammonium nitrate: a protein crystallization reagent, *Acta Crystallogr. Sect. D Biol. Crystallogr.* 55 (1999) 2037–2038. doi:10.1107/S0907444999011774.
- [28] D.F. Kennedy, C.J. Drummond, T.S. Peat, J. Newman, Evaluating Protic Ionic Liquids as Protein Crystallization Additives, *Cryst. Growth Des.* 11 (2011) 1777–1785.
- [29] K. Shi, F. Cui, H. Bi, Y. Jiang, T. Song, Polycationic peptide guided spherical ordered self-assembly of biomacromolecules., *Biomaterials*. 33 (2012) 8723–32. doi:10.1016/j.biomaterials.2012.08.037.
- [30] H.P. Merkle, A. Jen, A crystal clear solution for insulin delivery A hybrid protein cocrystal of insulin and a lipophilically modified derivate provides smoother and longer lasting control of glucose levels, *Nat. Biotechnol.* 20 (2002) 798–90.
- [31] A. Jen, K. Madörin, K. Vosbeck, T. Arvinte, H.P. Merkle, Transforming growth factor beta-3 crystals as reservoirs for slow release of active TGF-beta3., *J. Control. Release*. 78 (2002) 25–34. <http://www.ncbi.nlm.nih.gov/pubmed/11772446>.
- [32] W. Fraunhofer, G. Winter, D.W. Borhani, S. Gottschalk, C.H. Cowles, S. Kim, *Compositions and Methods for Crystallizing Antibodies*, 2014.
- [33] A. Koenigsdorfer, S. Gottschalk, H.-J. Krause, G. Winter, D.W. Borhani, W. Fraunhofer, *Crystalline anti-hTNF-alpha antibodies*, 2014.
- [34] C. Govardhan, N. Khalaf, C.W. Jung, B. Simeone, A. Higbie, S. Qu, et al., Novel long-acting crystal formulation of human growth hormone., *Pharm. Res.* 22 (2005) 1461–70. doi:10.1007/s11095-005-6021-x.
- [35] M. Chan-Huot, L. Duma, J.-B. Charbonnier, J.-E. Herbert-Pucheta, L. Assairi, Y. Blouquit, et al., Large-Scale Production of Microcrystals and Precipitates of Proteins and Their Complexes, *Cryst. Growth Des.* 12 (2012) 6199–6207. doi:10.1021/cg301378j.
- [36] Y. Zang, B. Kammerer, M. Eisenkolb, K. Lohr, H. Kiefer, Towards protein crystallization as a process step in downstream processing of therapeutic antibodies: screening and optimization at microbatch scale., *PLoS One*. 6 (2011) e25282. doi:10.1371/journal.pone.0025282.
- [37] T. Morita, Y. Horikiri, H. Yamahara, T. Suzuki, H. Yoshino, Formation and isolation of spherical fine protein microparticles through lyophilization of protein-poly(ethylene glycol) aqueous mixture., *Pharm. Res.* 17 (2000) 1367–73. <http://www.ncbi.nlm.nih.gov/pubmed/11205729>.

- [38] Y.F. Maa, P.A. Nguyen, J.D. Andya, N. Dasovich, T. Sweeney, S.J. Shire, et al., Effect of Spray Drying and Subsequent Processing Conditions on Residual Moisture Content and Physical-Biochemical Stability of Protein Inhalation Powders.pdf, *Pharm. Res.* 15 (1998) 768–775.
- [39] H.R. Costantino, L. Firouzabadian, K. Hogeland, C. Wu, C. Beganski, K.G. Carrasquillo, et al., Protein spray-freeze drying. Effect of atomization conditions on particle size and stability., *Pharm. Res.* 17 (2000) 1374–83. <http://www.ncbi.nlm.nih.gov/pubmed/11205730>.
- [40] H.R. Costantino, L. Firouzabadian, C. Wu, K.G. Carrasquillo, K. Griebenow, S.E. Zale, et al., Protein spray freeze drying. 2. Effect of formulation variables on particle size and stability., *J. Pharm. Sci.* 91 (2002) 388–95. <http://www.ncbi.nlm.nih.gov/pubmed/11835198>.
- [41] M. a Winters, B.L. Knutson, P.G. Debenedetti, H.G. Sparks, T.M. Przybycien, C.L. Stevenson, et al., Precipitation of proteins in supercritical carbon dioxide., *J. Pharm. Sci.* 85 (1996) 586–94. doi:10.1021/js950482q.
- [42] M.J. Pikal, D.R. Riggsbee, The stability of insulin in crystalline and amorphous solids: observation of greater stability for the amorphous form., *Pharm. Res.* 14 (1997) 1379–87. <http://www.ncbi.nlm.nih.gov/pubmed/9358550>.
- [43] A. a Elkordy, R.T. Forbes, B.W. Barry, Stability of crystallised and spray-dried lysozyme., *Int. J. Pharm.* 278 (2004) 209–19. doi:10.1016/j.ijpharm.2004.02.027.
- [44] J.M. Broering, A.S. Bommarius, Evaluation of Hofmeister effects on the kinetic stability of proteins., *J. Phys. Chem. B.* 109 (2005) 20612–9. doi:10.1021/jp053618+.
- [45] J.T. Chin, S.L. Wheeler, A.M. Klibanov, Communication to the Editor On Protein Solubility in Organic Solvents, 44 (1994) 140–145.
- [46] N.. Shah, R.D. Ludescher, Influence of hydration on the internal dynamics of hen egg white lysozyme in the dry state, *Photochem. Photobiol.* 58 (1993) 169–174.
- [47] M.F. Dunn, Zinc-ligand interactions modulate assembly and stability of the insulin hexamer -- a review., *Biometals.* 18 (2005) 295–303. doi:10.1007/s10534-005-3685-y.
- [48] K. Petersen, Crystalline Amorphous Insulin-Zinc Compounds with Prolonged Action, *Science* (80-. ). 116 (1952) 394–398.
- [49] M.L. Brader, M. Sukumar, A.H. Pekar, D.S. McClellan, R.E. Chance, D.B. Flora, et al., Hybrid insulin cocrystals for controlled release delivery., *Nat. Biotechnol.* 20 (2002) 800–4. doi:10.1038/nbt722.
- [50] Y. Jiang, K. Shi, S. Wang, X. Li, F. Cui, A morphological screening of protein crystals for interferon delivery by metal ion-chelate technology., *Drug Dev. Ind. Pharm.* 36 (2010) 1389–97. doi:10.3109/03639045.2010.481303.

- [51] S. Puhl, L. Li, L. Meinel, O. Germershaus, Controlled Protein Delivery from Electrospun Non-wovens: Novel Combination of Protein Crystals and Biodegradable Release Matrix., *Mol. Pharm.* 11 (2014) 2372–2380. doi:10.1021/mp5001026.
- [52] S. Puhl, D. Ilko, L. Li, U. Holzgrabe, L. Meinel, O. Germershaus, Protein release from electrospun nonwovens: Improving the release characteristics through rational combination of polyester blend matrices with polidocanol, *Int. J. Pharm.* 477 (2014) 273–281. doi:10.1016/j.ijpharm.2014.10.047.
- [53] M. Hrynyk, M. Martins-Green, A.E. Barron, R.J. Neufeld, Sustained prolonged topical delivery of bioactive human insulin for potential treatment of cutaneous wounds., *Int. J. Pharm.* 398 (2010) 146–54. doi:10.1016/j.ijpharm.2010.07.052.
- [54] G.S. Mack, Pfizer dumps Exubera., *Nat. Biotechnol.* 25 (2007) 1331–2. doi:10.1038/nbt1207-1331.
- [55] U.S. Food and Drug Administration, FDA approves Afrezza to treat diabetes, (2014). <http://www.fda.gov/newsevents/newsroom/pressannouncements/ucm403122.htm>.
- [56] W. Nuffer, J.M. Trujillo, S.L. Ellis, Technosphere Insulin (Afrezza): A New, Inhaled Prandial Insulin., *Ann. Pharmacother.* (2014). doi:10.1177/1060028014554648.
- [57] G. Lee, Spray-Drying of Proteins, *Pharm. Biotechnol.* 13 (2002) 135–158.
- [58] C. Klingler, B.W. Müller, H. Steckel, Insulin-micro- and nanoparticles for pulmonary delivery., *Int. J. Pharm.* 377 (2009) 173–9. doi:10.1016/j.ijpharm.2009.05.008.
- [59] K.J. Brodbeck, S. Pushpala, a J. McHugh, Sustained release of human growth hormone from PLGA solution depots., *Pharm. Res.* 16 (1999) 1825–9. <http://www.ncbi.nlm.nih.gov/pubmed/10644069>.
- [60] S. Takada, Y. Yamagata, M. Misaki, K. Taira, T. Kurokawa, Sustained release of human growth hormone from microcapsules prepared by a solvent evaporation technique., *J. Control. Release.* 88 (2003) 229–42. <http://www.ncbi.nlm.nih.gov/pubmed/12628330>.
- [61] M. Körber, R. Bodmeier, Development of an in situ forming PLGA drug delivery system I. Characterization of a non-aqueous protein precipitation., *Eur. J. Pharm. Sci.* 35 (2008) 283–92. doi:10.1016/j.ejps.2008.07.007.







## **2 Controlled Protein Delivery from Electrospun Non-Wovens: Novel Combination of Protein Crystals and a Biodegradable Release Matrix**

Sebastian Puhl, Linhao Li, Lorenz Meinel, Oliver Germershaus

Reprinted (adapted) with permission from *Molecular Pharmaceutics* 2014, 11, 2372–2380.  
Copyright (2014) American Chemical Society.  
[dx.doi.org/10.1021/mp5001026](http://dx.doi.org/10.1021/mp5001026)

## **Abstract**

Poly- $\epsilon$ -caprolactone (PCL) is an excellent polymer for electrospinning and matrix-controlled drug delivery combining optimal processability and good biocompatibility. Electrospinning of proteins has been shown to be challenging via the use of organic solvents, frequently resulting in protein unfolding or aggregation. Encapsulation of protein crystals represents an attractive but largely unexplored alternative to established protein encapsulation techniques because of increased thermodynamic stability and improved solvent resistance of the crystalline state. We herein explore the electrospinning of protein crystal suspensions and establish basic design principles for this novel type of protein delivery system. PCL was deployed as a matrix, and lysozyme was used as a crystallizing model protein. By rational combination of lysozyme crystals 0.7 or 2.1  $\mu\text{m}$  in diameter and a PCL fiber diameter between 1.6 and 10  $\mu\text{m}$ , release within the first 24 h could be varied between approximately 10 and 100%. Lysozyme loading of PCL microfibers between 0.5 and 5% was achieved without affecting processability. While relative release was unaffected by loading percentage, the amount of lysozyme released could be tailored. PCL was blended with poly(ethylene glycol) and poly(lactic-co-glycolic acid) to further modify the release rate. Under optimized conditions, an almost constant lysozyme release over 11 weeks was achieved.

## 2.1 Introduction

The first report of electrospinning dates back to the 1930s [1,2]. Besides good processability and high versatility with regard to attainable structures of the products, electrospun non-wovens are quite suitable as controlled release matrices for drug delivery. With the increasing availability of biocompatible polymers being suitable for electrospinning, controlled drug release from non-woven scaffolds has received an increasing amount of attention. Potential applications of non-wovens range from transdermal delivery and wound dressing to tissue engineering after surgical intervention [3]. Poly- $\epsilon$ -caprolactone (PCL) is a biocompatible and biodegradable polymer with proven suitability for controlled drug delivery applications [4]. The solubility in various organic solvents as well as its ability to form fibers under mechanical stress renders PCL an ideal candidate for electrospinning [5]. PCL biodegradation in vivo is slow and primarily driven by enzymatic degradation. In vitro, its structure remains intact over months [6]. Poly(lactic-co-glycolic acid) (PLGA) represents a well-established polymer for drug delivery with a degradation rate that is higher than that of PCL but is hampered by significant shrinkage of its non-wovens [7]. The combination of PCL and PLGA leads to easily processable polymer blends, mechanically stable non-wovens, and allows the fine-tuning of release properties [8]. However, PCL and PLGA both are rather hydrophobic polymers, and poor wettability frequently is a challenge for efficient drug release [9]. Therefore, hydrophilic polymers, such as poly(ethylene glycol) (PEG) or poly-(ethyleneimine), have been used to improve wettability as well as to induce pore formation and resulted in successful efforts to improve drug release [9–11]. The controlled release of proteins is a long-standing challenge to formulation scientists because of the complex structure, multiple degradation pathways, and resulting stability issues. Unfortunately, electrospinning often relies on the use of organic solvents that may detrimentally affect protein integrity and thus their biological activity. Electrospinning of water in oil emulsions and generation of lipophilic complexes of hydrophilic proteins are common solutions [9,10]. Nevertheless, proteins are still prone to interactions with

the solvent or the solvent–water interface, rendering them susceptible to denaturation. Considering these challenges, the aim of this work was to establish alternative strategies for the encapsulation of proteins. Compared to the amorphous state, crystals are characterized by higher thermodynamic stability and a reduced solvent-exposed surface area, rendering protein crystals potentially more suitable for direct processing in organic solvents [12–14]. As an example,  $\alpha$ -amylase was shown to withstand treatment with organic solvents after crystallization [15]. In addition, crystals represent the most concentrated form of a protein, therefore allowing high drug loading [12]. Finally, crystal dissolution can be controlled in many ways, e.g., by modifying crystal size, crystal morphology, excipients, and dissolution media [12,16]. Because of these properties, the encapsulation of protein crystals into polymeric matrices by electrospinning may represent an alternative approach alleviating several of the problems encountered during generation of protein drug delivery systems. Lysozyme was selected as a model protein on the basis of its well-established crystallization conditions, allowing the generation of crystals with a controlled size and morphology [17]. Moreover, lysozyme is well-established for wound treatment [18–20]. Lysozyme crystals with a well-controlled, narrow size distribution were prepared, and the impact of PCL fiber diameter and size of incorporated protein crystals on drug release was studied. Furthermore, lysozyme loading was varied to identify the effect on processability and release. We then used PCL/PEG and PCL/PLGA blends to improve the hydrophilicity, microporosity, and degradability of the fibers to modify drug release kinetics.

## **2.2 Experimental section**

### **2.2.1 Materials**

Chicken egg white lysozyme (~70000 units/mg), PCL ( $M_w = 70000$ – $90000$ ), *Micrococcus lysodeikticus*, polysorbate 80 (PS80), fluorescein isothiocyanate (FITC), and tetrafluoroacetic acid [high-performance liquid chromatography (HPLC) grade] were purchased from Sigma-

Aldrich (Munich, Germany). Poly(D,L-lactide-co-glycolide) 50:50 (Resomer RG 502H,  $M_w = 7000\text{--}17000$ , free acid) was a gift from Evonik Industries (Essen, Germany). Poly(ethylene glycol) 3000 was obtained from MERCK Schuckardt (Hohenbrunn, Germany). The bicinchoninic acid (BCA) assay kit was purchased from Thermo Scientific (Rockford, IL). Acetonitrile (gradient grade) was purchased from VWR Prolabo (Fontenaysous-Bois, France). Chloroform, ethanol, sodium phosphate, sodium hydroxide, sodium chloride, sodium azide, and acetic acid were of analytical grade.

### **2.2.2 Lysozyme Crystallization and Crystal Size Determination**

Lysozyme crystallization was performed according to the method of Falkner et al. with modifications [17]. Lysozyme was dissolved in 10 mL of sodium acetate buffer (pH 3.5) at a concentration of  $8.0\text{ mg mL}^{-1}$ . Twenty milliliters of precipitation buffer consisting of 20% sodium chloride, 10% PEG 3000, and 500 mM sodium acetate (pH 3.5) at  $-4$  or  $8\text{ }^\circ\text{C}$  was poured quickly into the lysozyme solution and the mixture stirred at 500 rpm. Crystal formation took place within seconds. After being washed twice with an ethanol/chloroform mixture (3:10 volume ratio), crystals were dried under a mild vacuum. Particle size distributions of particles above approximately  $1\text{ }\mu\text{m}$  were determined by laser diffraction analysis (LS 230, Beckman Coulter, Brea, CA) and below approximately  $1\text{ }\mu\text{m}$  by dynamic light scattering (DelsaNano HC, Beckman Coulter).

### **2.2.3 FITC Labeling of Lysozyme**

Lysozyme was dissolved in 0.1 M carbonate buffer (pH 9.0) at a concentration of  $2.0\text{ mg mL}^{-1}$ . FITC ( $1.0\text{ mg mL}^{-1}$ , dissolved in DMSO) was added at a volume ratio of 1:12.5 to the lysozyme solution and the mixture stirred for 6 h at room temperature. Subsequently, the solution was dialyzed (Spectra/Por dialysis membrane, cutoff of 6–8 kDa, Spectrum Laboratories, Rancho Dominguez, CA) against 5 L of deionized water for 2 h and lyophilized.

The average molar degree of modification was 1.47 mol (mol of FITC)<sup>-1</sup> per lysozyme. Labeled crystals were produced using a 1:30 labeled:unlabeled lysozyme molar ratio according to the procedure described above.

#### **2.2.4 PCL Electrospinning**

Electrospinning was performed with a dc power supply HCP 140-350000 instrument from FuG Elektronik (Rosenheim, Germany) and a syringe pump (type 540200, TSE Systems, Bad Homburg, Germany). PCL fibers were produced by electrospinning onto a static receiver plate using a focusing ring 20 cm in diameter using a setup similar to that described previously [21]. Protein crystals were suspended in ethanol at a concentration of 3.0 mg mL<sup>-1</sup>. After homogenization in an ultrasonic bath (Branson 3200, Branson, Danbury, CT) for 20 s, chloroform and the respective polymers were added. Ethanol and chloroform were mixed in a volume ratio of 1:6. Using this procedure, stable protein crystal suspensions in a concentrated PCL solution, suitable for electrospinning, were obtained. Suspensions were transferred into a syringe with an attached metal spinneret (22 gauge). A copper ring with a 20 cm diameter was electrically charged like the metal spinneret and placed in a vertical plane around it. The electrospinning conditions, composition of the polymer solution, and lysozyme crystal size were varied, resulting in different combinations of crystal size and fiber diameter (Table 1). For each sample, 1 mL of a polymer suspension was electrospun, resulting in round non-wovens with almost identical diameters. The loading of the non-wovens was calculated to be 0.2% m/m. Pure PCL non-wovens with lysozyme loadings of 0.5, 1.0, 2.5, and 5.0% were produced using 2.1 μm lysozyme crystals with minor adjustments.

A solution of 18% m/V PCL was electrospun with a flow rate of 10 mL h<sup>-1</sup>. The collector was placed at a distance of 35 cm, and the voltage was set to 27 kV. The resulting fiber diameter was 7.11 ± 3.01 μm. Furthermore, different amounts of PEG or PLGA were admixed to the PCL/crystal suspension and electrospun in a similar fashion (Tables 2 and 3). Concentrations

of admixed PEG or PLGA were calculated relative to total dry polymer mass (% m/m). All experiments were performed in triplicate, and the data represent averages  $\pm$  the standard deviation (SD).

| Crystal size [ $\mu\text{m}$ ] | PCL [%] m/V | Flowrate [ml h <sup>-1</sup> ] | Collector distance [cm] | Voltage [kV] | Fiber Diameter $\pm$ SD [ $\mu\text{m}$ ] |
|--------------------------------|-------------|--------------------------------|-------------------------|--------------|---|
| 2.1                            | 14          | 1                              | 20                      | 25           | 1.7 $\pm$ 0.5                             |
| 0.7                            | 14          | 1                              | 20                      | 25           | 1.6 $\pm$ 0.4                             |
| 2.1                            | 14          | 5                              | 25                      | 25           | 3.9 $\pm$ 0.5                             |
| 0.7                            | 14          | 5                              | 25                      | 25           | 3.5 $\pm$ 0.8                             |
| 2.1                            | 18          | 10                             | 25                      | 25           | 5.3 $\pm$ 0.7                             |
| 0.7                            | 18          | 10                             | 25                      | 25           | 5.2 $\pm$ 0.5                             |
| 2.1                            | 25          | 15                             | 35                      | 25           | 10.1 $\pm$ 0.8                            |
| 0.7                            | 25          | 15                             | 35                      | 25           | 10.3 $\pm$ 1.0                            |

**Table 1:** Electrospinning conditions and resulting average fiber diameters of pure PCL fibers

| PEG content [%] m/m | Crystal size [ $\mu\text{m}$ ] | PCL [%] m/V | Flowrate [ml h <sup>-1</sup> ] | Collector distance [cm] | Voltage [kV] | Fiber Diameter $\pm$ SD [ $\mu\text{m}$ ] |
|---------------------|--------------------------------|-------------|--------------------------------|-------------------------|--------------|---|
| 2                   |                                |             |                                |                         |              | 6.8 $\pm$ 1.1                             |
| 5                   |                                |             |                                |                         |              | 6.9 $\pm$ 0.9                             |
| 10                  | 2.1                            | 25          | 15                             | 40                      | 27           | 5.8 $\pm$ 0.9 *                           |
| 20                  |                                |             |                                |                         |              | 5.6 $\pm$ 1.1 *                           |

\* Fiber diameters are statistically significant smaller as compared to PCL/PEG 2 % (p<0.001)

**Table 2:** Electrospinning conditions and resulting average fiber diameters of PCL/PEG blends

| PLGA content [%]<br>m/m | Crystal size[ $\mu\text{m}$ ] | PCL [%]<br>m/V | Flowrate<br>[ml h <sup>-1</sup> ] | Collector distance<br>[cm] | Voltage<br>[kV] | Fiber Diameter<br>$\pm$ SD [ $\mu\text{m}$ ] |
|-------------------------|-------------------------------|----------------|-----------------------------------|----------------------------|-----------------|--|
| 2                       |                               |                |                                   |                            |                 | 9.9 $\pm$ 3.4                                |
| 10                      | 2.1                           | 25             | 15                                | 40                         | 27              | 8.2 $\pm$ 4.4 *                              |

\* Fiber diameters are statistically significant smaller as compared to PCL/PLGA 2 % (p<0.024)

**Table 3:** Electrospinning conditions and resulting average fiber diameters of PCL/PLGA blends

### 2.2.5 In Vitro Release

The generated non-wovens were dried in vacuum overnight and weighed. Afterward, the entire non-woven (approximately 150–300 mg) was cut into smaller pieces and incubated in 3.0 mL of PBS (pH 7.4) with 0.1% sodium azide at 37 °C. At each time point, 200  $\mu\text{L}$  of the release medium was withdrawn and replaced by the same volume of buffer. To minimize the impact of the variable wettability of scaffolds and to delineate the effect of fiber diameter and crystal size, polysorbate 80 was added to the release medium during release from pure PCL non-wovens. In contrast, the medium used during release from PCL/PEG and PCL/PLGA blends was without PS 80. The lysozyme concentration was measured by RP-HPLC (LaChrom Ultra with L-2400 UV detector, VWR Hitachi and RP18 Licrosphere 100 column, Merck, Darmstadt, Germany) at 220 nm ( $\lambda$ ) with a water/TFA to acetonitrile gradient (Table S1 of the Supporting Information), yielding a limit of quantification of 2.56  $\mu\text{g mL}^{-1}$ . The BCA assay (Pierce BCA assay kit, ThermoScientific) was used for lysozyme quantification in the case of PCL/PEG and PCL scaffolds where release medium without polysorbate 80 was used, and the limit of quantification was 1.20  $\mu\text{g mL}^{-1}$ . Fifty microliters of sample was mixed with 200  $\mu\text{L}$  of the BCA reagent solution. After incubation at 60 °C for 30 min, the absorbance was determined at a wavelength ( $\lambda$ ) of 562 nm (Spectra max 250, Molecular Devices, Sunnyvale, CA).



### **2.2.6 Relative Bioactivity of Lysozyme**

The relative bioactivity of lysozyme was determined as described previously [22]. Briefly, the *Micrococcus lysodeikticus* cell wall preparation was suspended in 1.0 mL of 0.1 M KH<sub>2</sub>PO<sub>4</sub> (pH 6.2) at a concentration of 200 mg L<sup>-1</sup>, and 33.3 μL of the sample solution was added. After the sample had been stirred for 5 s, the decline in absorbance measured at 570 nm was recorded for 2 min (Genesys 10S, Thermo Scientific). The relative biological activity of lysozyme was determined in reference to a calibration curve constructed using fresh lysozyme and setting its bioactivity to 100%. The slope of the decline was proportional to the lysozyme activity, and the limit of quantification was 0.96 μg mL<sup>-1</sup> lysozyme.

### **2.2.7 Morphology and Fiber Diameter**

Scanning electron microscopy (SEM) images were recorded using a JSM-7500F field emission scanning electron microscope (Jeol, Tokyo, Japan) with an acceleration voltage of 5 kV. The fiber diameter was determined using ImageJ (National Institutes of Health, Bethesda, MD). For each preparation, 60 individual fiber diameters were measured manually perpendicular to the fiber surface. For all preparations, samples of non-wovens were drawn regularly during release studies. Samples were washed with purified water, dried under vacuum overnight, studied by SEM, and compared with the fresh non-wovens. For fluorescence microscopy, pure PCL fibers containing 5.0% FITC-labeled lysozyme crystals were electrospun onto cover slips. Electrospinning conditions were the same as those for 10.1 μm pure PCL fibers. Fluorescence images were recorded using an Axio Observer Z1 epifluorescence microscope (Zeiss, Oberkochen, Germany) with excitation at 450–490 nm ( $\lambda$ ), a beam splitter at 495 nm ( $\lambda$ ), and emission at 500–550 nm ( $\lambda$ ) using a Plan-Apochromat 63×/1.40 objective and an AxioCam MRm camera.

### 2.2.8 Wettability of the Non-Wovens

Direct measurement of the contact angle using sessile drop goniometry is difficult for non-wovens because of the rough surface and high capillarity. Consequently, we determined the sorption rate of release buffer to characterize the wettability of the non-wovens using a tensiometer (K12, Krüss GmbH, Hamburg, Germany). The non-wovens were cut into pieces of equal size (9 mm × 18 mm) and connected to the balance of the tensiometer. The short side of the sample was immersed exactly 0.5 mm into the release buffer (PBS with 0.1% sodium azide). The mass increase was recorded over 10 min, and the squared mass was plotted versus time. The Washburn theory describes the relationship between the time and the adsorbed mass of liquid as follows [23,24].

$$t = A \cdot m^2 \quad (1)$$

$$A = \frac{\eta}{c \cdot \rho^2 \cdot \sigma \cdot \cos\theta} \quad (2)$$

where  $m$  is the sorbed mass of water,  $\eta$  is the viscosity of the immersion liquid,  $c$  is the capillarity of the sample,  $\rho$  is the density of the immersion liquid,  $\sigma$  is the surface tension of the immersion liquid, and  $\theta$  is the contact angle between the immersion liquid and non-woven. Assuming similar capillarity, the sorbed mass of water directly correlates with the contact angle between the liquid and non-woven and, therefore, represents a simple measure for assessing the wettability of non-wovens.

### 2.2.9 Statistical Analysis

All data are reported as means  $\pm$  the standard deviation of at least three independent experiments unless specified otherwise. Statistical significance was calculated with a Student's  $t$  test for comparison of two groups or one-way analysis of variance using multiple comparisons versus

control by the Holm–Sidak method for comparison of multiple groups with an overall significance level of 0.05 (SigmaPlot 12, Systat Software, San Jose, CA).

## 2.3 Results

### 2.3.1 Morphology of Lysozyme Crystals and Non-Wovens

Lysozyme crystals were produced at a yield of approximately 92%, achieving narrow size distributions and minimal aggregation (Figure S1 of the Supporting Information). Two different crystals with diameters of  $0.7 \pm 0.1$  and  $2.1 \pm 0.7$   $\mu\text{m}$  were used in this study (Figure 1A,B). The purity of the resulting crystal powder was determined to be 85.9% for the 0.7  $\mu\text{m}$  crystals and 85.6% for the 2.1  $\mu\text{m}$  crystals. The relative biological activity was fully retained after incubation in the solvents used for electrospinning. The fiber diameter, shape, and surface were examined using SEM. It is to be noted that single lysozyme crystals were not observed outside a fiber. Electrospinning of pure PCL was highly reproducible, allowing the repeated production of nonwovens with narrow fiber size distributions (Table 1 and Figure S2A of the Supporting Information). The surface of the fibers appeared to be smooth, and no pores were observed (Figure 1C–F). Electrospinning process parameters had to be adapted for PCL/PEG blends as compared to the protocol used for PCL to account for the decreased viscosity of the solution (Table 2). Nevertheless, a statistically significant decrease in fiber diameter from  $6.8 \pm 1.1$   $\mu\text{m}$  for blends containing 2% PEG to  $5.6 \pm 1.1$   $\mu\text{m}$  for the 20% PEG blend was observed. However, the high degree of uniformity of fiber diameters was not compromised under the modified conditions (Figure S2B of the Supporting Information).

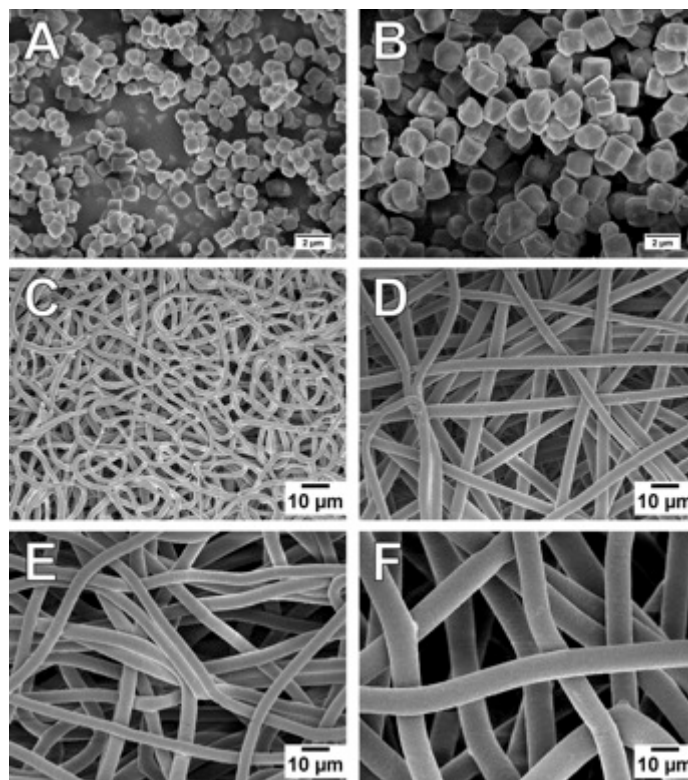
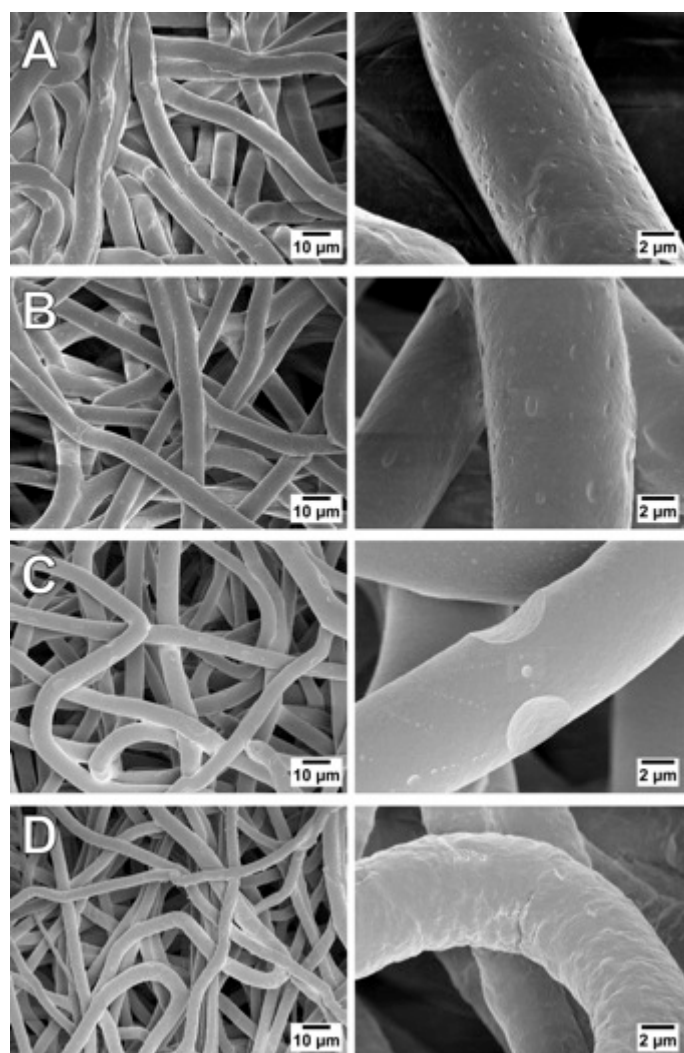


Figure 1. Scanning electron micrographs detailing the morphology of lysozyme crystals (A and B) and electrospun non-wovens (C–F). Lysozyme crystals approximately 0.7  $\mu\text{m}$  (A) and 2.1  $\mu\text{m}$  (B) in average diameter were used in this study. Non-wovens were generated by electrospinning from PCL solutions in a chloroform/ethanol mixture containing suspended lysozyme crystals. Average fiber diameters were approximately 1.6 (C), 3.6 (D), 5.2 (E), and 10.2  $\mu\text{m}$  (F).

The addition of PEG resulted in the formation of pores or depressions on the surface, whose size increased with increasing PEG content (Figure 2A–C). At 20% PEG, the fiber morphology changed to a coarse, wrinkled surface with no distinct pores (Figure 2D). The PCL/PLGA spinning process was less stable than PCL or PCL/PEG spinning, resulting in an increasing relative standard deviation of fiber diameters from 9.8% for pure PCL fibers to 34.8% in the case of 2% PLGA and 53.5% for 10% PLGA fibers (Figure S2C of the Supporting Information). Again, with an increasing PLGA content, a statistically significant decrease in fiber diameter from  $9.9 \pm 3.4$  to  $8.2 \pm 4.4$   $\mu\text{m}$  and an increase in surface roughness were observed (Figure 3A,B). PCL/PLGA blends with a PLGA content of >10% resulted in reduced viscosity and phase separation and thus were not suitable for electrospinning.



**Figure 2.** Scanning electron micrographs of PCL/PEG blend nonwovens at 2% (A), 5% (B), 10% (C), and 20% PEG (D) at low (left) and high (right) magnifications.

During release, no change in fiber morphology was detected by SEM in the case of PCL/PEG scaffolds, while minimal shrinking and formation of few large pores were observed in the case of PCL/PLGA nonwovens (Figure S3 of the Supporting Information).

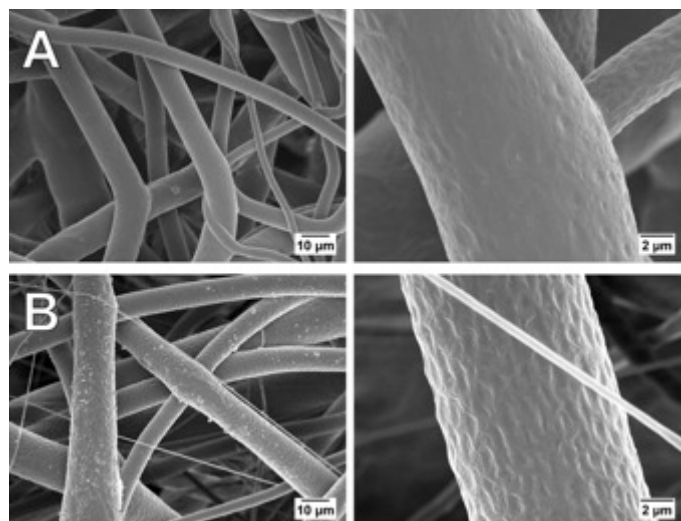


**Figure 3.** Scanning electron micrographs of PCL/PLGA blend nonwovens at 2% (A) and 10% PLGA (B) at low (left) and high (right) magnifications.

Using fluorescence microscopy, it was confirmed that crystals kept their shape after being incorporated into electrospun fibers and that all crystals were located within the fibers (Figure 4). Crystals were evenly and discretely distributed within individual fibers and could be observed within the entire non-woven. The distance to the fiber surface appeared to be irregular. The effect of processing on the morphology and distribution of lysozyme crystals was evaluated in detail by comparing unprocessed lysozyme crystals suspended in air (Figure 4, inset A) to crystals in PCL cast as a film using the same lysozyme crystal/PCL suspension that was used for electrospinning (Figure 4, inset B). The size and morphology of lysozyme crystals after suspension in PCL in a chloroform/ethanol mixture and film casting were unchanged compared to those of unprocessed lysozyme crystals. Lysozyme crystals in electrospun fibers had the same morphology but appeared to be slightly smaller than those in cast films, which may be explained by the curvature of fibers resulting an optically reduced size of particles within the fiber.

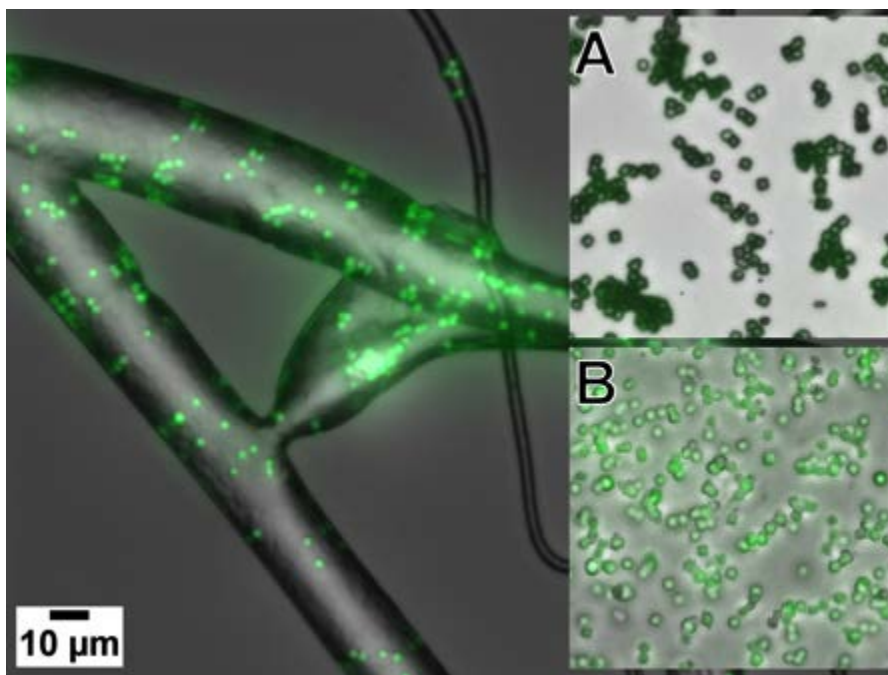


**Figure 4.** Figure 4. Distribution of FITC-labeled lysozyme crystals in a PCL non-woven prepared using 2.1 µm lysozyme crystals, a 25% PCL solution, and a drug loading of 5%. Inset A shows unprocessed lysozyme crystals suspended in air, while inset B shows lysozyme crystals embedded in a film cast from the same crystal suspension in a PCL solution used for electrospinning of the fibers. The scale bar applies to the main image and the insets.

### 2.3.2 Effect of Scaffold Composition on Lysozyme Release, Relative Bioactivity, and Sorption of Release Buffer

The release of lysozyme from PCL fibers depended on fiber diameter as well as on the size of the protein crystals. The burst release was efficiently controlled by both parameters (Figure 5A, B). For both 0.7 and 2.1 µm lysozyme crystals, a statistically significant inverse relation of burst release to fiber diameter was observed (Figure 5C). Furthermore, burst release from fibers with a similar diameter was consistently and statistically significantly higher for larger protein crystals (Figure 5C). Interestingly, this was confirmed even for the combination of 2.1 µm crystals with 1.5 µm fibers, potentially because of the coating of the crystals with a thin PCL film controlling the release. Using pure PCL as a scaffold material, only the amount of burst differed; the subsequent release was in all cases minimal and was not affected by fiber diameter or crystal size (Figure 5A, B).

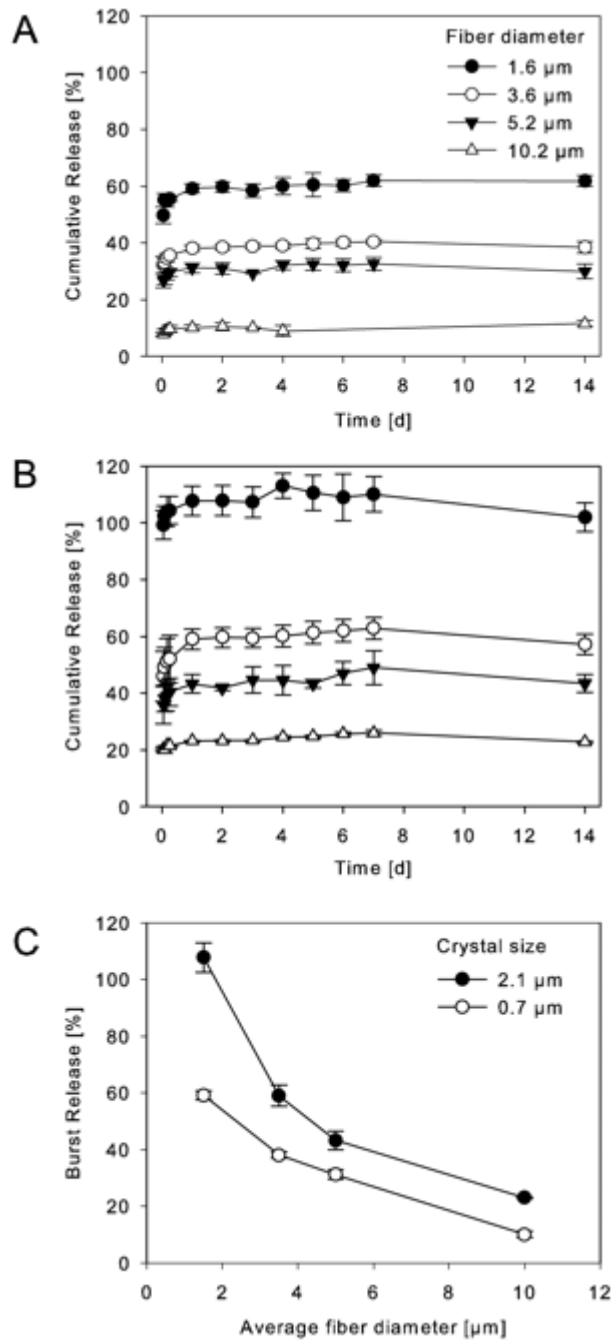


**Figure 5.** Release of lysozyme from pure PCL non-wovens with average fiber diameters of 1.6, 3.6, 5.2, and 10.2 μm using approximately 0.7 μm (A) and 2.1 μm (B) lysozyme crystals. (C) Relationship among fiber diameter, crystal size, and burst release. The averages and standard deviations of three independent experiments are shown.

The effect of lysozyme loading under otherwise identical conditions was varied to delineate the drug loading potential of the delivery system as well as the effect of loading on drug release (Figure 6). Processability was not affected within the chosen loading range. Interestingly, for drug loading between 0.5 and 5%, no effect of loading on relative lysozyme release was



observed (Figure 6A). Absolute drug release is shown in Figure 6B, confirming that the amount of lysozyme released could be directly controlled by the loading. A linear relationship between the absolute amount of lysozyme released after 24 h and drug loading was found (Figure 6C;  $R^2 = 0.982$ ).

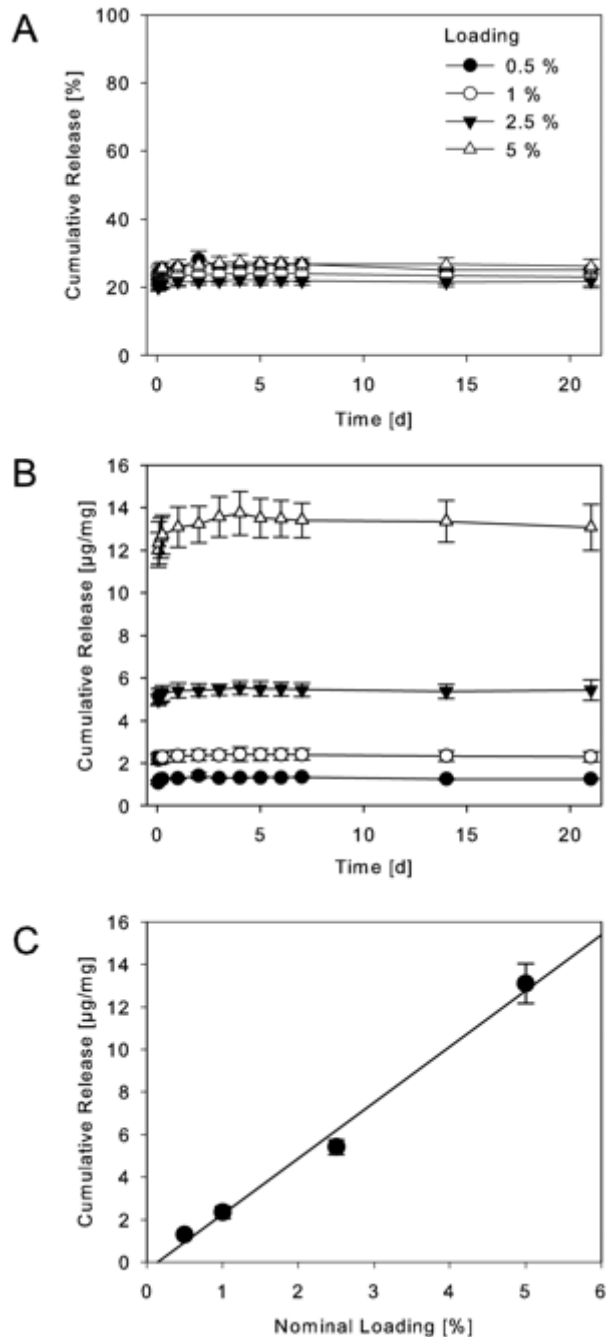


**Figure 6.** Effect of variation of lysozyme loading on the release from pure PCL non-wovens with an average fiber diameter of  $7.1 \mu\text{m}$  and using approximately  $2.1 \mu\text{m}$  lysozyme crystals. Cumulative relative release (A) and cumulative absolute release (B) of lysozyme. A linear relationship between loading and burst release was observed (C). The averages and standard deviations of three independent experiments are shown.

PEG was added to the system in different ratios as a pore forming agent and to improve wettability of non-wovens compared to that of pure PCL as described previously [9, 10] and as confirmed by sorption experiments (see below). Addition of up to 10% PEG had no significant effect on the release pattern compared to the effect of pure PCL (Figure 7A). At 20% PEG, a significant increase in the level of released lysozyme was found for the first 21 days, followed by minimal release thereafter (Figure 7A). Therefore, PCL/PLGA blends were used to further improve the release by increasing the level of polymer degradation (Figure 7B). After addition of 10% PLGA, a burst of around 5% of total encapsulated lysozyme was observed, which was significantly higher than the burst from pure PCL scaffolds under otherwise comparable conditions. Thereafter, lysozyme was released at an almost constant rate for ~5 weeks. However, lysozyme degradation products were detected by RP-HPLC after ~1 week (Figure S4 of the Supporting Information). After 5 weeks, no further increase in the magnitude of the lysozyme main peak was observed in the release medium, and the pH value of the release buffer decreased to 3.3, most likely because of acidic PLGA degradation products. As exchange of the release medium was minimal (approximately 7% of the medium was exchanged per time point), the decrease in pH led to degradation of already released lysozyme, resulting in a decreasing cumulative lysozyme concentration after incubation for 5 weeks. At 2% PLGA, the level of lysozyme degradation was significantly reduced and an almost constant release rate was observed for 11 weeks. Under these conditions, the pH decreased to 5.2 within 11 weeks. For both PCL/PLGA blends, the level of lysozyme release was statistically significantly higher than the level of release from pure PCL scaffolds.

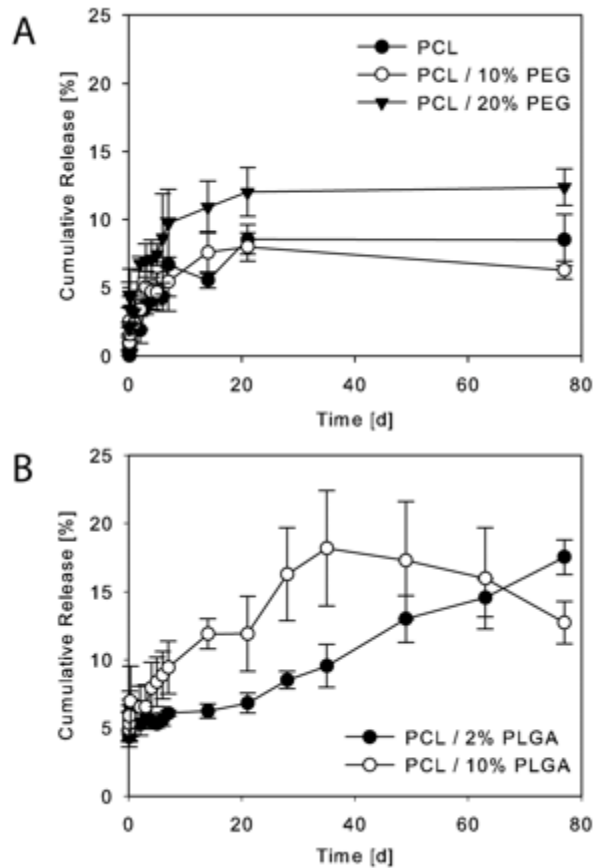


**Figure 7.** Release of lysozyme from PCL/PEG and PCL/PLGA scaffolds at a constant fiber diameter and crystal size. The effect of addition of increasing amounts of PEG (A) and PLGA (B) relative to pure PCL is shown. Results are presented as averages and standard deviations of three independent experiments.

The relative bioactivity of samples taken at the end of the release study was determined and related to the content determined by RP-HPLC. Lysozyme released from pure PCL or PCL/PEG scaffolds showed no decrease in relative bioactivity after 3 weeks. The relative bioactivity of lysozyme released from PCL/PLGA scaffolds after 11 weeks was  $84.5 \pm 1.8\%$  in the case of 2% PCL/PLGA blends, whereas the relative bioactivity in the case of 10% PCL/PLGA blends was significantly lower ( $67.0 \pm 8.3\%$ ). Sorption measurements were performed to assess the wettability of the scaffolds (Figure 8). In contrast to classic wicking experiments, the rate of buffer sorption was determined per area of the non-woven in contact with the solution but the contact angle was not calculated because of the unknown scaffold porosity. Pure PCL non-wovens showed the least sorption with only little buffer uptake during the experiment. As

expected, the addition of polysorbate 80 to the release medium resulted in a statistically significantly increased level of sorption, i.e., improved wetting of scaffolds. Addition of 10 and 20% PEG but not of 2 or 5% PEG resulted in a significantly increased level of sorption. In contrast, the wettability of PCL/PLGA blends was not significantly increased compared to that of pure PCL scaffolds.

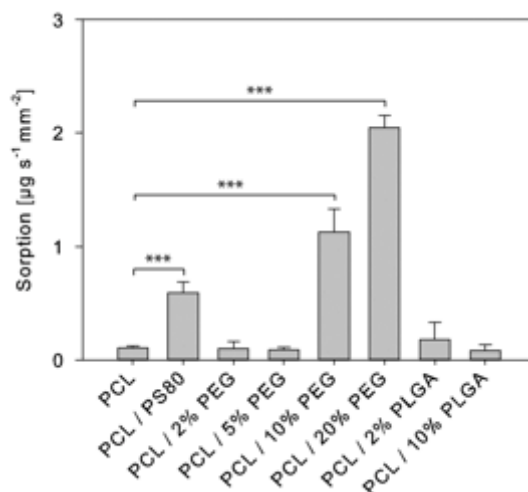


**Figure 8.** Dependence of sorption of release buffer by electrospun non-wovens on polymer composition and addition of surfactant. The averages and standard deviations of three independent experiments are shown.

## 2.4 Discussion

The application of protein crystals is an emerging strategy for addressing several problems related to the processing, storage, and delivery of biologic drugs [15,25–28]. Notably, protein crystals possess higher thermodynamic stability, smaller contact surface area, and higher purity than the amorphous state [12,29]. The control of crystallization conditions allows the generation of particles of varying size and with almost monomodal size distribution (Figure 1A,B) [17]. Furthermore, the crystalline state opens new avenues for the development of electrospun protein delivery systems, from a processing perspective as well as with regard to the control of release profiles. Organic solvents that otherwise would lead to denaturation of the protein can be used during electrospinning of protein crystal suspensions [15]. Of course, solvents must be carefully selected such that protein crystals neither dissolve nor unfold or aggregate during processing.

Lysozyme crystals could be dispersed in a mixture of chloroform and ethanol without a detectable loss of relative biological activity. After incorporation of lysozyme crystals into electrospun scaffolds composed of PCL and PCL/PEG or PCL/PLGA blends, the lysozyme crystal integrity and overall morphology were retained. Sedimentation during the electrospinning operation was successfully prevented by high viscosities of concentrated polymer solutions, resulting in a homogeneous lysozyme crystal distribution within the scaffolds (Figure 4). The release of protein from non-woven scaffolds is often characterized by significant burst release at early time points, of which the extent is in many cases related to the conditions of scaffold preparation or scaffold composition [30,31]. However, control of burst release is rarely considered a design feature of a drug delivery system despite the fact that the release of a defined loading dose would in many cases be desirable from a pharmacokinetic perspective [32,33]. As shown herein, burst release can be modified in a manner independent of the subsequent release rate by means of a rational combination of lysozyme crystal size and PCL fiber diameter (Figure 5), therefore opening new options for controlled protein delivery. We hypothesize that the variable burst release can be explained primarily using geometrical considerations. For a constant fiber diameter, the likelihood that parts of a protein crystal are located at or very close to the fiber surface positively correlates with crystal size, and therefore, the level of burst release increases with an increasing ratio of crystal size to fiber diameter. By SEM, no crystals or parts of crystals exposed at the fiber surface were found (Figure 1). We therefore assume that burst release originates from lysozyme crystals that are very close to the surface and are covered only with a thin PCL film, allowing fast diffusion of water and dissolved lysozyme. An interesting feature of a drug delivery system composed of protein crystals embedded in non-woven polymer fibers is the ability to vary drug loading within broad margins without affecting relative drug release (Figure 6A–C). Absolute protein release can therefore be directly defined by variation of drug loading. Subsequent lysozyme release was negligible in all cases because of the fact that PCL degradation under *in vitro* release conditions

is very slow in general and further reduced in the case of non-woven scaffolds [34]. Apart from release driven by polymer degradation, solid state diffusion and desorption of encapsulated drugs from nanopores may contribute to the release of protein from PCL scaffolds [30,35]. A classic approach to further improve release under such circumstances is to increase the porosity of the scaffolds by blending with, e.g., low- molecular weight PEG.11 Furthermore, the wettability of PCL/PEG fibers is significantly improved compared to that of pure PCL by addition of PEG (Figure 8). However, up to 10% PEG content, the release profiles were comparable to those of pure PCL fibers. Increasing the PEG content to 20% changed the fiber morphology and resulted in increased release rates within the first 3 weeks (Figures 2D and 7A). In contrast to our findings, a pronounced effect of addition of PEG to PCL fibers containing dissolved/amorphous lysozyme on release rate was found by Li et al., highlighting the profound differences between a drug delivery system within which a molecular dispersion of drug is used and a system representing a coarse drug suspension in a polymer matrix [10]. Finally, PCL/PLGA blends were employed to tailor the release rate. In contrast to simple pore formation as in the case of PEG, the combination of PLGA and PCL was selected to improve release because of the following three effects. First, the PLGA degradation rate is much higher than that of PCL, resulting in an increased overall degradation rate of the polymer blend. Second, PLGA degradation results in the local release of acidic degradation products that may catalyze and hence increase the level of PCL ester hydrolysis [36]. Third, in contrast to PCL, PLGA is known to show significant swelling during release, potentially resulting in weakening of the scaffold structure with improved penetration of the release medium [37]. Water sorption was not affected by the addition of PLGA compared to pure PCL scaffolds (Figure 8). Consequently, improved release as a result of increased wettability of the scaffolds may be excluded. Both PLGA blends showed an increased burst effect compared to pure PCL and significantly increased release rates (Figure 7B). The level of lysozyme degradation was increased during release from PCL/PLGA scaffolds and positively correlated with PLGA

content. PLGA degradation is known to negatively affect protein integrity and stability because of the generation of acidic degradation products [38]. The *in vitro* release setup chosen herein resulting in minimal exchange of release medium at each sampling time point exaggerates the detrimental effects of PLGA degradation. In an *in vivo* setting, a higher fluid exchange rate and, therefore, a reduced level of protein degradation may be assumed. Nevertheless, the PLGA content must be carefully balanced to achieve an appropriate release rate while reducing the level of protein degradation. Despite the improved release of lysozyme from PCL/PLGA compared to pure PCL non-wovens, the morphology remained largely unchanged throughout the release except for pore formation (Figure S4 of the Supporting Information). In summary, our results could pave the way to the controlled release of crystalline proteins embedded in electrospun nonwovens. We have provided evidence that the burst release, wettability, and release rate can be tailored, allowing the specific requirements in various applications of protein-loaded nonwovens to be fulfilled.

## **2.5 Conclusion**

Incorporating crystallized proteins into non-wovens offers numerous possibilities for the delivery of peptides and proteins. Relevant fields of application of non-wovens for controlled protein delivery are the treatment of dermal wounds and localized drug release after surgical interventions, e.g., after tumor excision. We show that protein crystals can successfully be embedded into electrospun non-wovens while preserving protein relative bioactivity. The burst effect could be controlled by a rational combination of fiber diameter, crystal size, and loading. Release rates following burst from pure PCL scaffolds were constant and independent of crystal size, fiber diameter, and loading. The wettability of non-wovens was controlled by addition of a hydrophilic porogen to the PCL matrix, and the release rate was increased at PEG concentrations of 20%. Admixing PLGA to PCL resulted in non-wovens with a tunable release rate achieving an almost linear release over 11 weeks under optimized conditions.

## 2.6 References

- [1] A. Formhals, Apparatus for Producing Artificial Filaments from Material such as Cellulose Acetate, US1975504. (1934).
- [2] A. Formhals, Method and apparatus for spinning, US2158416. (1937).
- [3] A.J. Meinel, O. Germershaus, T. Luhmann, H.P. Merkle, L. Meinel, Electrospun matrices for localized drug delivery: current technologies and selected biomedical applications., *Eur. J. Pharm. Biopharm.* 81 (2012) 1–13. doi:10.1016/j.ejpb.2012.01.016.
- [4] T.K. Dash, V.B. Konkimalla, Poly- $\epsilon$ -caprolactone based formulations for drug delivery and tissue engineering: A review., *J. Control. Release.* 158 (2012) 15–33. doi:10.1016/j.jconrel.2011.09.064.
- [5] a. Cipitria, a. Skelton, T.R. Dargaville, P.D. Dalton, D.W. Hutmacher, Design, fabrication and characterization of PCL electrospun scaffolds—a review, *J. Mater. Chem.* 21 (2011) 9419. doi:10.1039/c0jm04502k.
- [6] D.R. Chen, J.Z. Bei, S.G. Wang, Polycaprolactone microparticles and their biodegradation, 67 (2000) 455–459.
- [7] X. Zong, S. Li, E. Chen, B. Garlick, K. Kim, D. Fang, et al., Prevention of Postsurgery-Induced Abdominal Adhesions by Electrospun Bioabsorbable Nanofibrous Poly(lactide-co-glycolide)-Based Membranes, *Ann. Surg.* 240 (2004) 910–915. doi:10.1097/01.sla.0000143302.48223.7e.
- [8] X. Cao, M.S. Shoichet, Delivering neuroactive molecules from biodegradable microspheres for application in central nervous system disorders, *Biomaterials.* 20 (1999) 329–339. doi:10.1016/S0142-9612(98)00172-0.
- [9] S. Mareschek, A. Greiner, T. Kissel, Electrospun biodegradable nanofiber nonwovens for controlled release of proteins., *J. Control. Release.* 127 (2008) 180–7. doi:10.1016/j.jconrel.2008.01.011.
- [10] Y. Li, H. Jiang, K. Zhu, Encapsulation and controlled release of lysozyme from electrospun poly( $\epsilon$ -caprolactone)/poly(ethylene glycol) non-woven membranes by formation of lysozyme-oleate complexes., *J. Mater. Sci. Mater. Med.* 19 (2008) 827–32. doi:10.1007/s10856-007-3175-6.
- [11] C. Lu, W. Lin, Permeation of Protein from Porous Poly ( $\epsilon$ -caprolactone) Films, 2001 (2002) 220–225. doi:10.1002/jbm.10120.
- [12] B. Shenoy, Y. Wang, W. Shan, A.L. Margolin, Stability of crystalline proteins., *Biotechnol. Bioeng.* 73 (2001) 358–69. <http://www.ncbi.nlm.nih.gov/pubmed/11320506>.
- [13] M.X. Yang, B. Shenoy, M. Disttler, R. Patel, M. McGrath, S. Pechenov, et al., Crystalline monoclonal antibodies for subcutaneous delivery., *Proc. Natl. Acad. Sci. U. S. A.* 100 (2003) 6934–9. doi:10.1073/pnas.1131899100.



- [14] A. a Elkordy, R.T. Forbes, B.W. Barry, Integrity of crystalline lysozyme exceeds that of a spray-dried form., *Int. J. Pharm.* 247 (2002) 79–90. <http://www.ncbi.nlm.nih.gov/pubmed/12429487>.
- [15] S. Pechenov, B. Shenoy, M.X. Yang, S.K. Basu, A.L. Margolin, Injectable controlled release formulations incorporating protein crystals., *J. Control. Release.* 96 (2004) 149–58. doi:10.1016/j.jconrel.2004.01.019.
- [16] C. Müller, J. Ulrich, The dissolution phenomenon of lysozyme crystals, *Cryst. Res. Technol.* 47 (2012) 169–174. doi:10.1002/crat.201100553.
- [17] J.C. Falkner, A.M. Al-somali, J.A. Jamison, J. Zhang, S.L. Adrianse, R.L. Simpson, et al., Generation of Size-Controlled , Submicrometer Protein Crystals, *Chem. Mater.* 13 (2005) 2679–2686.
- [18] V.B. Bueno, D.F.S. Petri, Xanthan hydrogel films: molecular conformation, charge density and protein carriers., *Carbohydr. Polym.* 101 (2014) 897–904. doi:10.1016/j.carbpol.2013.10.039.
- [19] N. Charensriwilaiwat, P. Opanasopit, T. Rojanarata, T. Ngawhirunpat, Lysozyme-loaded, electrospun chitosan-based nanofiber mats for wound healing., *Int. J. Pharm.* 427 (2012) 379–84. doi:10.1016/j.ijpharm.2012.02.010.
- [20] T. Nakatsuji, R.L. Gallo, Antimicrobial peptides: old molecules with new ideas., *J. Invest. Dermatol.* 132 (2012) 887–95. doi:10.1038/jid.2011.387.
- [21] Q.P. Pham, U. Sharma, A.G. Mikos, Electrospun poly(epsilon-caprolactone) microfiber and multilayer nanofiber/microfiber scaffolds: characterization of scaffolds and measurement of cellular infiltration., *Biomacromolecules.* 7 (2006) 2796–805. doi:10.1021/bm060680j.
- [22] Y.H. Liao, M.B. Brown, G.P. Martin, Turbidimetric and HPLC assays for the determination of formulated lysozyme activity., *J. Pharm. Pharmacol.* 53 (2001) 549–54. <http://www.ncbi.nlm.nih.gov/pubmed/11341373>.
- [23] E.W. Washburn, Note on a method of determining the distribution of pore sizes in a porous material, *Phys. Rev.* 7 (1921) 115–116.
- [24] E.W. Washburn, The Dynamics of capillary flow, *Phys. Rev.* 17 (1921).
- [25] Y. Zang, B. Kammerer, M. Eisenkolb, K. Lohr, H. Kiefer, Towards protein crystallization as a process step in downstream processing of therapeutic antibodies: screening and optimization at microbatch scale., *PLoS One.* 6 (2011) e25282. doi:10.1371/journal.pone.0025282.
- [26] D. Hebel, S. Huber, B. Stanislawski, D. Hekmat, Stirred batch crystallization of a therapeutic antibody fragment., *J. Biotechnol.* 166 (2013) 206–11. doi:10.1016/j.jbiotec.2013.05.010.

- [27] M.A. Miller, J.D. Engstrom, B.S. Ludher, K.P. Johnston, Low viscosity highly concentrated injectable nonaqueous suspensions of lysozyme microparticles, 26 (2011) 1067–1074. doi:10.1021/la9023426.Low.
- [28] C. Govardhan, N. Khalaf, C.W. Jung, B. Simeone, A. Higbie, S. Qu, et al., Novel long-acting crystal formulation of human growth hormone., *Pharm. Res.* 22 (2005) 1461–70. doi:10.1007/s11095-005-6021-x.
- [29] A. a Elkordy, R.T. Forbes, B.W. Barry, Stability of crystallised and spray-dried lysozyme., *Int. J. Pharm.* 278 (2004) 209–19. doi:10.1016/j.ijpharm.2004.02.027.
- [30] M. Gandhi, R. Srikar, A.L. Yarin, C.M. Megaridis, R.A. Gemeinhart, Mechanistic Examination of Protein Release from Polymer Nanofibers, *Mol. Pharm.* 6 (2009) 641–647.
- [31] M.R. Williamson, H.-I. Chang, A.G. a Coombes, Gravity spun polycaprolactone fibres: controlling release of a hydrophilic macromolecule (ovalbumin) and a lipophilic drug (progesterone)., *Biomaterials.* 25 (2004) 5053–60. doi:10.1016/j.biomaterials.2004.02.027.
- [32] a. Finkelstein, Local Drug Delivery via a Coronary Stent With Programmable Release Pharmacokinetics, *Circulation.* 107 (2003) 777–784. doi:10.1161/01.CIR.0000050367.65079.71.
- [33] J. Zeng, A. Aigner, F. Czubayko, T. Kissel, J.H. Wendorff, A. Greiner, Poly(vinyl alcohol) nanofibers by electrospinning as a protein delivery system and the retardation of enzyme release by additional polymer coatings., *Biomacromolecules.* 6 (2005) 1484–8. doi:10.1021/bm0492576.
- [34] N. Bolgen, Y.Z. Menciloglu, K. Acatay, I. Vargel, E. Piskin, In vitro and in vivo degradation of non-woven materials made of poly( $\epsilon$ -caprolactone) nanofibers prepared by electrospinning under different conditions, *J. Biomater. Sci. Polym. Ed.* 16 (2005) 1537–1555.
- [35] R. Srikar, a L. Yarin, C.M. Megaridis, a V Bazilevsky, E. Kelley, Desorption-limited mechanism of release from polymer nanofibers., *Langmuir.* 24 (2008) 965–74. doi:10.1021/la702449k.
- [36] G.L. Siparsky, K.J. Voorhees, F. Miao, Hydrolysis of Polylactic Acid ( PLA ) and Polycaprolactone ( PCL ) in Aqueous Acetonitrile Solutions : Autocatalysis, *J. Environ. Polym. Degrad.* 6 (1998).
- [37] M. Shive, J. Anderson, Biodegradation and biocompatibility of PLA and PLGA microspheres., *Adv. Drug Deliv. Rev.* 28 (1997) 5–24. <http://www.ncbi.nlm.nih.gov/pubmed/10837562>.
- [38] G. Crotts, T.G. Park, Protein delivery from poly ( lactic-co-glycolic acid ) biodegradable microspheres : release kinetics and stability issues, *J. Microencapsul.* 15 (1998) 699–713.





### **3 Protein release from electrospun nonwovens: Improving the release characteristics through rational combination of polyester blend matrices with polidocanol**

Sebastian Puhl, David Ilko, Linhao Li, Ulrike Holzgrabe, Lorenz Meinel, Oliver Germershaus

This chapter was originally published in *International Journal of Pharmaceutics* 477 (2014) 273–281,  
[dx.doi.org/10.1016/j.ijpharm.2014.10.047](https://doi.org/10.1016/j.ijpharm.2014.10.047)  
Reprinted with permission from Elsevier (License number 3524390790232)

## **Abstract**

Nonwoven scaffolds consisting of poly- $\epsilon$ -caprolactone (PCL), poly(lactic-*co*-glycolic acid) (PLGA) and polidocanol (PD), and loaded with lysozyme crystals were prepared by electrospinning. The composition of the matrix was varied and the effect of PD content in binary mixtures, and of PD and PLGA content in ternary mixtures regarding processability, fiber morphology, water sorption, swelling and drug release was investigated. Binary PCL/PD blend nonwovens showed a PD-dependent increase in swelling of up to 30% and of lysozyme burst release of up to 45% associated with changes of the fiber morphology. Furthermore, addition of free PD to the release medium resulted in a significant increase of lysozyme burst release from pure PCL nonwovens from approximately 2% to 35%. Using ternary PCL/PD/PLGA blends, matrix degradation could be significantly improved over PCL/PD blends, resulting in a biphasic release of lysozyme with constant release over 9 weeks, followed by constant release with a reduced rate over additional 4 weeks. Based on these results, protein release from PCL scaffolds is improved by blending with PD due to improved lysozyme desorption from the polymer surface and PD-dependent matrix swelling.

### 3.1 Introduction

Nonwovens prepared by electrospinning are extremely versatile scaffolds allowing the controlled and localized delivery of various drugs in a broad variety of applications ranging from tissue engineering to topical gene delivery. The large surface area of electrospun nonwovens, their versatility with regards to attainable structures as well as the large number of biocompatible polymers suitable for electrospinning such as poly- $\epsilon$ -caprolactone (PCL), poly(lactic-*co*-glycolic acid) (PLGA), poly(ethylene glycol) (PEG) or poly(L-lysine) (PLL) constitute the exceptional suitability of nonwoven scaffolds for drug delivery [1,2]. PCL is frequently used as a polymer matrix for various drug delivery applications, including the production of electrospun nonwovens, because of its biodegradability, biocompatibility, advantageous material characteristics such as low glass transition- and melting temperature, and broad solvent compatibility as well as its excellent mechanical properties [3–5]. Moreover, PCL has been used in several FDA approved drug delivery systems and implants, as suture material and adhesion barrier [6]. Despite these advantages, release of hydrophilic, high molecular weight drugs was frequently found to be challenging because of PCLs semicrystalline nature, slow degradation and high hydrophobicity [7,8], requiring copolymerization or blending with hydrophilic polymers or polymers possessing a higher degradation rate such as PLGA [9–12].

In previous studies we observed that the combination of PCL nonwovens and protein crystals allows control of both, amount of burst release as well as long-term release rate through variation of protein crystal – fiber size ratio, degree of loading and polymer matrix composition [12]. However, despite the significant variability achieved through the novel combination of electrospun fibers and protein crystals, the low amount of total released protein and limited control over release rate required further optimization. Furthermore, blending of PCL with PEG and PLGA alone, while in part successful, still resulted in slow and incomplete protein release.

Within this study we explore the mode of protein release from pure and blended PCL matrices containing protein crystals. We hypothesize that besides polymer degradation and drug diffusion, wettability of the nonwoven, swelling of the polymer matrix and desorption play an important role in protein release from nonwoven scaffolds. Therefore, we studied the effect of matrix composition on protein release using electrospun nonwovens consisting of a novel blend of PCL, polidocanol (PD) and PLGA. PD is used in pharmaceutical and cosmetic formulations as an O/W emulsifier and as an active pharmaceutical ingredient for topical therapy, as local anesthetic and antipruritic drug at concentrations between 3 and 8 % m/m, and as sclerosant after injection into varicose veins at concentrations between 0.25 and 3 % m/m. Because of its surface activity and well-established topical application, PD may represent a valuable excipient to improve the material characteristics of PCL nonwovens.

### **3.2 Materials and Methods**

PCL (Mw 70000-90000), chicken egg white lysozyme and trifluoroacetic acid (HPLC grade) were purchased from Sigma-Aldrich (Munich, Germany). Polidocanol (Macrogoli aether laurilicum 9, Ph.Eur. 6.0) was bought from Fagron (Barsbüttel, Germany). Poly(D,L-lactide-co-glycolide) 50:50 (Resomer RG 502H, Mw 7000-17000) was a kind gift from Evonik Industries (Essen, Germany). Acetonitrile (gradient grade) was purchased from VWR Prolabo (Fontenay-sous-Bois, France). Poly(ethylene glycol) 6000 was obtained from MERCK Schuckardt (Hohenbrunn, Germany). Chloroform, ethanol, sodium phosphate, sodium hydroxide, sodium chloride, sodium azide and acetic acid were of analytical grade.

#### **3.2.1 Lysozyme crystallization and crystal size determination**

Lysozyme crystallization was performed according to the method of Falkner et al. [13] with modifications as described before [12]. Lysozyme was dissolved in 100 mM sodium acetate buffer pH 3.5 at a concentration of 8.0 mg/ml. Precipitation buffer consisting of 20 % sodium



chloride, 10 % PEG 6000 and 500 mM sodium acetate at pH 3.5 at 8 °C was poured quickly into the lysozyme solution and stirred at 500 rpm. Mixing ratio of precipitation buffer to lysozyme solution was 2:1. After centrifugation at 3500g for 5 minutes to separate crystals, they were washed twice with ethanol/chloroform (volume ratio 3:10). Finally, crystals were dried over night under mild vacuum. Average particle size of crystals was measured by laser diffraction analysis using ethanol as dispersion medium (LS 230, Beckman Coulter, Brea, CA).

### 3.2.2 PCL electrospinning

Electrospinning was performed using a custom-built apparatus consisting of a DC power supply HCP 140-350000 (FuG Elektronik, Rosenheim, Germany) and a syringe pump (Type 540200, TSE Systems, Bad Homburg, Germany). Nonwovens were produced by electrospinning onto a stationary copper plate using a similar setup as described before [12,14]. Protein crystals were dispersed in ethanol at a concentration of 3.0 mg/ml and homogenized for 20 seconds using an ultrasonic bath (Branson 3200, Branson, Danbury, CT). Subsequently, chloroform and the particular polymers were added. Ethanol and chloroform were mixed in a volume ratio of 1:6. Ratios of polidocanol and PLGA were calculated as dry mass in relationship to PCL (m/m %) and compositions are summarized in **Table 1**. No sedimentation, dissolution or disintegration of the protein crystals was observed during processing in polymer solution. The resulting suspensions were filled into a syringe with an attached gauge 22 metal needle. The needle was centered within a copper ring of 20 cm diameter consisting of copper wire of 2 mm diameter placed in a vertical plane around it and both were connected to the DC power supply and charge was adjusted to 27 kV. The flow rate was set to 10 ml/h and the stationary copper plate was placed at a distance of 40 cm from the needle. The lysozyme crystal loading of the nonwovens was calculated individually. Average loading was  $0.15 \pm 0.04$  % m/m. All data is depicted as results from triplicated experiments and represents the average  $\pm$  standard deviation (SD).

| <b>Name</b>     | <b>PCL [%]</b> | <b>PD [%]</b> | <b>PLGA [%]</b> |
|-----------------|----------------|---------------|-----------------|
| PCL             | 100            | --            | --              |
| PCL/PD2         | 98             | 2             | --              |
| PCL/PD10        | 90             | 10            | --              |
| PCL/PD20        | 80             | 20            | --              |
| PCL/PD50        | 50             | 50            | --              |
| PCL/PD20/PLGA2  | 78             | 20            | 2               |
| PCL/PD20/PLGA10 | 70             | 20            | 10              |

**Table 1:** Compositions of the electrospun nonwovens. All ratios are expressed as % m/m.

### 3.2.3 Morphology and fiber diameter

SEM images were recorded using a JSM-7500F field emission scanning electron microscope (Jeol, Tokyo, Japan) with an acceleration voltage of 2 kV. ImageJ (NIH, Bethesda, MD) was used to determine the fiber diameter. Sixty individual fiber diameters were manually measured vertically to the fiber surface for every preparation. Samples were cut out of the incubated nonwovens and washed with purified water, dried under mild vacuum overnight and studied by SEM using fresh nonwovens as reference.

### 3.2.4 Wettability and sorption rate of the nonwovens

Contact angle measurements were performed using casted films as substitutes for electrospun nonwovens using a drop shape analysis (DSA 10, Krüss GmbH, Hamburg, Germany). Films were used instead of nonwovens to avoid bias by variable capillarity and uneven surfaces, respectively. Polymer blends were coated on a glass microscope slide and allowed to dry under ambient conditions. A drop of release medium was placed on the polymer films and contact angle was measured over time.

Sorption of PBS release medium into capillaries of the nonwovens was determined similar as described before [12]. According to the Washburn theory the sorption rate is correlated to contact angle and wettability of a nonwoven [15].

$$t = A \cdot m^2 \quad (1)$$

$$A = \frac{\eta}{c \cdot \rho^2 \cdot \sigma \cdot \cos\theta} \quad (2)$$

$$\frac{m^2}{t} = \frac{c \cdot \rho^2 \cdot \sigma \cdot \cos\theta}{\eta} \quad (3)$$

where  $m$  is the sorbed mass of water,  $\eta$  is the viscosity of the immersion liquid,  $c$  is the capillarity of the sample,  $\rho$  is the density of the immersion liquid,  $\sigma$  is the surface tension of the immersion liquid, and  $\theta$  is the contact angle between immersion liquid and nonwoven. Briefly, for each nonwoven composition the short side of a sample with the size of 9 mm x 36 mm was dipped 0.1 mm deep into the release medium using a tensiometer (K12, Krüss GmbH, Hamburg, Germany). Mass increase per area nonwoven over time was recorded and depicted as the sorption rate expressed as ( $\mu\text{g/s}/\text{mm}^2$ ).

### 3.2.5 Swelling of polymer blends

Swelling of the polymer blends was investigated similar as described before [16]. Films of the same compositions as those of nonwovens were used to avoid any bias from variability of the capillarity of nonwovens. Films of all the respective polymer-compositions were casted on a glass plate, dried at room temperature and weighed. Masses ranged from 150 to 350 mg and films were approximately 1 mm thick with a diameter of approximately 15 mm. The films were then immersed into 4 ml of PBS and incubated for 24 h at 37 °C. Subsequently, the polymer films were dried on the outside with a paper towel and weighed. Since PD was known to leach from the polymer films resulting in substantial mass loss, samples were dried at RT for 72 hours and weighed again to determine the absolute amount of water absorbed. Swelling is expressed as the swelling ratio  $Q_m$  according to equation 4.

$$Q_m = \frac{W_s - W_d}{W_d} \quad (4)$$

$W_s$  and  $W_d$  represent the weight of the sample after swelling and the weight of the sample after drying for 72 hours, respectively.

### **3.2.6 Differential scanning calorimetry**

Differential scanning calorimetry (DSC) analysis was performed using a DSC 8000 (Perkin Elmer, Waltham, MA). Electrospun samples of approximately 3 mg were accurately weighed into aluminum pans and heated twice in a cycle from -50 °C to 150 °C with a heating rate of 20 K/min. For analysis the second heating step was used.

### **3.2.7 In vitro release**

Potential residual solvents in the nonwovens after preparation were removed by storage at reduced pressure over night. Afterwards, the nonwovens were weighed (approx. 150-300 mg) and cut into smaller pieces. For release studies they were placed into 4.0 ml PBS, pH 7.4 with 0.1 % sodium azide at 37 °C. Sink conditions both for lysozyme and PD were guaranteed at all times. At defined time points, 250  $\mu$ l of the release medium were sampled and replaced by the same volume of fresh buffer. In additional experiments, free PD at a concentration of 0.112 mg/ml, 15 mg/ml or 45 mg/ml was added to the release medium prior to incubation of pure PCL nonwovens and 0.112 mg/ml of free PD was added to the medium prior to incubation of PCL/PD50 nonwovens. The concentrations were chosen as follows: 0.112 mg/ml equals twice the critical micelle concentration (CMC), a concentration of 15 mg/ml PD was found after incubating PCL/PD20 nonwovens, and a concentration of 45 mg/ml PD was found after incubation of PCL/PD50 nonwovens. These additional release experiments were performed to decipher the role of PD during lysozyme release. Lysozyme concentrations were determined using RP-HPLC as described before [12].

Polidocanol concentration was measured using an Agilent 1100 LC system (Waldbronn, Germany) equipped with a binary pump, an online degasser and a thermostated column

compartment. For detection a charged aerosol detector (Corona<sup>®</sup> CAD, Thermo Scientific, Idstein, Germany) was used because of the lack of chromophores in PD (Ilko et al., 2014). The gas inlet pressure (nitrogen) was 35 psi, the filter was set to “none” and the range to 100 pA. The optimized method used a Kinetex C18 (100 x 3.0 mm, 2.6  $\mu$ m particle size) analytical column from Phenomenex (Aschaffenburg, Germany). The column compartment was maintained at 40 °C. The mobile phase consisted of water-acetonitrile (15:85, V/V) at a flow rate of 0.6 ml/min. The injection volume was 10  $\mu$ l. Samples were diluted with mobile phase to give a PD concentration of about 10 to 100  $\mu$ g/ml. Quantification was done by establishing a five point calibration curve over a range from 5 to 150  $\mu$ g/ml and log-log transformation of concentration and peak area. Limit of quantification was determined at 0.86  $\mu$ g/ml of PD.

### **3.2.8 Relative bioactivity of lysozyme**

Relative bioactivity was determined using *Micrococcus lysodeikticus* cell wall preparation as described before [17,18]. Briefly, bacteria were suspended in 1.0 ml of a 0.1 M  $\text{KH}_2\text{PO}_4$ , pH 6.2 at a concentration of 200 mg/l. Then 33.3 $\mu$ l of the sample solution was added and stirred for 5 seconds. The subsequent decline of absorbance at 570 nm was recorded for 3 minutes using a UV-spectrophotometer (Genesys 10S, Thermo Scientific, Rockford, IL). The slope of the decline was proportional to lysozyme bioactivity and the limit of quantification was found to be 0.96  $\mu$ g/ml lysozyme. Bioactivity of the individual samples was determined using a calibration curve constructed using fresh lysozyme. Relative biological activity of lysozyme is expressed in reference to the lysozyme amount as determined by HPLC.

### **3.2.9 Statistical analysis**

All data are reported as mean  $\pm$  standard deviation of at least three independent experiments unless specified otherwise. Statistical significance was calculated by one-way ANOVA using

multiple comparisons by the Holm-Sidak method for comparison of multiple groups with an overall significance level of 0.05 (Origin Pro, Northampton, MA).

### 3.3 Results

#### 3.3.1 Morphology of nonwovens

Nonwovens were generated from PCL or blends using electrospinning as established before [12]. Blending of PCL or PCL/PLGA with PD had no negative impact on processability within the investigated PD concentration range and required no adaption of the pre-established electrospinning parameters. As shown before, processing of lysozyme crystals in organic solvents during electrospinning did not negatively affect lysozyme bioactivity or crystal morphology and the high viscosities of polymer solutions prevented sedimentation of lysozyme crystals during processing [12]. Narrow fiber diameter distributions were obtained for all preparations except for PCL/PD20/PLGA10 nonwovens (**Figure 1 F and G**). Fiber diameters of the nonwovens were found to be reproducible between individual experiments. Overall, SEM micrographs revealed reduction of fiber surface roughness and separation between fibers with increasing PD ratio (**Figure 1 A-D**). Nonwovens prepared from ternary blends containing PCL, PLGA and PD had an average fiber diameter of  $4.2 \pm 2.7 \mu\text{m}$  (PCL/PD20/PLGA2) and  $6.5 \pm 11.1 \mu\text{m}$  (PCL/PD20/PLGA10). With both blends a less homogenous distribution of fiber diameters was observed with an apparently bimodal distribution in the case of PCL/PD20/PLGA2 and the presence of large beads in the case of PCL/PD20/PLGA10 (**Figure 1 E and F**).

After incubation of PCL/PD nonwovens in release medium, fiber diameters were virtually unchanged but the fiber surface roughness appeared to be increased with noticeable wrinkles and indentations (**Figure 1 G and Figure 2 A-D**). The surface roughness after incubation seemed to positively correlate with PD content as assessed by SEM. No further changes of fiber morphology were detected after the first 6 hours of incubation (data not shown).

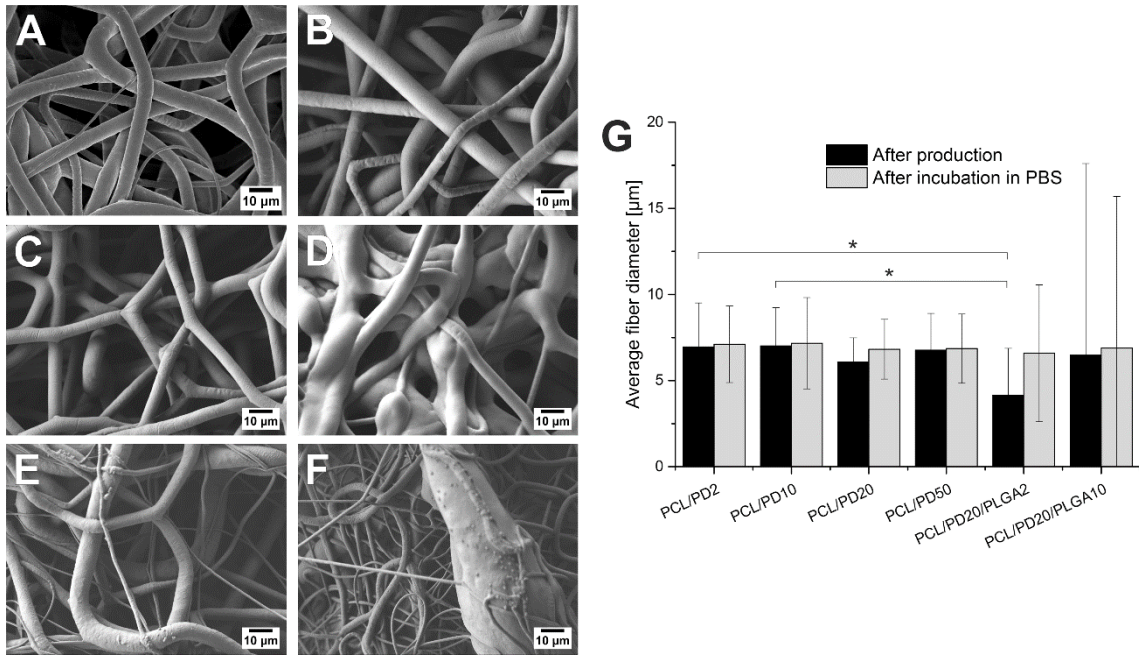


**Figure 1:** Morphology and fiber diameter of electrospun nonwovens: PCL/PD2 (A), PCL/PD10 (B), PCL/PD20 (C), PCL/PD50 (D), PCL/PD20/PLGA2 (E), PCL/PD20/PLGA10 (F), and average fiber diameter of the dried electrospun nonwovens before and after incubation in release medium for 8 weeks (G).

Similar patterns were found after incubation of nonwovens containing 20 % PD and 2 % or 10 % PLGA (**Figure 2 E and F**). Surface morphology of both preparations was quite comparable to nonwovens consisting of PCL and 20 % PD only, after incubation for 6 hours. After an extended incubation of 9 weeks, PCL/PD20/PLGA10 nonwovens showed signs of fiber degradation in the form of cracks and fractures but fiber diameter remained virtually unchanged (**Figure 2 G and H**).

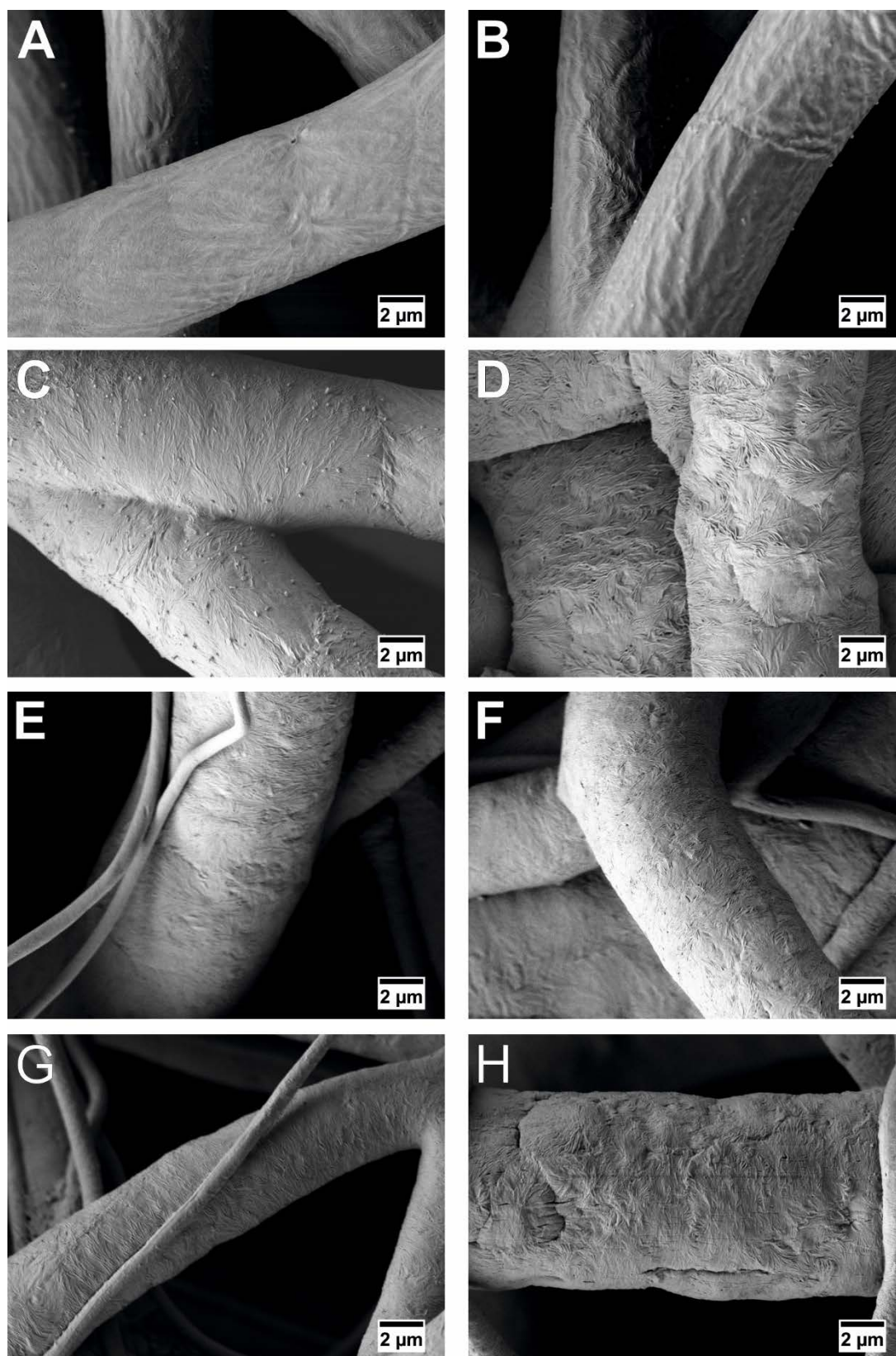


**Figure 2.** Morphology of nonwovens after incubation in release medium for 1 day: PCL/PD2 (A), PCL/PD10 (B), PCL/PD20 (C), PCL/PD50 (D), PCL/PD20/PLGA2 (E), PCL/PD20/PLGA10 (F). Morphology of formulations containing PLGA after 8 weeks of incubation in release medium: PCL/PD20/PLGA2 (G), and PCL/PD20/PLGA10 (H).



### 3.3.2 Differential scanning calorimetry

Melting points of PCL and PD were determined by DSC with 59.6 °C and 23.8 °C, respectively, being in good agreement with previously reported results [19,20]. Glass transition point of PLGA was observed at 44.4 °C (**Figure 3 A**) [21]. PCL/PD blends showed a decreasing melting temperature with increasing PD content (**Figure 3 B**). Below 10 % PD, neither glass transition nor melting of PD was detected, while above 10 % PD glass transition but no melting of PD was observed. At 50 % PD both, glass transition and melting of PD were detected. Both ternary blend formulations additionally showed glass transition of PLGA between 50 and 60 °C, however not clearly separated from melting of PCL.

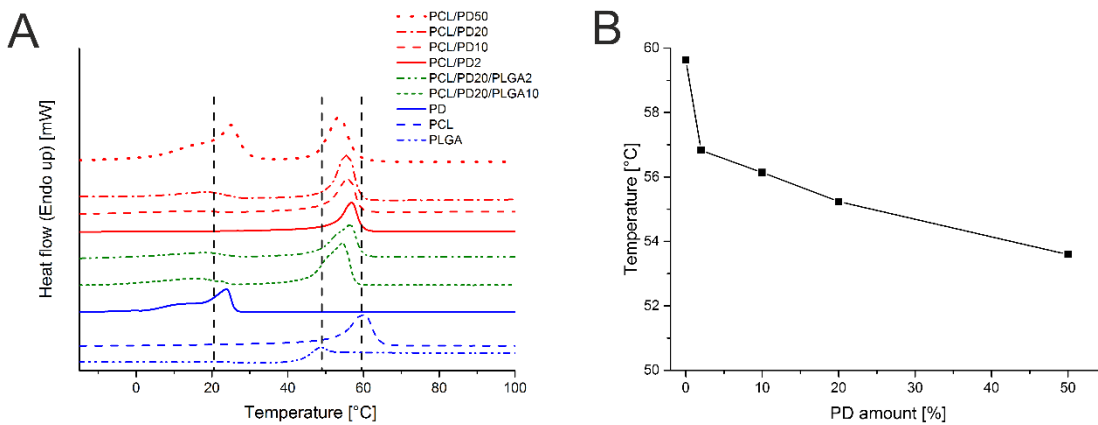


**Figure 3:** DSC analysis of pure polymers and electrospun polymer blends (A). Vertical lines represent the melting respectively glass transition point of the pure polymers. Effect of PD content on melting temperature of PCL/PD nonwovens (B).

### 3.3.3 Contact angle, sorption rate and swelling behavior

The contact angle of PBS with pure PCL films was found to be  $85.3 \pm 4.9^\circ$ . Because of the surface activity of PD, contact angles were considerably reduced for films containing PD and fast spreading of the drop complicated analysis. A significant reduction of the contact angle to  $72.6 \pm 4.9^\circ$  was observed in the case of samples containing 2 % PD. For samples containing higher percentages of PD, contact angles could not be determined because of fast spreading of the liquid on the surface and thus were considered to be  $0^\circ$ .

In addition, sorption of incubation medium to nonwovens was investigated (**Figure 4 A**). The sorption rate is influenced by the contact angle as well as the capillarity of the nonwovens and thus may describe the initial contact of release medium with nonwovens and the general wettability of nonwovens [15]. Interestingly, sorption of PBS into the nonwovens was found to decrease with increasing PD concentration. With nonwovens containing 50 % PD sorption was not completed within the timeframe of wicking experiments, signified by PBS sorption only within the first 5 mm of the total 36 mm length of the sample. Addition of PLGA resulted in a significant increase of the sorption rate compared to nonwovens containing PCL and PD alone. The swelling of pure PCL films was found to be negligible (**Figure 4 B**). However, with increasing PD content in the polymer films the swelling ratio increased linearly ( $R^2 = 0.995$ ) and the correlation between PD content and swelling ratio was found to be statistically significant ( $p < 0.0001$ ). Addition of PLGA had no statistically significant effect on swelling within the investigated time frame of 24 h, i.e. swelling was comparable to PCL/PD nonwovens with the same PD content. Incubation of pure PCL films with 15 mg/ml PD in the release medium resulted in a small but significant increase of swelling ( $0.73 \pm 0.14$  %) compared to pure PCL films without addition of PD ( $0.46 \pm 0.003$  %).

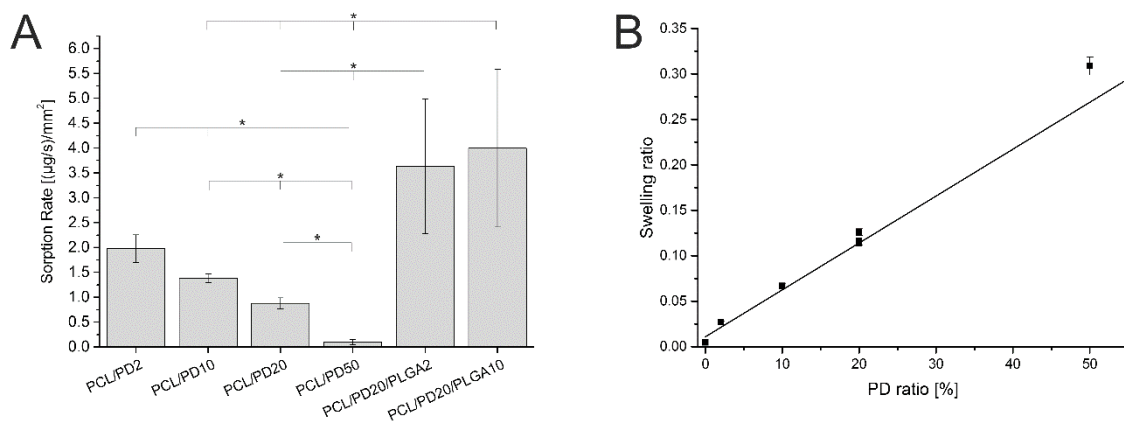


**Figure 4:** Effect of nonwoven composition on sorption of PBS (A) and on swelling of PCL/PD and PCL/PD/PLGA films (B).

### 3.3.4 Polidocanol release

Maximum PD concentrations were reached after incubation for approx. 1 hour in release medium for all nonwovens (**Figure 5**). Relative PD release depended on the PD content of nonwovens, generally increasing with increasing PD content. However, at high PD content of 50 % PD/PCL only  $80.5 \pm 5.7$  % of PD contained in the nonwovens was released.

Addition of free PD to the release medium prior to incubation of pure PCL nonwovens revealed that PD adsorbed to the nonwovens, resulting in a drop of free PD concentration in the medium from  $112 \mu\text{g/ml}$  to  $12.9 \pm 3.1 \mu\text{g/ml}$ . However, at higher free PD concentration of 15 or 45 mg/ml in release medium no drop of the PD concentration after addition of the nonwovens was observed, most likely because of the limited amount of PD absorbed being not detectable at high total concentration.

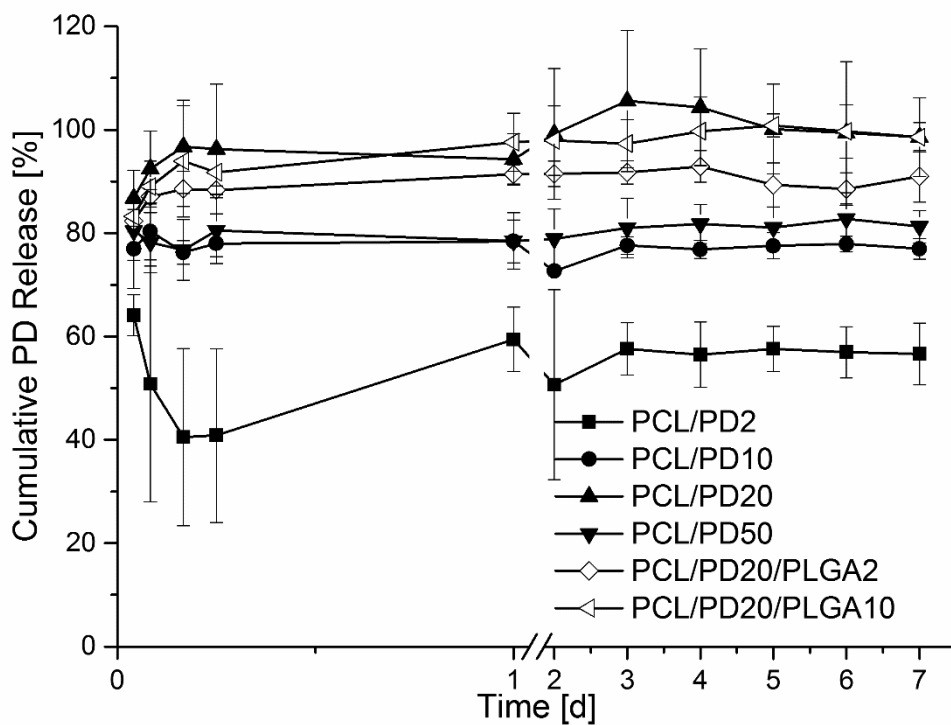


**Figure 5:** Cumulative release of polidocanol from nonwovens prepared from PCL/PD or PCL/PD/PLGA blends.

### 3.3.5 Lysozyme release

Lysozyme release from pure PCL fibers was found to be low with  $1.98 \pm 0.5$  % and  $8.5 \pm 1.1$  % of total encapsulated protein released after 1 day and 3 weeks, respectively (**Figure 6 A**). Hence, under these conditions, very low burst release and a very low release rate was found. A PD concentration dependent increase of burst release was obtained using binary mixtures of PCL and PD, with higher PD content in the nonwoven resulting in higher burst release of up to  $45.4 \pm 1.5$ % at 50 % PD after 1 day incubation (**Figure 6 A**). Similarly, lysozyme burst release from nonwovens consisting of PCL, 20 % PD and 2 % or 10 % PLGA, respectively, was significantly increased compared to pure PCL nonwovens (**Figure 6 B**). However, compared to nonwovens consisting of the binary blend PCL/PD20, burst release from ternary blend nonwovens was significantly lower ( $17.5$  % for PCL/PD20 versus approximately 10% for PCL, PCL/PD20/PLGA2 or PCL/PD20/PGLA10). The release rate from nonwovens produced from binary mixtures of PCL/PD was negligible after burst and comparable to the one from ternary mixtures (PCL/PD/PLGA) within the first week of release. Solely PCL/PD50 nonwovens showed a slow release up to 7 days. Subsequently, only nonwovens containing PLGA showed an accelerated release, which was more pronounced with higher PLGA content, achieving an almost constant release rate. With 10 % PLGA (PCL/PD20/PLGA10)  $42.8 \pm 1.5$  % of encapsulated lysozyme was released after 4 weeks. Subsequently, lysozyme concentration decreased in the case of the PCL/PD20/PLGA10 nonwovens because of PLGA degradation products resulting in a pH drop in the release buffer from 7.4 to 3.3 and inducing protein degradation. This effect was a direct result of the setup chosen for release studies. The volume of release medium withdrawn for analysis and replaced by fresh release medium at each time point was small compared to the total volume of release medium, resulting in accumulation of both released lysozyme and PLGA degradation products in the release buffer. Nonwovens containing 2 % PLGA showed an almost linear release of lysozyme from week 2 until week 9 resulting in cumulative release of  $43.6 \pm 2.7$  % after 9 weeks. Thereafter, lysozyme release rate

dropped considerably and was almost constant during the following 4 weeks. The pH of the release buffer at the end of the incubation was 5.2.

The effect of the presence of PD in the release medium was investigated by adding free PD to the release medium before incubation of the nonwovens. Addition of 0.112 mg/ml PD (approximately twice the CMC of PD) to the release medium prior to incubation of pure PCL nonwovens led to a significant increase of lysozyme burst release after 1 day incubation from  $1.98 \pm 0.54\%$  without PD in the release medium to  $24.5 \pm 2.52\%$  (**Figure 6 C**). Addition of 15 mg/ml PD (equal to the PD concentration after release from PCL/PD20 nonwoven) and 45 mg/ml (equal to the PD concentration after release from PCL/PD50 nonwoven) resulted in further increased burst release, most prominently at the higher PD concentration (**Figure 6 C**). Addition of 0.112 mg/ml PD to the release medium prior of incubation of PCL/PD50 nonwovens resulted in increased burst release compared to the same nonwovens incubated without PD addition to the release medium (**Figure 6 D**).

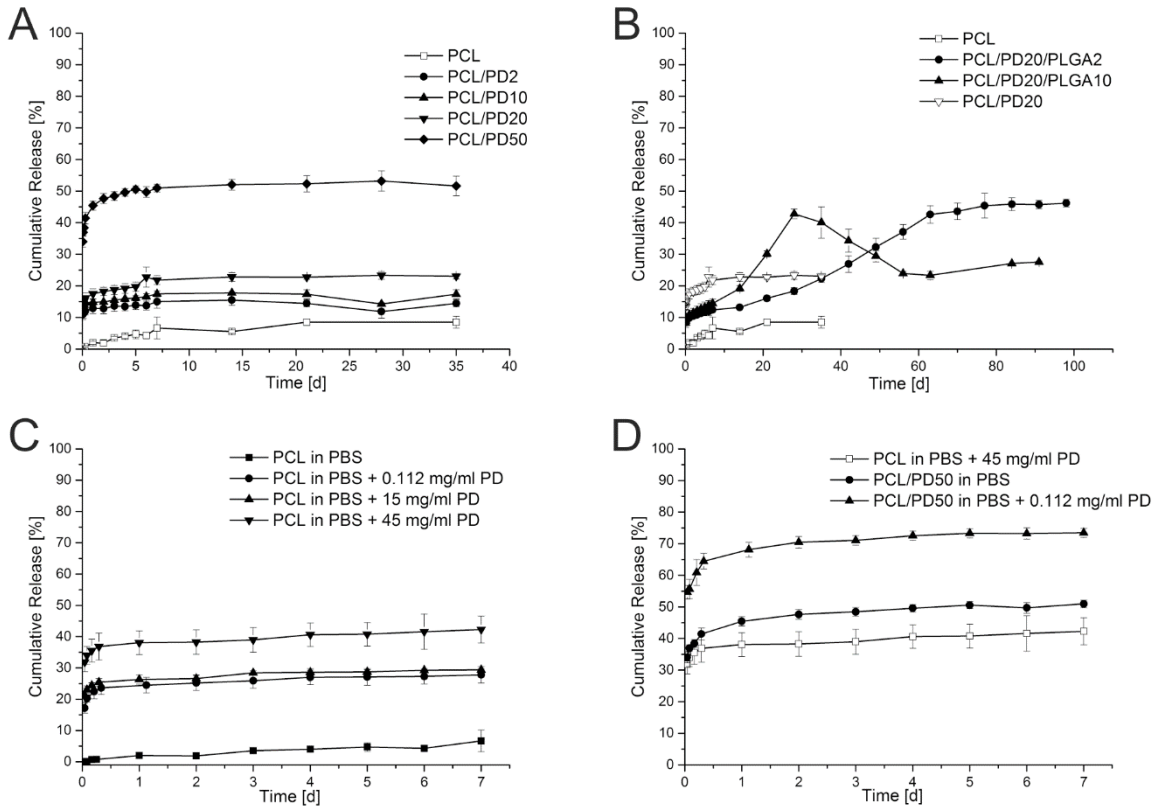


**Figure 6:** Effect of nonwoven composition and addition of PD into release medium prior to incubation of the nonwovens on cumulative lysozyme release. The effect of PD content in PCL/PD blend nonwovens (A), PLGA content in PCL/PD/PLGA blend nonwovens (B), concentration of free PD in the release medium in combination with nonwovens of pure PCL (C), and concentration of free PD in combination with PCL/PD blend nonwoven (D) on lysozyme release is shown.

### 3.3.6 Bioactivity

Lysozyme retained its biological activity after electrospinning including after suspending in the respective organic solvents [12]. Moreover, bioactivity was investigated throughout the release study. After 5 weeks incubation, bioactivity was mostly retained for all nonwoven compositions (average of all samples  $104.9 \pm 13.0$  %). Release from nonwovens containing PLGA was investigated for 13 weeks and biological activity was determined until the end of incubation. Relative bioactivity was strongly reduced to  $53.7 \pm 18.9$  % after 13 weeks release from nonwovens containing 10% PLGA. In contrast, relative bioactivity of lysozyme after release from nonwovens containing 2 % PLGA activity was found to be  $108.9 \pm 10.7$  % (**Table 2**).

| Sample               | Time     | Bioactive Lysozyme [%] |
|----------------------|----------|------------------------|
| 2 % PD               | 5 weeks  | 102.4 ± 9.6            |
| 10 % PD              | 5 weeks  | 110.3 ± 14.7           |
| 20 % PD              | 5 weeks  | 106.1 ± 8.6            |
| 50 % PD              | 5 weeks  | 88.9 ± 18.0            |
| 20 % PD<br>2 % PLGA  | 5 weeks  | 112.9 ± 7.0            |
|                      | 9 weeks  | 105.1 ± 3.2            |
|                      | 13 weeks | 108.9 ± 10.7           |
| 20 % PD<br>10 % PLGA | 5 weeks  | 109.2 ± 10.9           |
|                      | 9 weeks  | 100.7 ± 46.6           |
|                      | 13 weeks | 53.7 ± 18.9            |

**Table 2:** Relative bioactivity of released lysozyme determined at selected time points during the release study.

### 3.4 Discussion

With its broad solvent compatibility, high structural stability and optimal processability by electrospinning, PCL offers numerous advantages as a polymer matrix for electrospun drug delivery systems. PCL on the other hand is a semicrystalline, hydrophobic and slowly degrading polymer, resulting in significant challenges, most notably related to drug release, when applied as a polymer matrix for the delivery of large, hydrophilic drugs [7]. Therefore, PCL based copolymers or blends are needed that maintain most of the advantageous properties of PCL, most importantly its superior processability, while improving the release of large, hydrophilic drugs from the scaffold [22,23]. We have recently shown that the encapsulation of protein crystals into electrospun nonwovens is a promising new approach towards protein delivery from

nonwovens in terms of processing, loading capacity and control over burst and long-term release [12]. We herein apply this novel strategy and investigate the physicochemical properties and release characteristics of nonwoven blends composed of PCL, PLGA and PD in an attempt to identify compositions that improve the release of lysozyme.

Electrospinning of PCL/PD blends was straightforward up to a PD content of 50 %. Characterization of the morphology of nonwovens by SEM revealed that fiber surface roughness and the separation between fibers decreased with increasing PD content (**Figure 1 A-D**). Analysis of the melting points of PCL/PD blends by DSC on the one hand showed that homogeneous mixtures were obtained up to a PD content of approximately 20 %. Above this point a separate melting peak of PD was observed, which may be attributed to partial phase separation of PCL and PD (**Figure 3**). On the other hand, an increase of the PD content resulted in melting point depression of PCL, i.e. PD acted as a plasticizer in the PD/PCL blends. Therefore, the morphological changes observed by SEM with increasing PD content can be attributed to the melting point depression of PCL/PD blends and, above 20 % PD, phase separation, potentially leading to coating of the fiber surface with PD. The fiber morphology was distinctly different prior and after incubation for 1 day in the release medium. After incubation, the fiber surface showed wrinkles and indentations, which appeared to increase with increasing PD content (**Figure 2 A-F**). These structural changes after incubation are interpreted as a result of matrix swelling during incubation in release medium (**Figure 4 B**) followed by shrinking during drying of the nonwovens prior to SEM imaging on the one hand and PD leaching from the fibers on the other hand.

The water sorption into capillaries of the nonwovens was investigated to estimate their overall wettability. Surprisingly, water sorption decreased with increasing PD ratios, which was in contrast to the significantly decreasing contact angles. Examination of the swelling behavior of the polymer compositions revealed a linear increase of swelling ratios with increasing PD concentrations. Swelling takes place inside each fiber while sorption takes place in capillaries



between the fibers of the nonwovens. With increasing fiber diameters due to swelling, capillarity of the nonwovens is reduced. According to the Washburn Theory the sorption rate is inversely proportional to the capillarity explaining the decrease of water sorption while wettability increases.

PD release from nonwovens occurred within the first hour of incubation in all cases (**Figure 5**). Furthermore, relative PD release increased with increasing PD content up to PCL/PD20. The low molecular weight and hydrophilicity of PD leads to immediate dissolution of solvent-accessible PD. The fraction of solvent-accessible PD increases with increasing PD content because of a) geometrical consideration similar to the release of lysozyme at increasing lysozyme loading [12] and b) increased swelling of the matrix (**Figure 4 B**), resulting in improved water penetration into the polymer matrix [24,25]. However, at a higher PD content of 50 % (PCL/PD50) relative release was reduced to  $80.5 \pm 5.7$  % compared to almost complete release observed with PCL/PD20. Considering the results of SEM and DSC analysis, where partial phase separation was identified above a PD content of 20% (**Figures 1 A-D and Figure 3**), we conclude that with PCL/PD50 no further increase of water penetration into the polymer matrix was achieved resulting in reduction of relative release of PD. Moreover, increased swelling may partly bind PD in a gel composed of PCL, PD and water.

Apart from its release from the nonwoven matrix, PD also adsorbs to the PCL surface, though a relatively low amount is required to saturate the latter. When incubating pure PCL nonwovens in release medium containing 0.112 mg/ml of free PD, the concentration of free PD decreased to about a tenth of initial concentrations. Incubating pure PCL nonwovens in release media with higher free PD concentrations did not lead to higher adsorption, or the adsorbed amount was not detectable in relation to the high concentration of free PD.

Lysozyme burst release from PCL/PD scaffolds increased with increasing PD content. In addition, close evaluation of the initial phase of lysozyme release revealed a gradual change of release profile with increasing PD content (**Figure 6 A**). To explain these observations a release

model based on a) PD-induced desorption of lysozyme from the polymer matrix and b) increased matrix swelling with increasing PD content and thus a diffusion controlled mechanism is proposed [25,26]. Recently, Srikar et al. reported a model describing the release of hydrophilic drugs from electrospun, slowly degrading polymer matrices [27]. Within this model it is assumed that drug release is primarily controlled by drug desorption from nanopores and from the polymer surface. Furthermore, the model assumes that only drug present at the surface can be released, whereas encapsulated drug is not or only very slowly released. Based on this model, both, increasing the solvent accessible fraction of lysozyme and improving desorption of lysozyme from the polymer surface would result in increased release [28]. The rapid release of PD from the nonwovens (**Figure 5**) results in morphological changes of the fiber structure, signified by formation of wrinkles and indentations as observed by SEM (**Figure 2 A-F**). The observed structural changes are a consequence of swelling of the polymer matrix, as discussed above, resulting in an increased solvent accessible surface. Increasing the PD content therefore resulted in increased lysozyme burst release. Furthermore, PD efficiently adsorbs to the PCL surface (see above), displacing and releasing lysozyme from the scaffold. Addition of PD to the release medium during release of lysozyme from pure PCL nonwovens confirmed the assumed desorption-controlled release mechanism resulting in increased burst release while the subsequent release rate was unaffected (**Figure 6 C**).

On the other hand, swelling of the polymer matrix is assumed to increase diffusion distance and potentially tortuosity, resulting in slower lysozyme release [29]. According to Higuchi's law, solubility within the polymer matrix is substantial for a diffusional release [30]. In a study by Li et al. release of lysozyme from PCL nonwovens was successfully increased through formation of lysozyme-oleate complexes, improving the solubility of the drug in the polymer matrix, as well as blending with PEG to enhance the wettability of the polymer matrix [31]. Because of the poor solubility of lysozyme in the polymer matrix, pure PCL and PCL/PD blends with low PD content showed little diffusional release of the protein. With increasing PD ratios

swelling and thus water uptake into the polymer matrix was increased, thus allowing diffusional release. Consequently, we observed increasing diffusional release characteristics with increasing PD content, most prominently in the case of PCL/PD50 nonwovens showing a release up to 7 days (**Figure 6 A**). When incubating the PCL/PD blend nonwovens in release medium supplemented with PD, burst release was increased significantly but release profile was almost unaffected (**Figure 6 D**). This observation is attributed to increased desorption of lysozyme prior to swelling of the matrix with PD present in the release medium.

Despite the achieved improvements of lysozyme desorption and solvent accessible surface through blending of PCL with PD, the low degradation rate of PCL limited drug release subsequent to the initial burst. Through generation of nonwovens consisting of PCL, PD and PLGA, degradability of the polymer matrix is significantly improved as shown before [12]. Matrix swelling and improved drug desorption induced by PD proved to be effective also with the ternary blend (**Figure 4 B**). Consequently we identified three release mechanisms: desorption, diffusion and matrix degradation while the latter added a significant increase of overall protein release. Furthermore, sorption of release medium to nonwovens was improved compared to PCL/PD nonwovens, most likely because of increased capillarity of nonwovens resulting from broader fiber diameter distributions (**Figure 1 E-G**).

In summary, the rational combination of PCL, serving as slowly biodegradable, structurally stable component, PLGA, which improves polymer matrix degradability and PD inducing matrix swelling and drug desorption led to marked improvement of lysozyme release. The improved release of hydrophilic drugs from PCL or PCL/PLGA matrices achieved by using PD as matrix component and the identification of the release mechanism for such scaffolds may significantly improve the utilization of PCL nonwovens for topical drug delivery and tissue engineering. Furthermore, PD's ability to improve drug release from polymer matrices is according to our knowledge described for the first time herein.

Although the goal of incorporation of PD into fibers was to improve lysozyme release, pharmacological activity of PD is to be expected from all nonwoven preparations since minimum effective concentrations for topical application are reached. In the case of topical application of nonwoven scaffolds as wound dressings, pharmacologic activity of PD might be considered beneficial. However, potential side effects should be considered as well.

Future research might harness the concept of improved matrix swelling and improved desorption by addition of surfactants as a guiding principle for the design of polyester based drug delivery systems. PD proved to be an effective excipient with regards to this concept, however its pharmacological activity might limit its use. Therefore, future research might focus on finding alternative surfactants without pharmacologic activity that improve swelling and drug desorption from polyester matrices.

### **3.5 Conclusion**

Novel PCL/PD and PCL/PD/PLGA blend nonwovens with encapsulated lysozyme crystals were characterized with regards to physical properties and lysozyme release. Blending of PCL and PD resulted in reduction of the contact angle and increased swelling depending on PD content. Ternary blends of PCL, PD and PLGA showed similar properties to PCL/PD nonwovens. The total fraction of lysozyme released from PCL/PD nonwovens increased with increasing PD content and addition of PLGA to PCL/PD blends resulted in controlled release over up to 13 weeks with cumulative release of up to approximately 50 % of encapsulated lysozyme. Lysozyme release was shown to depend on both matrix swelling and desorption, which both is facilitated by PD. Addition of PLGA lead to a concentration dependent augmentation of matrix degradation resulting in controlled release of lysozyme.

### 3.6 References

- [1] A.J. Meinel, O. Germershaus, T. Luhmann, H.P. Merkle, L. Meinel, Electrospun matrices for localized drug delivery: current technologies and selected biomedical applications., *Eur. J. Pharm. Biopharm.* 81 (2012) 1–13. doi:10.1016/j.ejpb.2012.01.016.
- [2] J.H. Wendorff, S. Agarwal, A. Greiner, *Electrospinning: Materials, Processing, and Applications*, Wiley-VCH, Weinheim, Germany, 2012.
- [3] a. Cipitria, a. Skelton, T.R. Dargaville, P.D. Dalton, D.W. Hutmacher, Design, fabrication and characterization of PCL electrospun scaffolds—a review, *J. Mater. Chem.* 21 (2011) 9419. doi:10.1039/c0jm04502k.
- [4] T.K. Dash, V.B. Konkimalla, Poly- $\epsilon$ -caprolactone based formulations for drug delivery and tissue engineering: A review., *J. Control. Release.* 158 (2012) 15–33. doi:10.1016/j.jconrel.2011.09.064.
- [5] X. Qin, D. Wu, Effect of different solvents on poly(caprolactone) (PCL) electrospun nonwoven membranes, *J. Therm. Anal. Calorim.* 107 (2011) 1007–1013. doi:10.1007/s10973-011-1640-4.
- [6] P. a Gunatillake, R. Adhikari, Biodegradable synthetic polymers for tissue engineering., *Eur. Cell. Mater.* 5 (2003) 1–16; discussion 16. <http://www.ncbi.nlm.nih.gov/pubmed/14562275>.
- [7] D.R. Chen, J.Z. Bei, S.G. Wang, Polycaprolactone microparticles and their biodegradation, 67 (2000) 455–459.
- [8] X. Wang, Y. Wang, K. Wei, N. Zhao, S. Zhang, J. Chen, Drug distribution within poly( $\epsilon$ -caprolactone) microspheres and in vitro release, *J. Mater. Process. Technol.* 209 (2009) 348–354. doi:10.1016/j.jmatprotec.2008.02.004.
- [9] M. Shive, J. Anderson, Biodegradation and biocompatibility of PLA and PLGA microspheres., *Adv. Drug Deliv. Rev.* 28 (1997) 5–24. <http://www.ncbi.nlm.nih.gov/pubmed/10837562>.
- [10] T. Briggs, T.L. Arinzeh, Examining the formulation of emulsion electrospinning for improving the release of bioactive proteins from electrospun fibers., *J. Biomed. Mater. Res. A.* 102 (2014) 674–84. doi:10.1002/jbm.a.34730.
- [11] Y. Liu, H. Jiang, Y. Li, K. Zhu, Control of Dimensional Stability and Degradation Rate in Electrospun Composite Scaffolds Composed of Poly(D,L-lactide-co-glycolide) and Poly(epsilon-caprolactone), 26 (2008) 63–71.
- [12] S. Puhl, L. Li, L. Meinel, O. Germershaus, Controlled Protein Delivery from Electrospun Non-wovens: Novel Combination of Protein Crystals and Biodegradable Release Matrix., *Mol. Pharm.* 11 (2014) 2372–2380. doi:10.1021/mp5001026.

- [13] J.C. Falkner, A.M. Al-somali, J.A. Jamison, J. Zhang, S.L. Adrianse, R.L. Simpson, et al., Generation of Size-Controlled, Submicrometer Protein Crystals, *Chem. Mater.* 13 (2005) 2679–2686.
- [14] Q.P. Pham, U. Sharma, A.G. Mikos, Electrospun poly(epsilon-caprolactone) microfiber and multilayer nanofiber/microfiber scaffolds: characterization of scaffolds and measurement of cellular infiltration., *Biomacromolecules.* 7 (2006) 2796–805. doi:10.1021/bm060680j.
- [15] E.W. Washburn, The Dynamics of capillary flow, *Phys. Rev.* 17 (1921).
- [16] S. Sahoo, A. Sasmal, R. Nanda, a. R. Phani, P.L. Nayak, Synthesis of chitosan–polycaprolactone blend for control delivery of ofloxacin drug, *Carbohydr. Polym.* 79 (2010) 106–113. doi:10.1016/j.carbpol.2009.07.042.
- [17] G. Gorin, S.F. Wang, L. Papapavlou, Assay of lysozyme by its lytic action on *M. lysodeikticus* cells., *Anal. Biochem.* 39 (1971) 113–127. [http://www.ncbi.nlm.nih.gov/entrez/query.fcgi?cmd=Retrieve&db=PubMed&dopt=Citation&list\\_uids=5544583](http://www.ncbi.nlm.nih.gov/entrez/query.fcgi?cmd=Retrieve&db=PubMed&dopt=Citation&list_uids=5544583).
- [18] Y.H. Liao, M.B. Brown, G.P. Martin, Turbidimetric and HPLC assays for the determination of formulated lysozyme activity., *J. Pharm. Pharmacol.* 53 (2001) 549–554. <http://www.ncbi.nlm.nih.gov/pubmed/11341373>.
- [19] H. Bittiger, R.H. Marchessault, W.D. Niegisch, Crystal structure of poly-ε-caprolactone, *Acta Crystallogr. Sect. B Struct. Crystallogr. Cryst. Chem.* 26 (1970) 1923–1927. doi:10.1107/S0567740870005198.
- [20] D.M. Eckmann, Polidocanol for endovenous microfoam sclerosant therapy, *Expert Opin.* 18 (2009) 1919–1927.
- [21] W. Friess, M. Schlapp, Release mechanisms from gentamicin loaded poly(lactic-co-glycolic acid) (PLGA) microparticles., *J. Pharm. Sci.* 91 (2002) 845–55. <http://www.ncbi.nlm.nih.gov/pubmed/11920769>.
- [22] H. Jiang, Y. Hu, Y. Li, P. Zhao, K. Zhu, W. Chen, A facile technique to prepare biodegradable coaxial electrospun nanofibers for controlled release of bioactive agents., *J. Control. Release.* 108 (2005) 237–43. doi:10.1016/j.jconrel.2005.08.006.
- [23] C. Lu, W. Lin, Permeation of Protein from Porous Poly ( ε -caprolactone ) Films, 2001 (2002) 220–225. doi:10.1002/jbm.10120.
- [24] S.K. Dordunoo, A.M.C. Oktaba, W. Hunter, W. Min, T. Cruz, H.M. Burt, Release of taxol from poly ( ε -caprolactone ) pastes : effect of water-soluble additives, 44 (1997) 87–94.
- [25] Z. Karami, I. Rezaeian, P. Zahedi, M. Abdollahi, Preparation and performance evaluations of electrospun poly(epsilon-caprolactone) poly(lactic acid) and their hybrid (50-50) nanofibrous mats containing thymol as an herbal drug for effective wound healing.pdf, *J. Appl. Polym. Sci.* 129 (2013) 756–766.

- [26] Y.Y. Yang, T.S. Chung, N.P. Ng, Morphology, drug distribution, and in vitro release profiles of biodegradable polymeric microspheres containing protein fabricated by double-emulsion solvent extraction/evaporation method., *Biomaterials*. 22 (2001) 231–41. <http://www.ncbi.nlm.nih.gov/pubmed/11197498>.
- [27] R. Srikar, a L. Yarin, C.M. Megaridis, a V Bazilevsky, E. Kelley, Desorption-limited mechanism of release from polymer nanofibers., *Langmuir*. 24 (2008) 965–74. doi:10.1021/la702449k.
- [28] G. Crotts, H. Saha, T. Gwan Park, Adsorption determines in-vitro protein release rate from biodegradable microspheres : quantitative analysis of surface area during degradation, 47 (1997) 101–111.
- [29] E. Ron, L. Bromberg, Temperature-responsive gels and thermogelling polymer matrices for protein and peptide delivery., *Adv. Drug Deliv. Rev.* 31 (1998) 197–221. <http://www.ncbi.nlm.nih.gov/pubmed/10837626>.
- [30] T. Higuchi, Mechanism of Sustained- Action Medication, *J. Pharm. Sci.* 52 (1963) 1145–1149.
- [31] Y. Li, H. Jiang, K. Zhu, Encapsulation and controlled release of lysozyme from electrospun poly(epsilon-caprolactone)/poly(ethylene glycol) non-woven membranes by formation of lysozyme-oleate complexes., *J. Mater. Sci. Mater. Med.* 19 (2008) 827–32. doi:10.1007/s10856-007-3175-6.





## **4 Silk fibroin coating of protein crystals for controlled delivery**

The chapter is unpublished.

## **Abstract**

Protein encapsulation in polymeric drug delivery systems is bound to several limitations caused by instabilities of encapsulated macromolecules. Protein crystallization has been found to circumvent some of these instabilities. However, protein crystallization in a pharmaceutical useful scale displays a challenge with crystal size and purity being important but difficult to control parameters. Therapeutic use of such protein crystals may furthermore require modification of the protein release rate through encapsulation. Silk fibroin (SF) from the cocoons of *Bombyx mori* is a well-established protein suitable for encapsulation of small molecules as well as proteins for controlled drug delivery.

Lysozyme was used as a crystallizable protein and the effect of process- as well as formulation parameters of batch crystallization on crystal size were studied using statistical design of experiments. Lysozyme crystal size depended on temperature and sodium chloride and poly(ethylenglycole) concentration of precipitant solution. Under optimized conditions, lysozyme crystals in a size range of approximately 0.3 to 10  $\mu\text{m}$  were obtained. Furthermore, a solid-in-oil-in-water process for encapsulation of lysozyme crystals into SF was developed. Using this process, coating of protein crystals with another protein was achieved for the first time. Encapsulation resulted in a significant reduction of dissolution rate of lysozyme crystals, leading to prolonged release over up to 24 hours.

## 4.1 Introduction

One of the most exquisite challenges to formulation scientists nowadays is the development of biocompatible and biodegradable drug delivery systems for sustained, delayed or site-directed delivery of proteins or peptides. Polymeric drug delivery systems for controlled release are typically based on a limited number of mostly synthetic polymers, such as poly(lactic-co-glycolic acid), poly(caprolactone), poly(ethylenglycole). The natural polymer silk fibroin (SF) obtained from cocoons of *Bombyx mori* is increasingly gaining attention because of advantageous properties. Its biocompatibility and proven performance in controlled drug delivery applications combined with versatile processability and attractive mechanical characteristics made SF an emerging polymer in the fields of drug delivery and tissue engineering. The delivery of therapeutic proteins after encapsulation into SF could be demonstrated several times [1–12].

Most therapeutic proteins suffer from multiple instabilities, physically and chemically, and need to be stabilized for processing, storage and efficacious application. Especially with the aim of sustained release the protein needs to remain uncompromised over the entire time of storage and after application. In this regard SF has been shown to stabilize enzymes and may be assumed that such stabilization can be achieved for other proteins and appropriate conditions [13]. Moreover, crystallization of proteins was proven to result in their physical stabilization [14–16]. Apart from that protein delivery in the crystalline state is associated with additional advantages. The dense packaging in a crystalline structure offers high loading of the drug delivery system and viscosity of suspensions of protein crystals is reduced compared to a solution of the same concentration [17,18]. Resistance of protein crystals against harsh processing conditions such as organic solvents, elevated temperatures and mechanical stress (e.g. stirring, filling) is significantly improved compared to protein solutions. Consequently, the range of processing modalities suitable for encapsulation of protein crystals into polymeric drug delivery systems is significantly broader than for classic protein encapsulation. Yet

generating protein crystals in sufficient amounts and quality represents a challenge by itself. Batch crystallization, where vast amounts of monomodal crystals are formed, appears to be one of the most suitable methods [19–21]. For some proteins, protocols for batch crystallization are well accessible while especially for therapeutic proteins they hardly exist. Crystalline forms of insulin are the only examples that made it to the market so far. Besides that, methods for batch crystallization of monoclonal antibodies like rituximab, trastuzumab, infliximab [22] and anti-hTNF-alpha [23,24] or the human growth hormone (hGH) [25] have been reported.

On the other hand protein crystal solubility is an important parameter regarding processing as dissolution during encapsulation would likely detrimentally affect the crystalline state. Especially in the case of encapsulation of protein crystals into SF, the number of solvents that allow dissolution of SF, but are non-solvents for the protein crystal is limited. Contact of SF with certain organic solvents, e.g. methanol, leads to a conformational change in the protein structure, mostly  $\beta$ -sheet formation [26,27]. This transforms SF into a highly insoluble and crystalline state.

In this work we present new insights in the batch crystallization conditions for lysozyme by using experimental design. Interactions between the process and formulation parameters are being evaluated and precise conditions for the preparation of various monomodal lysozyme crystal (LC) sizes are defined.

Coating of these highly water soluble protein crystals with SF is demonstrated herein for the first time. The coating process is being visualized and physical characteristics of the final product determined. These SF coated lysozyme crystals (SFLC) are being studied in terms of release behavior and biological activity.

## 4.2 Materials and Methods

*Bombyx mori* cocoons were obtained from Trudel AG (Zurich, Switzerland). Chicken hen egg lysozyme, Fluorescein-isothiocyanate (FITC) and 5(6)-Carboxy-X-rhodamine N-succinylimidylester (Rhodamine-x) were obtained from Sigma-Aldrich. All other chemicals were of analytical grade and were obtained from Sigma-Aldrich.

### 4.2.1 Preparation of Lysozyme Crystals and Optimization of Crystallization by Design of Experiments

Lysozyme crystals were produced from bulk lysozyme without prior purification. Briefly, 24 mg/ml lysozyme was dissolved in 100 mM sodium acetate buffer, pH 3. The solution was filtered through a 0.22  $\mu\text{m}$  membrane filter (Versapor, Pall Life Sciences, Washington, NY) to remove undissolved compounds. Precipitation buffer (500 mM sodium acetate, pH 3.5, and with variable concentration of sodium chloride and PEG 6000) was poured quickly into the lysozyme solution at a defined temperature and stirred for 10 seconds. Crystal formation took place within a few seconds. Subsequently, crystals were washed 3 times with ethanol and hydrodynamic diameter was determined by laser diffraction (LS 230, Beckman Coulter, Brea, CA) and for particles below approx. 1  $\mu\text{m}$  by dynamic light scattering (DelsaNano HC, Beckman Coulter, Brea, CA). Modde 9 (Umetrics, Umea, Sweden) was used for the setup of a central composite face-centered (CCF) design with one center point. Three levels each of the factors sodium chloride concentration (10, 15, 20 %) and PEG 6000 concentration (3, 11.5, 20 %) in precipitation buffer as well as the temperature of the precipitation buffer (-4 , 2, 8  $^{\circ}\text{C}$ ) were evaluated. Hydrodynamic diameter of protein crystals was selected as response. In total 17 experiments were performed. Validity of the resulting model was evaluated by the goodness of fit ( $R^2$ ) and goodness of prediction ( $Q^2$ ). The statistical significance of each variable was evaluated at a level of  $p \leq 0.05$ . Backward elimination of each variable by eliminating insignificant terms was used to optimize the model.

In order to produce  $2.1 \pm 0.7 \mu\text{m}$  and  $5.1 \pm 1.8 \mu\text{m}$  crystals, which were used for coating with SF, twenty milliliters of precipitation buffer consisting of 20 % sodium chloride, 10 % PEG 6000 and 500 mM sodium acetate at pH 3.5 and at 8 °C and 20 °C were used, respectively. Crystals were washed with DCM/ethanol 10:3 and dried at 200 mbar overnight. Purity is expressed as the relation between the mass of the crystal powders and the absolute amount of lysozyme found by HPLC analysis of solutions of these powders.

#### **4.2.2 Silk fibroin extraction**

Extraction of SF from cocoons of *Bombyx mori* was conducted as described before [28]. Briefly, cocoons were cut into pieces and the larvae were removed. The cocoon pieces were incubated twice in 0.02 M  $\text{Na}_2\text{CO}_3$  solution at approximately 100°C for 1h each. Subsequently, SF was washed in ultrapure water 10 times and dried over night. A solution of 9 M LiBr was prepared in which the dried SF was dissolved at 55 °C until a clear solution was obtained and was adjusted to 20 % SF (m/V). This solution was stored at 8 °C until further use.

#### **4.2.3 Labeling of lysozyme with FITC and silk fibroin with Rhodamine-X**

Lysozyme was dissolved at a concentration of 2.0 mg/ml in a 0.1 M carbonate buffer, pH 9.0. FITC was dissolved in DMSO at a concentration of 1.0 mg/ml, added to lysozyme solution at a volume ratio of 1:12.5 and stirred for 6 hours at room temperature. Finally, the solution was dialyzed against ultra pure water for 2 hours and lyophilized. The average molar degree of modification was determined to be 5.13 mol /mol FITC per lysozyme. For the preparation of labeled lysozyme crystals, a ratio of 1:30 of labeled to unlabeled lysozyme was used, applying crystallization conditions as described above.

The SF solution was dialyzed against ultrapure water (Merck Millipore, Merck KGaA, Darmstadt, Germany) for 2 days, changing the water five times (Spectra/Por dialysis membrane tubes, cutoff 6-8 kDa, Spectrum Laboratories, Rancho Dominguez, CA). The purified SF

solution was then dialyzed against 0.1 M MES, 0.9 % NaCl, pH 5.6 for 1 day. Afterwards the SF solution had a concentration of 2 % m/V. 40 mM EDC and 190 mM NHS were added and stirred for 20 min at room temperature. 286  $\mu$ mol  $\beta$ -mercaptoethanol was added to quench the reaction and stirred for about 10 min. Then, 32  $\mu$ mol ethylendiamine was added and stirred for 2 h. This solution was dialyzed against 0.1 M phosphate buffer, pH 7.5 over night. Finally 20 $\mu$ mol Rhodamine-x was added, stirred for 2 hours and dialyzed against pure water protected from light over 2 days with a buffer exchange every 12 hours. The average molar degree of modification was determined to be 21.2 mol /mol Rhodamine-x per SF.

#### **4.2.4 Coating of protein crystals with silk fibroin and purification**

Silk fibroin solution was diluted 1:2 with ultrapure water to prepare a solution containing 10 % SF and 4.5 M LiBr. Rhodamine-x-labeled SF was added at a weight ratio of 1:100 to the unlabeled SF. Lysozyme crystals were dispersed in EtOH/DCM 3:10 (v/v) at a concentration of 40 mg/ml and homogenized in using an ultrasonic bath for 20 seconds (Branson 3200, Branson, Danbury, CT). Two hundred microliters of the crystal suspension were injected under stirring at 5000 rpm (Dremel 3000, Dremel, Racine, WI) into 2 ml of diluted SF solution. This S/O/W system was then stirred at 500 rpm for 1 hour at reduced pressure (500 mbar) to allow evaporation of DCM. The resulting suspension was washed twice with ultra pure water to remove LiBr. Subsequently, EtOH was added to induce  $\beta$ -sheet formation of SF and the suspension was agitated for 5 min. After another washing step with ultra pure water the solution was shock-frozen in liquid nitrogen and lyophilized.

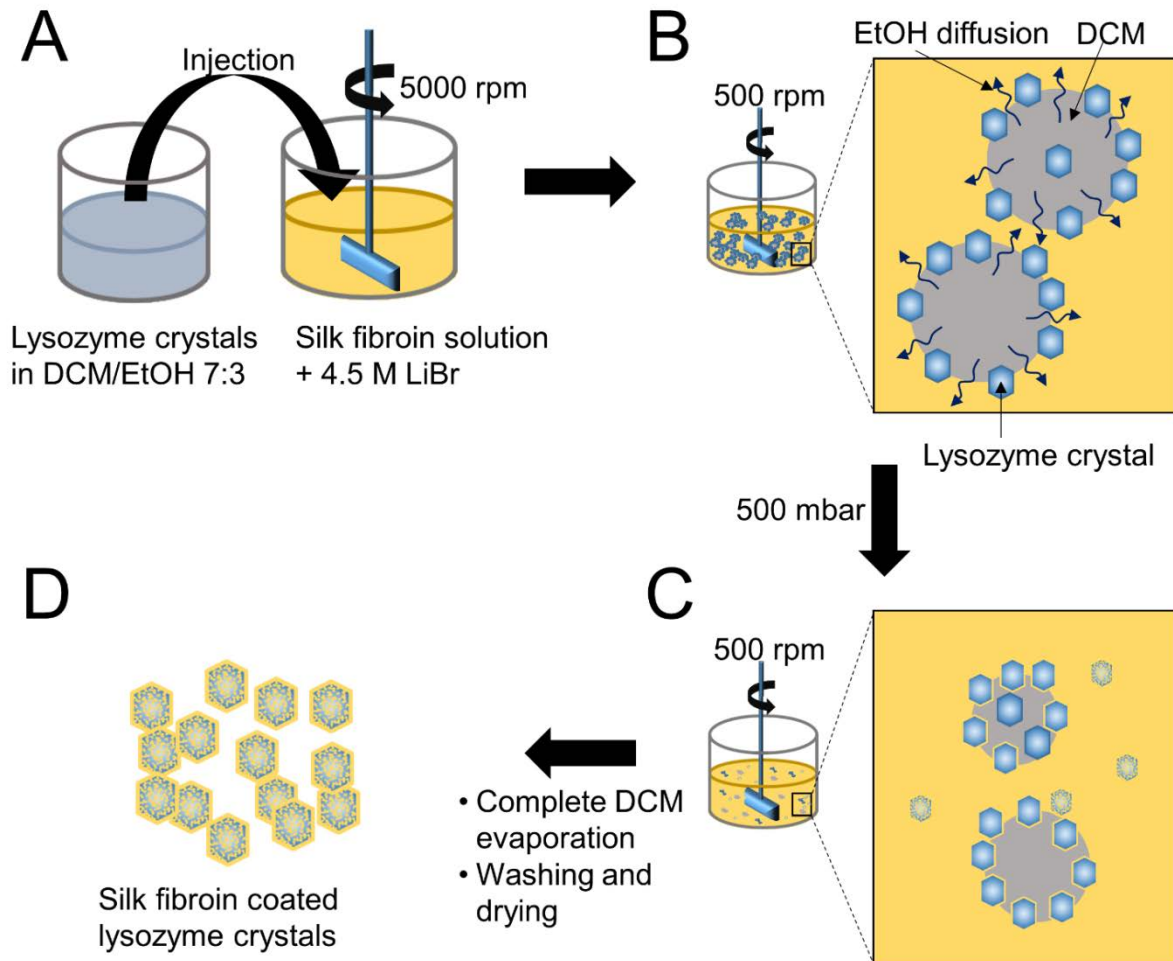


Figure 1: Schematic depiction of lysozyme crystals (LC) coating with silk fibroin (SF). (A) LC, dispersed in DCM/EtOH 7:3 were injected in a stirred (5000 rpm) SF solution. (B) The resulting S/O/W system was stirred under mild vacuum (500 mbar). LC were located at the interface between DCM and the SF solution. EtOH diffused from DCM into the SF solution inducing  $\beta$ -sheet formation of SF. (C) Over time DCM evaporates and SF coated LC translocate into the SF solution. (D) After washing and freeze drying, SFLC were collected.

#### 4.2.5 Microscopic characterization

Scanning electron micrographs were recorded using a JSM-7500F field emission scanning electron microscope (FESEM, Jeol, Tokyo, Japan) using an acceleration voltage of 5 kV. Negative phase contrast microscopy was performed using an Olympus BX 40 microscope (Olympus, Tokyo, Japan) and a VisiCam® 1.3 and VisiCam® Analyzer Software (VWR International, Radnor, PA) was used for image acquisition.



For confocal laser scanning microscopy (CLSM) a Leica TCS SP2 microscope was used (Leica Microsystems, Wetzlar, Germany). FITC and Rhodamine-X were detected separately using an argon laser at 488 nm and a krypton laser at 568 nm, respectively. A total number of 15 z-positions with an approx. heights of 0.3  $\mu\text{m}$  each was recorded for each sample.

#### **4.2.6 Release studies**

Phosphate buffered saline (PBS) with 0.05 % sodium azide was used as release medium. Samples (2  $\mu\text{m}$  crystals: average mass 413  $\mu\text{g}$ ; 5  $\mu\text{m}$  crystals: average mass 966  $\mu\text{g}$ ) were accurately weighed and incubated in 1.5 ml release medium at a temperature of 37  $^{\circ}\text{C}$  and with orbital shaking at 900 rpm in a Thermomixer comfort (Eppendorf, Hamburg, Germany). At predefined time points an aliquot of 150  $\mu\text{l}$  was drawn, centrifuged to remove particles and the supernatant was stored at -80  $^{\circ}\text{C}$  until analysis. Lysozyme concentrations are expressed relatively to the absolute mass of silk fibroin coated lysozyme crystals (SFLC) incubated in PBS.

Lysozyme concentrations were determined using RP-HPLC (LaChrom Ultra with L-2400 UV-detector, VWR Hitachi and RP18 Licrosphere 100 column, Merck, Darmstadt, Germany) with UV detection at a wavelength of 220 nm as described before [29]. The limit of quantification was determined to be 2.56  $\mu\text{g}/\text{ml}$ .

#### **4.2.7 Relative Bioactivity**

Relative bioactivity of lysozyme was determined as described before [29]. Briefly, a dry cell wall preparation of *micrococcus lysodeikticus* was suspended at a concentration of 200 mg/l in 1.0 ml of a 0.1 M  $\text{KH}_2\text{PO}_4$  buffer at pH 6.2. Then 33.3  $\mu\text{l}$  of the lysozyme sample solution were added and stirred for 5 seconds. The decline of absorbance measured at 570 nm was recorded for 2 minutes (Genesys 10S, Thermo Scientific, Rockford, IL). Using linear regression, the slope of the decline was determined. A calibration relating the slope to the relative lysozyme

activity was created. The limit of quantification was  $0.96 \mu\text{g ml}^{-1}$  lysozyme. Bioactivity is reported relative to fresh bulk lysozyme.

#### 4.2.8 FTIR

Dry samples of lysozyme crystals, pure SF after EtOH treatment and the SFLC were measured with an FTIR-6100 (JASCO, Frankfurt, Germany) with a PIKE MIRacle single reflection ATR (PIKE Technologies, Madison, WI). Wavenumber ranged from  $600$  to  $4000 \text{ cm}^{-1}$  with a resolution of  $4 \text{ cm}^{-1}$ . 128 scans were combined and a Fourier self-deconvolution (FSD) of the IR was performed by Spectramanager IR software (JASCO, Frankfurt, Germany).

### 4.3 Results

#### 4.3.1 Controlled crystal formation of lysozyme

Within the limits chosen for design of experiments, crystal formation took place in less than a minute resulting in low polydispersity (**Fig. 2**). All factors were fitted with a linear model ( $R^2 = 0.94$ ;  $Q^2 = 0.81$ ). Model validity and reproducibility were calculated to be 0.91 and 0.90, respectively. All three factors evaluated in the DoE had a significant influence on the crystal size. Higher precipitant concentrations resulted in smaller crystal size, while increase of temperature yielded larger crystals. The parameter temperature strongly interacted with the parameters NaCl and PEG concentration (**Fig. 3**). At  $+2 \text{ }^\circ\text{C}$  NaCl and PEG had a comparable impact on the crystal size. Higher concentrations of both additives decreased the average crystal size approximately to the same extent. At a lower temperature of  $-4^\circ\text{C}$ , higher PEG concentration strongly decreased crystal size while NaCl concentration almost had no effect. In contrast, at  $+8^\circ\text{C}$ , NaCl concentration had a pronounced effect on crystal size while the effect of PEG concentration was negligible. After washing of lysozyme crystals, purity of the product was examined by HPLC and found to be in the range between 21.7 and 94.9 %. Smaller crystals

were harder to purify, while larger crystals could be obtained almost completely pure. Average purity was  $66.0 \pm 22.4$  %. Average relative bioactivity of lysozyme after dissolution of crystals was found to be  $85.1 \pm 11.9$  %.

| DoE number | NaCl [%] | PEG 6000 [%] | Temperature Precipitation buffer | Avg. crystal size [ $\mu\text{m}$ ] | Purity [%] | Bioactive [%] |
|------------|----------|--------------|----------------------------------|-------------------------------------|------------|---------------|
| 1          | 10       | 3            | -4                               | $6.7 \pm 2.26$                      | 81.7       | 88.9          |
| 2          | 20       | 3            | -4                               | $10.9 \pm 11.7$                     | 71.5       | 90.4          |
| 3          | 10       | 20           | -4                               | $0.631 \pm 0.57$                    | 63.5       | 97.6          |
| 4          | 20       | 20           | -4                               | $0.912 \pm 0.909$                   | 63.4       | 85.2          |
| 5          | 10       | 3            | 8                                | $37.6 \pm 19.1$                     | 21.8       | 46.7          |
| 6          | 20       | 3            | 8                                | $2.62 \pm 0.809$                    | 69.4       | 93.1          |
| 7          | 10       | 20           | 8                                | $11.5 \pm 2.52$                     | 64.8       | 89.9          |
| 8          | 20       | 20           | 8                                | $2.19 \pm 0.747$                    | 91.3       | 88.0          |
| 9          | 10       | 11.5         | 2                                | $9.49 \pm 1.25$                     | 25.9       | 70.9          |
| 10         | 20       | 11.5         | 2                                | $2.04 \pm 0.927$                    | 68.7       | 96.7          |
| 11         | 15       | 3            | 2                                | $6.35 \pm 2.87$                     | 94.2       | 86.3          |
| 12         | 15       | 20           | 2                                | $1.74 \pm 0.741$                    | 52.0       | 91.1          |
| 13         | 15       | 11.5         | -4                               | $1.52 \pm 1.01$                     | 36.3       | 74.2          |
| 14         | 15       | 11.5         | 8                                | $7.68 \pm 1.27$                     | 94.9       | 88.3          |
| 15         | 15       | 11.5         | 2                                | $5.84 \pm 3.14$                     | 67.2       | 85.9          |
| 16         | 15       | 11.5         | 2                                | $3.03 \pm 1.14$                     | 94.2       | 87.1          |
| 17         | 15       | 11.5         | 2                                | $3.76 \pm 2.61$                     | 61.5       | 85.9          |

Table 1: DoE setup describing the order in which the experiments were conducted, the three factors of each experiment as well as the resulting average crystal sizes, their purity and bioactivity, both expressed relative to the lysozyme amount found by HPLC

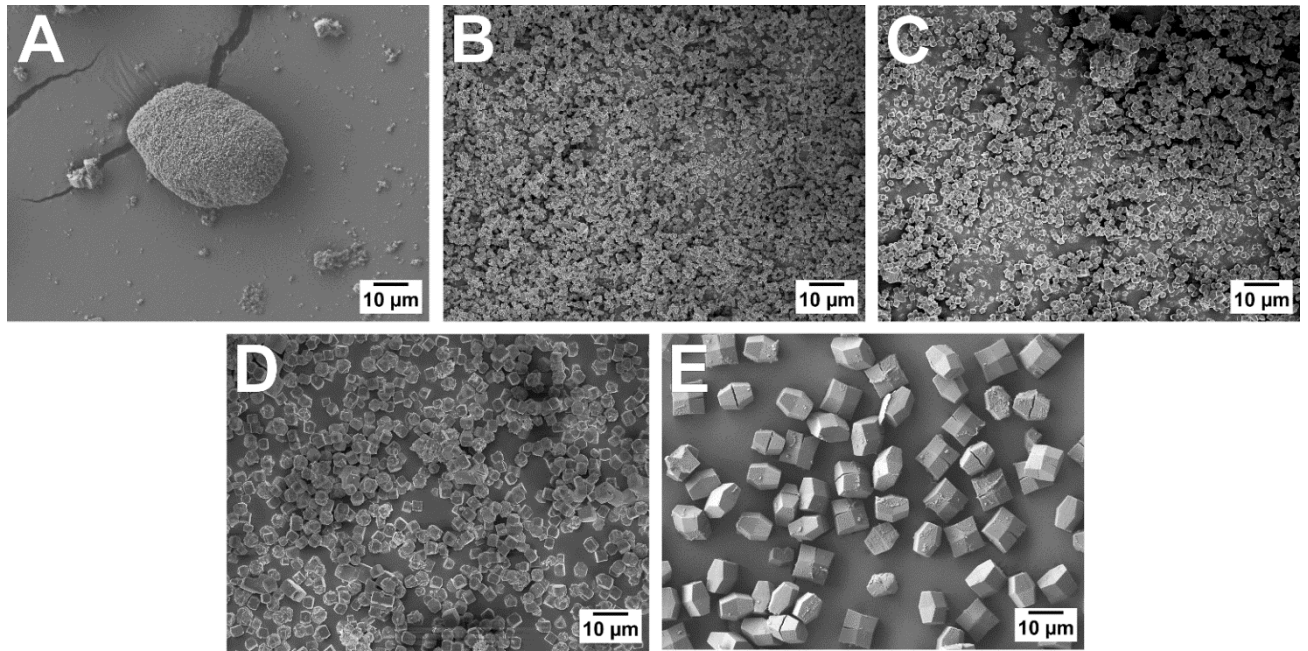


**Figure 2:** SEM images of lysozyme crystals with different average diameter: (A)  $319 \pm 91$  nm (B)  $699 \pm 106$  nm (C)  $2100 \pm 700$  nm (D)  $5099 \pm 1818$  nm (E)  $9498 \pm 1257$  nm (A) and (E) correspond to the crystals from the DoE with the numbers 3 (A) and 9 (E). (C) and (D) were used for the coating with SF and were produced as described. (B) was described as before [29]

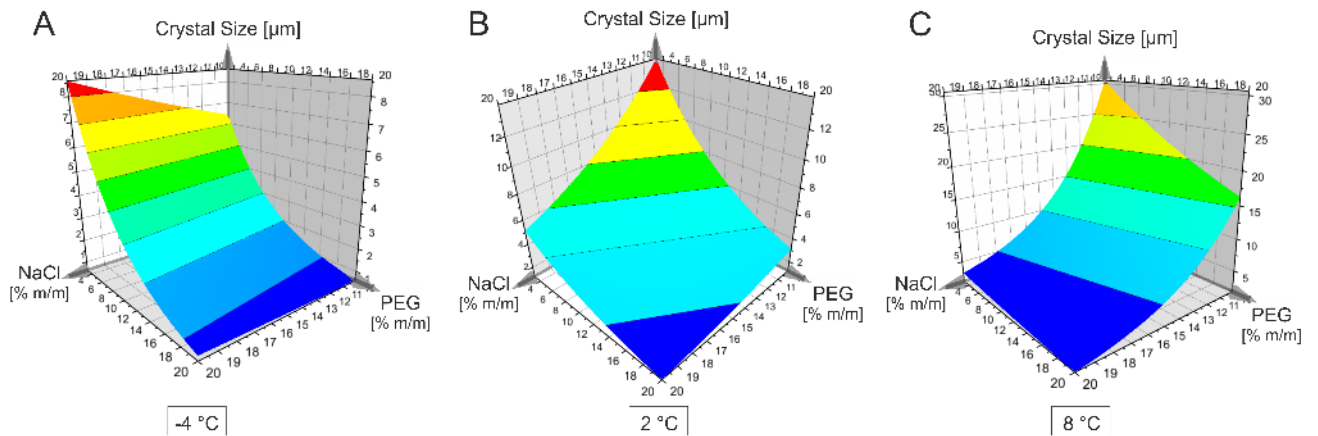


**Figure 3:** Response Surface Plots relating lysozyme crystal size to concentration of PEG and NaCl at three different temperatures: (A)  $-4^{\circ}\text{C}$  (B)  $+2^{\circ}\text{C}$  (C)  $+8^{\circ}\text{C}$

#### 4.3.2 SEM and light microscope pictures

During the lysozyme crystal coating process, samples were drawn at different time points and examined by light microscopy (**Fig. 4**). It was found that lysozyme crystals concentrate at the DCM/water interface and after complete evaporation of DCM, coated crystals remain suspended in the aqueous buffer.

SEM images of uncoated lysozyme crystals show smooth, uniformly sized particles with a characteristic rhombohedral structure (**Fig. 5 A and C**). After coating, particles had a rough surface and appeared rather spherical instead of the rhombohedral form (**Fig. 5 B and D**). Pores and larger gaps were observed on the surface and besides individual coated crystals, aggregates with irregular shape were found. Furthermore, the coating procedure resulted in smaller particle sizes. After coating, particle size was reduced to 62.7 % and 55.7% of the initial size for crystals of initially 5  $\mu\text{m}$  and 2  $\mu\text{m}$ , respectively.

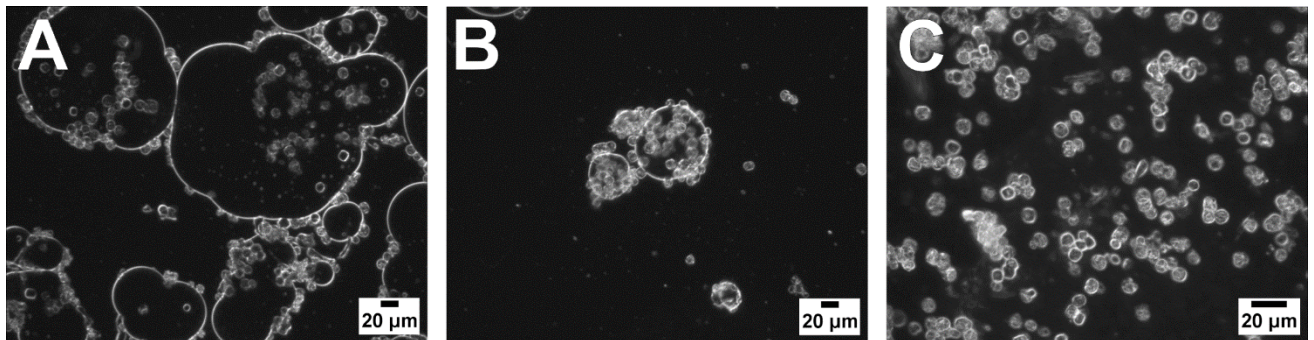


Figure 4: Light micrographs of lysozyme crystals during coating with SF. Crystals are suspended in the inner phase of the emulsion consisting of DCM/EtOH. After emulsification in SF solution, DCM is evaporated over time at reduced pressure. Micrographs are taken at (A) 0 min, (B) 30 min and (C) 60 min after emulsification.



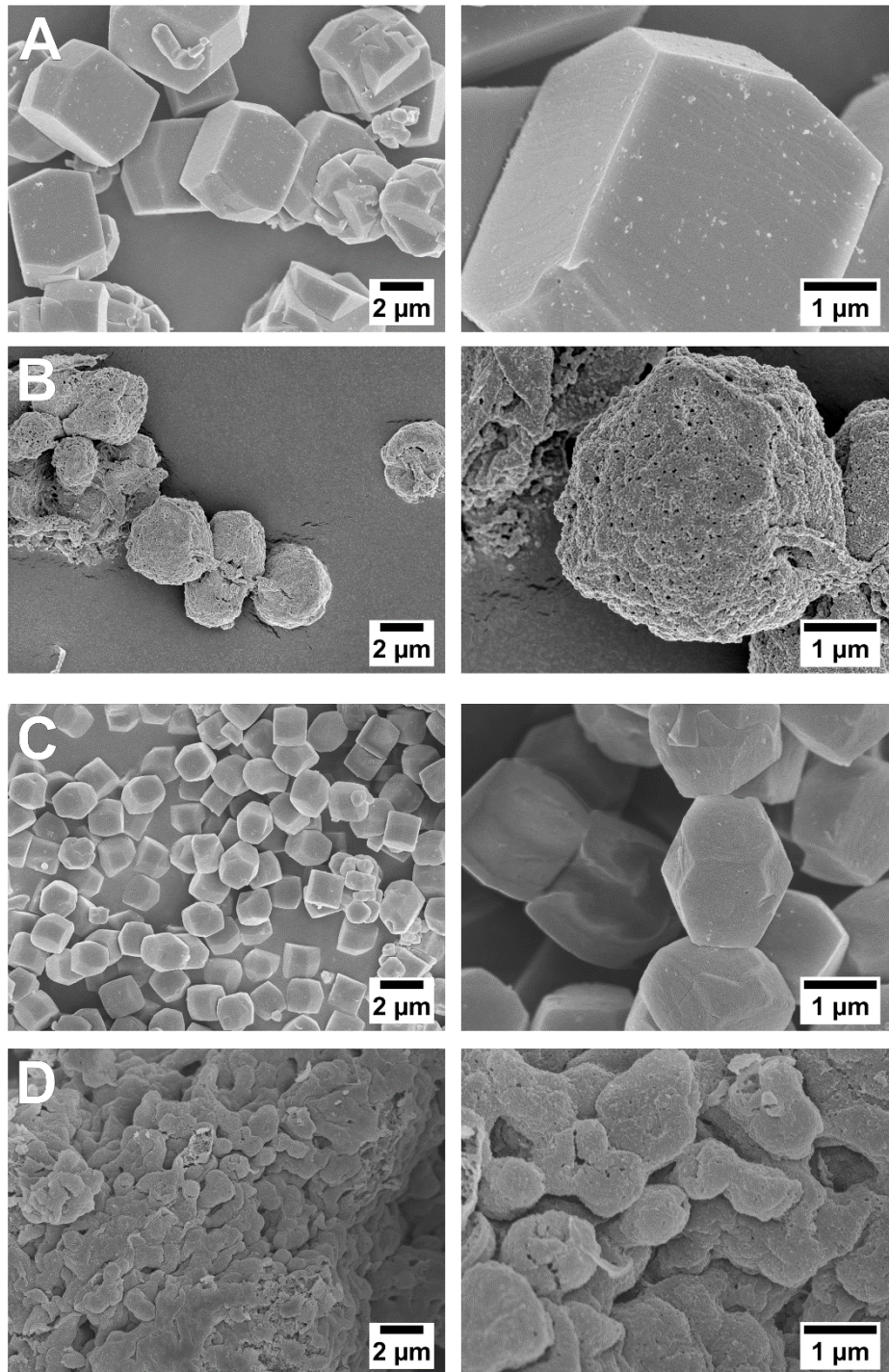


Figure 5: Scanning electron micrographs of lysozyme crystals at low (left) and high magnification (right): (A) uncoated 5  $\mu\text{m}$  crystals, (B) 5  $\mu\text{m}$  crystals after SF coating, (C) uncoated 2  $\mu\text{m}$  crystals and (D) 2  $\mu\text{m}$  crystals after SF coating.

### 4.3.3 CLSM analysis

After coating, FITC-labeled lysozyme crystals were found to be completely penetrated by Rhodamine-x-labeled SF. It appeared as if SF had filled preexisting channels in lysozyme crystals, resulting in a spot-like distribution of SF associated fluorescence at all investigated z-positions. In contrast, lysozyme fluorescence appeared to be homogeneous. CLSM images of SFLC taken after 3 days of incubation in release medium showed FITC-labeled lysozyme was not completely released. The macroscopic structure of labeled SF did not change during the 3 days and no erosion of the SF matrix could be observed.

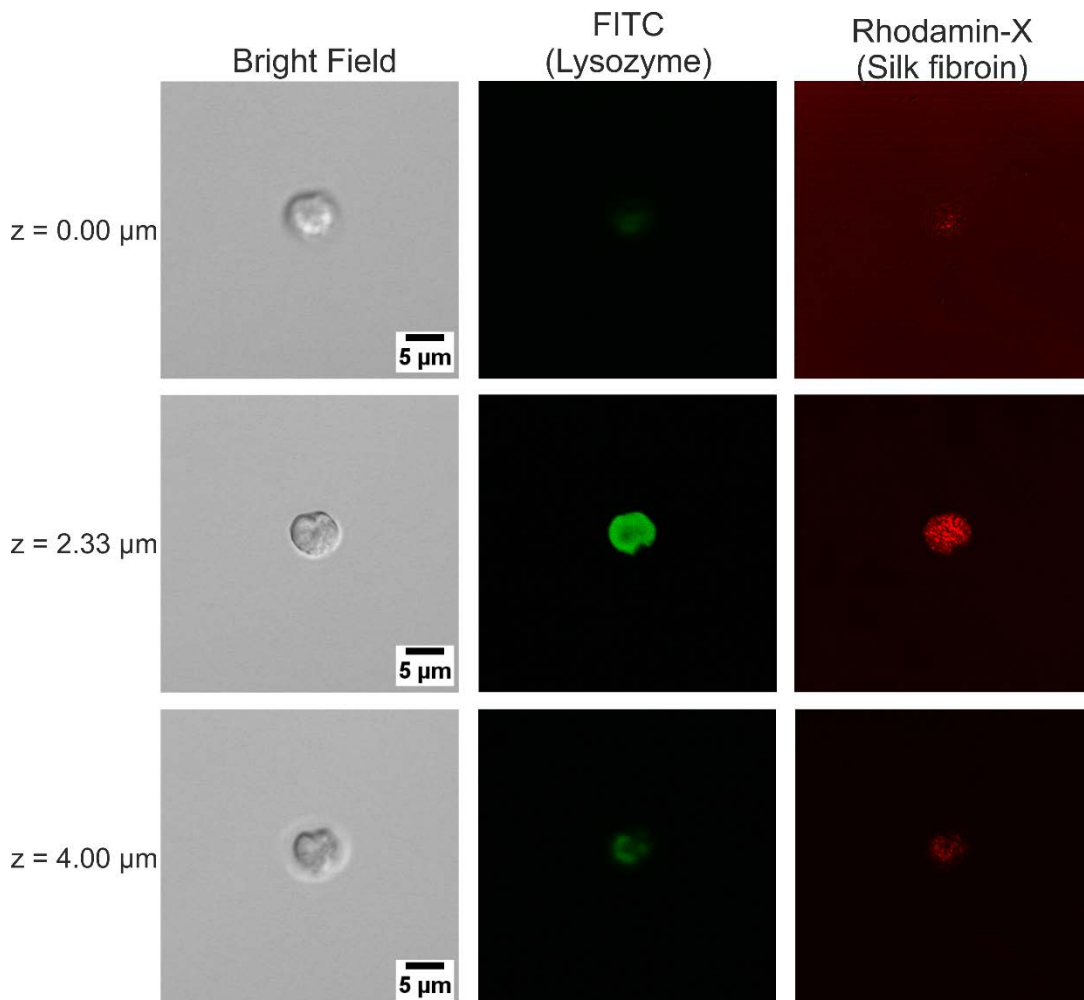


Figure 6: Representative confocal laser scanning micrographs of a SF coated lysozyme crystal. Depicted is the same crystals recorded at 15 different z-positions (shown are 0, 7 and 12). Lysozyme was labeled with FITC, whose fluorescence is shown in false color green. SF was modified with Rhodamine-X, shown in false color red.

#### 4.3.4 FTIR analysis

FTIR measurements of dried pure SF (after ethanol treatment), pure LC and SFLC were performed. Ethanol treated SF as well as LC showed distinctively different spectra in the range between wavenumber 1000 and 2000  $\text{cm}^{-1}$ . Characteristic absorption peaks of SF at 1620  $\text{cm}^{-1}$  (Amide I;  $\beta$ -sheet), 1698  $\text{cm}^{-1}$  (Amide I; t-Turns) indicating SF  $\beta$ -sheet formation were observed. Lysozyme peaks were observed at 1480  $\text{cm}^{-1}$ , 1645  $\text{cm}^{-1}$  (Amide I;  $\alpha$ -helix). SFLC showed a similar transmission spectrum with peaks at 1480  $\text{cm}^{-1}$ , 1620  $\text{cm}^{-1}$ , 1645  $\text{cm}^{-1}$  and 1698  $\text{cm}^{-1}$ .

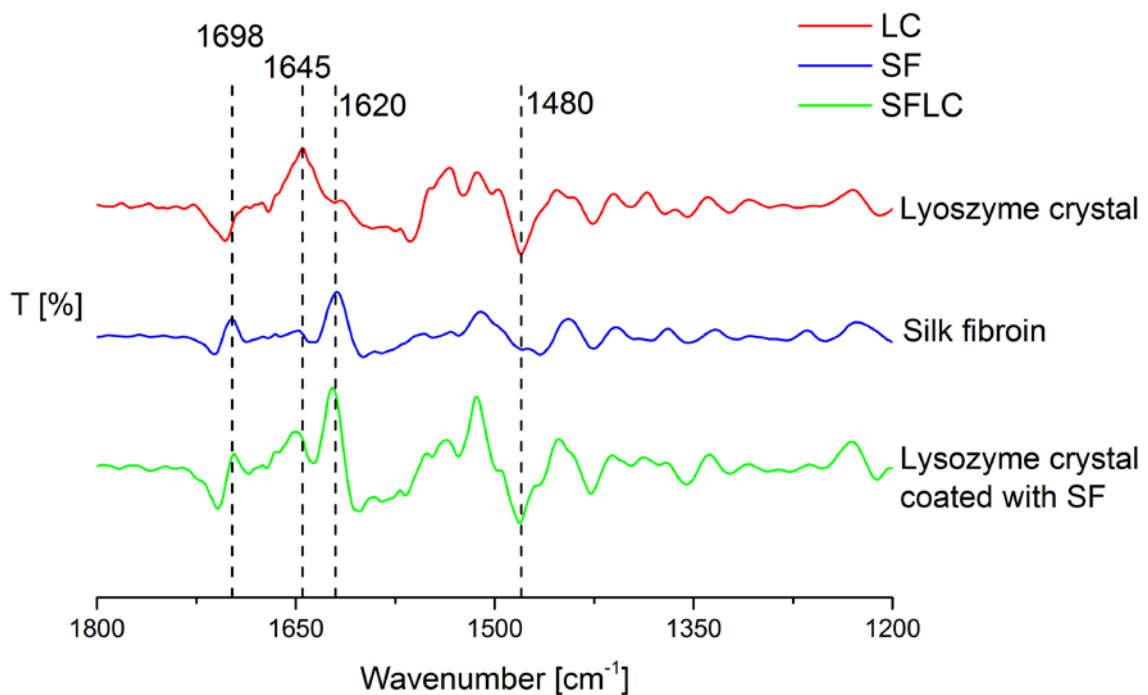


Figure 7: Second derivative FTIR spectra of SF, pure lysozyme crystals and lysozyme crystals coated with SF. Characteristic SF absorption peaks are indicated by the dotted lines.

#### 4.3.5 Lysozyme in vitro release and bioactivity

Lysozyme release from the SFLC showed a pronounced burst. In the case of 5  $\mu\text{m}$  SFLC burst release within the first hour of incubation reached a level of  $28.7 \pm 4.9\%$ . Afterwards a constant



release over the next 7 hours was observed. The amount of lysozyme released at the end of the incubation period was  $35.9 \pm 3.5$  % of the total mass of SFLC. Release from SFLC of  $2 \mu\text{m}$  also is characterized by a burst release of  $17.7 \pm 6.6$  % during the first hour of release. Total release leveled off after 24 h and  $30.0 \pm 9.1$  % was released. In contrast, uncoated lysozyme crystals instantly dissolved in PBS buffer (data not shown). The bioactivity of released lysozyme was not affected by the encapsulation procedure nor by release from the coated microcrystals. After 1 hour of release, bioactivity was found to be  $119.8 \pm 22.3$  % and after 3 days  $116. \pm 10.7$  %, relative to the amount of lysozyme as determined by HPLC.

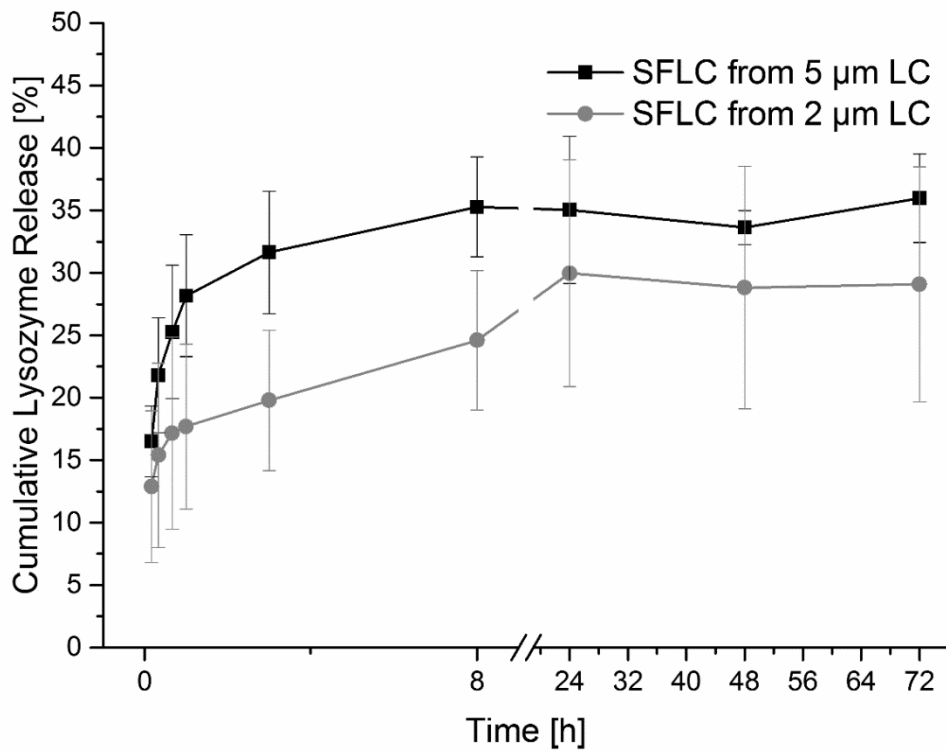


Figure 8: Cumulative release from SF coated lysozyme crystals with two different diameters,  $2 \mu\text{m}$  and  $5 \mu\text{m}$ . Pure lysozyme crystals dissolved within minutes (data not shown).

#### 4.4 Discussion

We crystallized lysozyme in a controlled manner and crystal sizes between approx. 0.3 and 20  $\mu\text{m}$  with monomodal size distributions were obtained. Lysozyme crystallization has been investigated before and several protocols for its crystallization exist [30,31]. In this study we studied the impact of the temperature on the precipitating agents. It is known, that the temperature itself influences solubility of proteins and thus supersaturation [18,32]. Up to a certain point, higher temperatures increase the solubility of lysozyme and thus reduce the tendency to form crystallization nuclei [31,33,34]. Fewer crystallization nuclei are formed simultaneously which grow to few but large crystals [35]. CCF experimental design allowed to examine the effects and interactions of the factors crystallization temperature, sodium chloride and PEG concentration. While the interaction between the precipitation agents NaCl and PEG were not significant, the interaction between the temperature and the former two were. At lower temperature, the effect of NaCl concentration on the crystal size decreased, while the effect of PEG concentration on the crystal size decreased with increasing temperature.

Previous studies found that the position of ions in the Hofmeister series, which is related to their affinity of being hydrated, directly affects their ability to crystallize proteins. The hydration of an ion correlates with its crystallization ability for proteins because of the competition of ions and protein for hydration [36]. For NaCl and lysozyme it was found that the Hofmeister series does not apply though and that ionic interactions are responsible for neutralizing the net charge of the protein, reducing its hydration and forcing it out of solution [37]. Formation of salt bridges between the carboxylates and amides of the protein molecules leading to lysozyme crystallization is thermodynamically not favored at low temperatures and thus variation of the ionic strength of NaCl does not affect crystallization at lower temperatures. The hydration of PEG, an amphiphilic neutral molecule, on the other hand increases with decreasing temperatures. The reason for this is that the strength of the H-bonds between water and PEG are decreasing faster with increasing temperatures than van der Waals forces. Consequently,

the amount of solvent molecules withdrawn from the protein decreases with increasing temperatures in the case of PEG.

Simple washing of protein crystals with a mixture of DCM and ethanol yielded lysozyme crystal purity between 26 and 95 % (**Table 1**). Smaller lysozyme crystals were harder to purify by washing, resulting in overall reduced purity (**Table 1**). Most likely this effect was related to differences in the efficiency of crystal separation by centrifugation and by the larger surface area of smaller protein crystals resulting in comparably larger amounts of adsorbed components from the precipitant solution. The bioactivity, relative to bulk lysozyme, was retained by this method and averaged at  $85.1 \pm 11.9$  %.

Lysozyme crystals were successfully encapsulated in SF to form microspheres for sustained dissolution. The challenge to encapsulate a water soluble protein crystal into a protein, that itself is dissolved in water, without the crystal being dissolved was approached by using a solid-in-oil-in-water (S/O/W) technique. The lysozyme crystals were homogeneously dispersed in a mixture of DCM and ethanol, which was selected because lysozyme crystals were not soluble in this solvent mixture. This suspension was injected under fast stirring in a silk fibroin solution in the presence of lithium bromide. Lithium bromide stabilizes SF, avoiding premature  $\beta$ -sheet formation and in addition delays the dissolution of lysozyme crystals. The presence of LiBr was a critical factor for the coating process because of otherwise rapid dissolution of lysozyme crystals in the S/O/W system. During the process lysozyme crystals were mainly located at the interface between aqueous and organic phase (**Fig. 4**). We hypothesize that ethanol was slowly diffusing towards the aqueous phase and resulting in SF  $\beta$ -sheet formation rendering SF water insoluble at the oil/water interface. Insoluble SF was then deposited on the protein crystals, leading to coating of lysozyme crystals with  $\beta$ -sheet rich SF. After complete DCM evaporation, coated lysozyme crystals could be collected by centrifugation and washing.

Fluorescent labeling of lysozyme with FITC and SF with Rhodamine-X, prior to crystallization and coating, revealed that SF was not only located on the surface of lysozyme crystals but also

penetrated the crystal bulk. We assume that the presence of channels along the crystallographic *c* axis in lysozyme crystals allowed SF penetration during the coating process [38]. Opposite net charges of SF and lysozyme, resulting from the different isoelectric points of around 4 and around 11 respectively, additionally supported the SF deposition on the surface and within channels of lysozyme crystals.

Successful coating was corroborated by FTIR analysis of pure and SF coated lysozyme crystals demonstrating the presence of crystallized lysozyme as well as  $\beta$ -sheet formation of SF coating. SF coating of lysozyme crystals of two different crystal diameters lead to significantly sustained release compared to pure lysozyme crystals. Burst release and subsequent release rate were further found to depend on lysozyme crystal size with large crystals (5  $\mu\text{m}$ ) resulting in a higher burst and rapid release, which leveled off after approx. 8 hours, whereas 2.1  $\mu\text{m}$  SFLCs showed a reduced burst and release for up to 24 h. This finding may be explained by electrostatic interactions between lysozyme and SF as described above. Such electrostatic interactions will in general result in sustained release of lysozyme from SF coated crystals while the weight ratio of SF to lysozyme will determine the amount of burst release and subsequent release rate. We hypothesize that in the case of 5  $\mu\text{m}$  SFLC saturation of the SF coat with lysozyme is reached rapidly due to the large amount of lysozyme present in the crystals. Therefore, burst release within 1 hour was significantly higher for 5  $\mu\text{m}$  crystals than for 2  $\mu\text{m}$  crystals. Release rate found after burst release was comparable for both crystal sizes but the duration of release was increased in the case of 2  $\mu\text{m}$  crystals. We assume that the relative amount of SF was higher for 2  $\mu\text{m}$  SFLC, resulting in a prolonged release duration.

Fluorescent micrographs of labeled SFLC after a 3 days of incubation in release medium showed remaining amounts of FITC, which we interpret as lysozyme that was not released. Given the hypothesis of electrostatic interaction between lysozyme and SF, it was expected that release would be incomplete. Lysozyme release may be improved by change of pH, increase of ionic strength of the release medium or addition of kosmotropic agents [28,39]. However, we

refrained from changing the release buffer composition in order to retain the physiologic relevance of the release study.

The release mechanism shows characteristics of both, desorptional and diffusional components. Hines et al. studied the release from SF films and described a release mechanism that is mainly driven by diffusion [40]. Due to the fact that the majority of lysozyme was released within approx. 8 hours, the desorptional phase dominated while diffusional release made only a minor contribution. High porosity of the SF coating is assumed to be responsible for rapid diffusion of lysozyme. The remaining lysozyme that was not released seemed to strongly adhere to SF due to the ionic interactions between lysozyme and SF. A long term release caused by polymer degradation as described in [40] was not observed in our study even after incubation over 7 days and longer.

#### **4.5 Conclusion**

The influence of the temperature on the crystallization excipients NaCl and PEG was demonstrated in this work. While NaCl loses impact on the nucleation of lysozyme with decreasing temperature, PEG's influence increases and at higher temperatures the matter is reversed. Many monomodal protein crystal sizes could be obtained in examined range of the conditions. Purification simply was achieved by washing in a mix of DCM and EtOH.

To the authors knowledge protein crystals were encapsulated in silk fibroin for the first time using an S/O/W technique. Complete penetration of SF into the protein crystals during the coating process was observed and lysozyme release lasted up to 24 hours under optimized conditions.

- [1] V.R. Sinha, A. Trehan, Biodegradable microspheres for protein delivery., *J. Control. Release.* 90 (2003) 261–80. <http://www.ncbi.nlm.nih.gov/pubmed/12880694>.

- [2] V. Karageorgiou, L. Meinel, S. Hofmann, A. Malhotra, V. Volloch, D. Kaplan, Bone morphogenetic protein-2 decorated silk fibroin films induce osteogenic differentiation of human bone marrow stromal cells., *J. Biomed. Mater. Res. A.* 71 (2004) 528–37. doi:10.1002/jbm.a.30186.
- [3] C. Kirker-Head, V. Karageorgiou, S. Hofmann, R. Fajardo, O. Betz, H.P. Merkle, et al., BMP-silk composite matrices heal critically sized femoral defects., *Bone.* 41 (2007) 247–55. doi:10.1016/j.bone.2007.04.186.
- [4] L. Uebersax, M. Mattotti, M. Papaloizos, H.P. Merkle, B. Gander, L. Meinel, Silk fibroin matrices for the controlled release of nerve growth factor (NGF)., *Biomaterials.* 28 (2007) 4449–60. doi:10.1016/j.biomaterials.2007.06.034.
- [5] X. Wang, E. Wenk, X. Hu, G.R. Castro, L. Meinel, X. Wang, et al., Silk coatings on PLGA and alginate microspheres for protein delivery., *Biomaterials.* 28 (2007) 4161–9. doi:10.1016/j.biomaterials.2007.05.036.
- [6] L. Uebersax, H.P. Merkle, L. Meinel, Insulin-like growth factor I releasing silk fibroin scaffolds induce chondrogenic differentiation of human mesenchymal stem cells., *J. Control. Release.* 127 (2008) 12–21. doi:10.1016/j.jconrel.2007.11.006.
- [7] X. Wang, X. Zhang, J. Castellot, I. Herman, M. Iafrafi, D.L. Kaplan, Controlled release from multilayer silk biomaterial coatings to modulate vascular cell responses., *Biomaterials.* 29 (2008) 894–903. doi:10.1016/j.biomaterials.2007.10.055.
- [8] X. Wang, T. Yucel, Q. Lu, X. Hu, D.L. Kaplan, Silk nanospheres and microspheres from silk/pva blend films for drug delivery., *Biomaterials.* 31 (2010) 1025–35. doi:10.1016/j.biomaterials.2009.11.002.
- [9] E. Wenk, A.R. Murphy, D.L. Kaplan, L. Meinel, H.P. Merkle, L. Uebersax, The use of sulfonated silk fibroin derivatives to control binding, delivery and potency of FGF-2 in tissue regeneration., *Biomaterials.* 31 (2010) 1403–13. doi:10.1016/j.biomaterials.2009.11.006.
- [10] N. Guziewicz, A. Best, B. Perez-Ramirez, D.L. Kaplan, Lyophilized silk fibroin hydrogels for the sustained local delivery of therapeutic monoclonal antibodies., *Biomaterials.* 32 (2011) 2642–50. doi:10.1016/j.biomaterials.2010.12.023.
- [11] P. Shi, J.C.H. Goh, Release and cellular acceptance of multiple drugs loaded silk fibroin particles., *Int. J. Pharm.* 420 (2011) 282–9. doi:10.1016/j.ijpharm.2011.08.051.
- [12] L. Li, S. Puhl, L. Meinel, O. Germershaus, Silk fibroin layer-by-layer microcapsules for localized gene delivery, *Biomaterials.* 35 (2014) 1–11. doi:10.1016/j.biomaterials.2014.05.062.
- [13] S. Lu, X. Wang, Q. Lu, X. Hu, N. Uppal, F.G. Omenetto, et al., Stabilization of enzymes in silk films., *Biomacromolecules.* 10 (2009) 1032–42. doi:10.1021/bm800956n.

- [14] B. Shenoy, Y. Wang, W. Shan, A.L. Margolin, Stability of crystalline proteins., *Biotechnol. Bioeng.* 73 (2001) 358–69.  
<http://www.ncbi.nlm.nih.gov/pubmed/11320506>.
- [15] A. a Elkordy, R.T. Forbes, B.W. Barry, Stability of crystallised and spray-dried lysozyme., *Int. J. Pharm.* 278 (2004) 209–19. doi:10.1016/j.ijpharm.2004.02.027.
- [16] A. a Elkordy, R.T. Forbes, B.W. Barry, Integrity of crystalline lysozyme exceeds that of a spray-dried form., *Int. J. Pharm.* 247 (2002) 79–90.  
<http://www.ncbi.nlm.nih.gov/pubmed/12429487>.
- [17] A. Jen, H.P. Merkle, Diamonds in the rough: protein crystals from a formulation perspective., *Pharm. Res.* 18 (2001) 1483–8.  
<http://www.ncbi.nlm.nih.gov/pubmed/11758753>.
- [18] S.K. Basu, C.P. Govardhan, C.W. Jung, A.L. Margolin, Protein crystals for the delivery of biopharmaceuticals., *Expert Opin. Biol. Ther.* 4 (2004) 301–17.  
doi:10.1517/14712598.4.3.301.
- [19] T. Lee, J. Vaghjiani, G. Lye, M. Turner, A systematic approach to the large-scale production of protein crystals., *Enzyme Microb. Technol.* 26 (2000) 582–592.  
<http://www.ncbi.nlm.nih.gov/pubmed/10793205>.
- [20] D. Hebel, S. Huber, B. Stanislawski, D. Hekmat, Stirred batch crystallization of a therapeutic antibody fragment., *J. Biotechnol.* 166 (2013) 206–11.  
doi:10.1016/j.jbiotec.2013.05.010.
- [21] C.N. Nanev, V.D. Tonchev, F. V. Hodzhaoglu, Protocol for growing insulin crystals of uniform size, *J. Cryst. Growth.* 375 (2013) 10–15. doi:10.1016/j.jcrysgr.2013.04.010.
- [22] M.X. Yang, B. Shenoy, M. Disttler, R. Patel, M. McGrath, S. Pechenov, et al., Crystalline monoclonal antibodies for subcutaneous delivery., *Proc. Natl. Acad. Sci. U. S. A.* 100 (2003) 6934–9. doi:10.1073/pnas.1131899100.
- [23] W. Fraunhofer, G. Winter, D.W. Borhani, S. Gottschalk, C.H. Cowles, S. Kim, *Compositions and Methods for Crystallizing Antibodies*, 2014.
- [24] A. Koenigsdorfer, S. Gottschalk, H.-J. Krause, G. Winter, D.W. Borhani, W. Fraunhofer, *Crystalline anti-hTNF-alpha antibodies*, 2014.
- [25] C. Govardhan, N. Khalaf, C.W. Jung, B. Simeone, A. Higbie, S. Qu, et al., Novel long-acting crystal formulation of human growth hormone., *Pharm. Res.* 22 (2005) 1461–70.  
doi:10.1007/s11095-005-6021-x.
- [26] G.H. Altman, F. Diaz, C. Jakuba, T. Calabro, R.L. Horan, J. Chen, et al., Silk-based biomaterials, *Biomaterials.* 24 (2003) 401–416. doi:10.1016/S0142-9612(02)00353-8.
- [27] R.L. Horan, K. Antle, A.L. Collette, Y. Wang, J. Huang, J.E. Moreau, et al., In vitro degradation of silk fibroin., *Biomaterials.* 26 (2005) 3385–93.  
doi:10.1016/j.biomaterials.2004.09.020.

- [28] O. Germershaus, V. Werner, M. Kutscher, L. Meinel, Deciphering the mechanism of protein interaction with silk fibroin for drug delivery systems., *Biomaterials*. 35 (2014) 3427–34. doi:10.1016/j.biomaterials.2013.12.083.
- [29] S. Puhl, L. Li, L. Meinel, O. Germershaus, Controlled Protein Delivery from Electrospun Non-wovens: Novel Combination of Protein Crystals and Biodegradable Release Matrix., *Mol. Pharm.* 11 (2014) 2372–2380. doi:10.1021/mp5001026.
- [30] M. V Saikumar, C.E. Glatz, M.A. Larson, Lysozyme crystal growth and nucleation kinetics, 187 (1998) 277–288.
- [31] J.C. Falkner, A.M. Al-somali, J.A. Jamison, J. Zhang, S.L. Adrianse, R.L. Simpson, et al., Generation of Size-Controlled , Submicrometer Protein Crystals, *Chem. Mater.* 13 (2005) 2679–2686.
- [32] A. Ducruix, R. Giegé, *Crystallization of Nucleic Acids and Proteins - A Practical Approach*, Second Edi, Oxford University Press, 1999.
- [33] E.L. Forsythe, R.A. Judge, M.L. Pusey, Tetragonal Chicken Egg White Lysozyme Solubility in Sodium Chloride Solutions, (1999) 637–640.
- [34] N. Asherie, Protein crystallization and phase diagrams., *Methods*. 34 (2004) 266–72. doi:10.1016/j.ymeth.2004.03.028.
- [35] C. Sagui, M. Grant, Theory of nucleation and growth during phase separation, *Phys. Rev. E*. 59 (1999) 4175–4187. doi:10.1103/PhysRevE.59.4175.
- [36] K.D. Collins, Ions from the Hofmeister series and osmolytes: effects on proteins in solution and in the crystallization process., *Methods*. 34 (2004) 300–11. doi:10.1016/j.ymeth.2004.03.021.
- [37] P. Retailleau, M. Riès-Kautt, a Ducruix, No salting-in of lysozyme chloride observed at low ionic strength over a large range of pH., *Biophys. J.* 73 (1997) 2156–63. doi:10.1016/S0006-3495(97)78246-8.
- [38] F.J. López-Jaramillo, a. B. Moraleda, L. a. González-Ramírez, a. Carazo, J.M. García-Ruiz, Soaking: the effect of osmotic shock on tetragonal lysozyme crystals, *Acta Crystallogr. Sect. D Biol. Crystallogr.* 58 (2002) 209–214. doi:10.1107/S090744490101914X.
- [39] N. a Guziewicz, A.J. Massetti, B.J. Perez-Ramirez, D.L. Kaplan, Mechanisms of monoclonal antibody stabilization and release from silk biomaterials., *Biomaterials*. 34 (2013) 7766–75. doi:10.1016/j.biomaterials.2013.06.039.
- [40] D.J. Hines, D.L. Kaplan, Mechanisms of controlled release from silk fibroin films, *Biomacromolecules*. 12 (2011) 804–12. doi:10.1021/bm101421r.







## 5 Conclusion and outlook

In this work new ways for protein encapsulation were explored with the final goal to develop novel approaches for controlled delivery of biologics. Lysozyme was chosen as a model protein and crystallized prior to all further processing. Over time, methods were refined progressively and finally a predictive model with the exact conditions for defined crystallization of lysozyme crystals with monomodal size of approximately 0.6 to 38  $\mu\text{m}$  were obtained. Two different approaches for the encapsulation of protein crystals, electrospinning and coating with silk fibroin by an S/O/W technique, were examined and a broad variety of release patterns were observed. However a perfect controlled release system, i.e. with linear and exhaustive release, could not be achieved.

The advantages of crystalline protein formulations have already been discussed before in detail. However, as described in chapter 1, they still have not been commonly accepted and are rarely applied while possible approaches for encapsulation have been described numerously before. Yet there seems to be a lack of suitable protocols for the crystallization of therapeutic proteins for which such a system would make sense. Moreover, at least in the beginning of the development of such a system, the cost-effectiveness is opposed to this gain in the patients' compliance as the effort for the development of controlled protein crystal delivery systems may be enormous. The example of insulin shows that preparations which guarantee a constant plasma level over an extended timeframe can be commercially very successful (e.g. insulin glargine). Additionally parenteral drugs show little compliance by patients and thus a decrease in necessary application frequency is likely to meet great acceptance. Growth hormones, insulin or antibodies are proteins that need to be administered regularly and the patients' compliance, and thus the entire treatment, would benefit. For example, the encapsulation of growth factors in electrospun nonwovens with subsequent application on damaged tissues appears to be a

perfect fit. Eventually the bigger effort during development could even lead to a cost reduction for the health care systems.

In chapter 2 and 3 protein crystals were encapsulated into the fibers of electrospun nonwovens which was reported in the literature for the first time. A well adjustable surface by variation of the fiber diameter combined with the possibility to modify the fiber composition demonstrated the electrospun nonwovens to be versatile controlled release systems. These nonwovens also require to be administered parenterally, but naturally an injection into the human body is no option. Possible applications rather are wound dressings, transdermal therapeutic systems (TTS) or a local drug delivery system after surgical interventions. With continuous degradation of the nonwovens a removal of it after treatment would not be necessary. The pharmaceutical industry has not picked up the commercial production of electrospun nonwovens yet. Only few information have reached the public, but production under aseptic conditions as well as in large scale seem to prevent the commercialization. Electrospun nonwovens find application as filter and are produced in large scale by respective companies. Hence large scale production has already been proven to be feasible and a transfer to the pharmaceutical industry thinkable.

As mentioned above it was well manageable to adapt the fiber diameter of the nonwovens. Combined with two different crystal sizes, a total of 8 setups were produced. A strong relationship between the fiber diameter and the crystal size ratio and the release was found. The smaller this ratio, the higher the burst release. Exhaustive release was achieved when nonwovens with the smallest average fiber diameter ( $1.7 \pm 0.5 \mu\text{m}$ ) were combined with the bigger crystals ( $2.1 \pm 0.7 \mu\text{m}$ ) and polysorbate 60 was added to the release medium externally. In the following experiments all further modifications on the nonwovens, i.e. variation in fiber composition, were performed under considerably disadvantageous conditions concerning the size ratios, in order to see the full effects of these modifications. A slight increase in overall protein release from the PCL nonwovens was obtained by the admixing of the hydrophilic PEG to the polymer solution prior to electrospinning. However while wettability was significantly

increased, release did not to the same extent. Partial matrix degradability was introduced to the system by adding PLGA to the PCL nonwovens and electrospin it together. While overall release could be increased, the nonwovens again suffered from bad wettability. Moreover acidic degradation products from PLGA detrimentally affected the protein concentration in the release medium. Polidocanol proved to be a more effective agent to increase wettability and it additionally altered fiber morphology and burst release significantly. The triple blend of PCL, polidocanol and PLGA finally led to the best result with a constant release rate over about nine weeks. Again acidic degradation products from PLGA decreased the lysozyme concentration in the release medium. A more favorable experiment setup with greater medium exchange at each sampling could circumvent this problem. In order to achieve an exhaustive release a possible approach could be to combine all gained experiences: A crystal size to fiber diameter ratio of about 1:1 and a matrix composition consisting of PCL, PD and PLGA. Moreover the influence of polymer degrading enzymes (e.g. lipase), as present within the human body, has not been examined, thus release based on PCL matrix degradation could not be observed.

Regarding the adaptability of the delivery system it was found that PCL can be combined easily with other polymers without losing the excellent electrospinnability. It is likely that more polymers can be found with properties to further enhance the release patterns and still maintain processability. More hydrophilic polymers with surface activity and/or different degradation behavior could offer beneficial modified release patterns with a constantly linear release rate and an exhaustive release.

In chapter 4 deeper insights on the lysozyme crystallization conditions and the resulting crystal size were given. Interactions between the two excipients NaCl and PEG as wells as the crystallization temperature were examined. These findings might be translatable to other protein crystallization methods and may be the basics for a rational decision which excipient is the best at a chosen temperature. The detailed descriptions of the lysozyme crystallization methods

might extend the knowledge of how to yield protein crystals in pharmaceutical useful scale and in conditions ready for delivery to the human body.

The coating of proteins crystals with another protein, i.e. silk fibroin, as demonstrated in chapter 4 has been reported for the first time. There are many advantages of this combination and they were discussed in this chapter. The aim was to obtain a controlled release system for the subcutaneous administration. Particle size and SF as coating material matched perfectly for that goal. Silk fibroin is a more and more emerging biopolymer gained from the cocoons of *Bombyx mori* and its biocompatibility has been proven before. However this system is not at its optimum yet and certain points leave room for improvement. Firstly during production there is a great loss of lysozyme crystal material caused by dissolution during coating with SF. Consequently the aim should be to find conditions that prevent the lysozyme crystals from dissolving while SF remains in solution until controlled beta-sheet-formation is induced by ethanol. These conditions might be achieved by selecting a proper salts added to the SF solution prior to the coating process. These salts might be chosen among those that are generally used to dissolve SF in the first place, e.g. LiBr, CaCl<sub>2</sub> or NaSCN. The second issue to be improved is the short release duration of 24 hours. To extent the short release duration it could be useful to recoat the SFLC with a second layer of SF using the same method again. A thicker SF coating might delays the lysozyme release.



## 6 Abbreviations

|       |  |
|-------|--|
| BCA   | Bicinchoninic Acid                     |
| DMSO  | Dimethylsulfoxide                      |
| DSC   | Differential Scanning Calorimetry      |
| FITC  | Fluorescein-isothiocyanate             |
| HPLC  | High Performance Liquid Chromatography |
| LC    | Lysozyme Crystal                       |
| LiBr  | Lithiumbromide                         |
| NaCl  | Natriumchloride                        |
| PBS   | Phosphate Buffer Saline                |
| PCL   | Poly ( $\epsilon$ -caprolactone)       |
| PD    | Polidocanol                            |
| PEG   | Poly (ethylen glycol)                  |
| PLGA  | Poly (lactic-co-glycolic acid)         |
| PS 80 | Polysorbate 80                         |
| RT    | Raumtemperatur                         |
| SD    | Standarddeviation (Standardabweichung) |
| SEM   | Scanning Electron Microscope           |
| SF    | Silk Fibroin                           |
| SFLC  | Silk Fibroin coated Lysozyme Crystal   |



## 7 Publications

Hiltensperger G., Jones NG., Niedermeier S., Stich A., Kaiser M., Jung J., Puhl S., Damme A., Braunschweig H., Meinel L., Engstler M., Holzgrabe U. ;Synthesis and Structure-Activity Relationships of New Quinolone-Type Molecules against *Trypanosoma brucei*.; *J Med Chem* (2013), 55(6), 2538-2548.

Li L., Puhl S., Meinel, L., Germershaus O.; Silk fibroin layer-by-layer microcapsules for localized gene delivery; *Biomaterials* (2014), 35(27), 7929-39

Puhl S., Li L., Meinel L., Germershaus O.; Controlled Protein Delivery from Electrospun Non-wovens: Novel Combination of Protein Crystals and Biodegradable Release Matrix; *Mol. Pharm.* (2014), 11(7), 2372-2380

Puhl S., Ilko D., Li L., Holzgrabe U., Meinel L., Germershaus O.; Protein release from electrospun nonwovens: Improving the release characteristics through rational combination of polyester blend matrices with polidocanol; *Int. J. Pharm.* (2014), 477(1-2), 273-281

Ilko D., Puhl S., Li L., Meinel L., Germershaus O., Holzgrabe U.; Simple and rapid high performance liquid chromatography method for the determination of polidocanol as bulk product and in pharmaceutical polymer matrices using charged aerosol detection; *J. Pharm. Biomed. Anal.* 104 (2014) 17–20

### Posters

Puhl, S., Meinel, L., Germershaus, O. Controlled Protein Delivery from Electrospun Non-Wovens: Novel Combination of Protein Crystals and Biodegradable Release Matrix; Poster Presentation, Controlled Release Society (CRS) Germany Local Chapter Meeting, 2013, Ludwigshafen, Germany

### Oral Presentations

Controlled release of proteins: Electrospinning of protein crystals in biodegradable polymer nonwovens; Controlled Release Society (CRS) Germany Local Chapter Meeting, 2014, Kiel, Germany

### Awards

- Best Poster Presentation, Controlled Release Society (CRS) Germany Local Chapter Meeting, 2013, Ludwigshafen, Germany
- Best Oral Presentation, Controlled Release Society (CRS) Germany Local Chapter Meeting, 2014, Kiel, Germany

## 8 Curriculum vitae

**Sebastian Puhl**  
**Geb.: 20.01.1986**

|                          |   |
|--------------------------|---|
| <b>02/2015</b>           | Process Expert<br>Novartis Pharma Productions   |
| <b>04/2011 – 01/2015</b> | Ph.D. Student<br>Julius-Maximilians-University Würzburg   |
| <b>01/2011</b>           | Approbation zum Apotheker   |
| <b>2009 – 2010</b>       | Praktisches Jahr  |
| 05/2010 – 11/2010        | Sanofi Aventis Deutschland GmbH, Medical Devices,<br>Production of Solostar Pen for Lantus (among other) under<br>GMP, Frankfurt / Main |
| 11/2009 – 05/2010        | Apotheke am Tübinger Tor, Reutlingen  |
| <b>10/2005 – 10/2009</b> | Friedrich-Alexander-University Erlangen-Nürnberg,<br>Studium der Pharmazie  |
| <b>05/2005</b>           | Abitur  |
| <b>1996 – 2005</b>       | Albert Schweitzer Gymnasium Erlangen, Germany   |

## 9 Acknowledgments

Sehr großer Dank gilt Prof. Dr. Oliver Germershaus. Sein großes Wissen, seine Geduld und nicht zuletzt seine Freundschaft haben zu dieser Arbeit unendlich viel beigetragen.

Auch Herr Prof. Dr. Dr. Lorenz Meinel gebührt sehr großer Dank. Durch die Aufnahme in seinen Arbeitskreis und das in mich gesetzte Vertrauen wurde all das erst möglich.

Der gesamte AK Meinel und AK Germershaus haben für viele schöne Stunden, beruflich und privat, gesorgt und dadurch diese Zeit zu einer unvergesslichen gemacht. Wir alle haben viele Höhen und Tiefen miteinander durchgestanden, es war oft stressig und hart doch dank euch bin ich (fast) immer gerne zur Arbeit gegangen. Vera Kohl möchte ich sehr für die angenehmen gemeinsamen Dienstreisen danken und für die super Zusammenarbeit, v.a. bei der Betreuung des ersten Teilpraktikums. Es war mir eine Ehre mir mit Marika Kutscher und Isabel Schultz ein Büro zu teilen. Joel Wurzel gilt besonderer Dank, mit dem man frustrierende Tage durch diverse Zerstreungen wieder ausgleichen konnte.

Linhao Li und David Ilko möchte ich für die gute Zusammenarbeit danken, durch die wir gemeinsam zu vielen Erfolgen gekommen sind.

Dr. Sascha Zügner, Doris Moret und Christine Schneider haben durch ihre immerwährende Hilfsbereitschaft und Unterstützung einen nicht unwesentlichen Teil zu dieser Arbeit beigetragen.

Großer Dank gilt auch Georg Walter, Matthias Völker und Karl Vollmuth, die immer mit Rat und Tat zur Seite standen, wenn technische oder handwerkliche Probleme zu lösen waren. Claudia Gehrig und Daniela Bunsen möchte ich für die viele Hilfe am SEM danken.

Abseits der Universität hat besonders Peter Stärtzel indirekt viel zu dieser Arbeit beigetragen. Dank ihm konnte eine Menge Stress und Frust bei einem gemütlichen Feierabendtrunk vergessen werden.

Bei meiner Freundin Kira Nultsch, die u.a. in besonders harten Zeiten zu mir gehalten hat, möchte ich mich ganz besonders bedanken. Durch sie konnte ich immer wieder Kraft tanken. Genauso möchte ich von ganzem Herzen meinen Eltern und Großeltern danken. Ohne Euch wäre ich niemals so weit gekommen. Vielen Dank, dass ich mich immer auf euch verlassen konnte und dass ihr mich immer unterstützt habt.

## Acknowledgments

## 10 Documentation of authorship

This section contains a list of the individual contribution for each author to the publications reprinted in this thesis.

| <b>M1</b>  | <b>Sebastian Puhl, Lorenz Meinel, Oliver Germershaus; Recent Advances in Crystalline and Amorphous Particulate Protein Formulations for Controlled Delivery. Unpublished manuscript</b> |          |          |
|--|---|----------|----------|
| <b>Author</b>  | <b>1</b>  | <b>2</b> | <b>3</b> |
| Particle production methods  | x   |          |          |
| Protein crystal delivery without further processing  | x   |          |          |
| Protein crystals delivery after further processing   | x   |          |          |
| Non-crystalline protein particles for delivery without further processing                          | x   |          |          |
| Non-crystalline protein particles for protein delivery with further processing, i.e. encapsulation | x   |          |          |
| Conclusion and outlook   | x   |          |          |
| Study design/concept development   | x   | x        | x        |
| Data analysis and interpretation   | x   |          | x        |
| Manuscript planning  | x   | x        | x        |
| Manuscript writing   | x   |          | x        |
| Correction of manuscript   |   | x        | x        |
| Supervision of Sebastian Puhl  |   | x        | x        |

| <b>P1</b>   | <b>Sebastian Puhl, Linhao Li, Lorenz Meinel, Oliver Germershaus (2014); Controlled Protein Delivery from Electrospun Non-Wovens: Novel Combination of Protein Crystals and a Biodegradable Release Matrix. Molecular Pharmaceutics 2014, 11, 2372–2380</b> |          |          |          |
|---|--|----------|----------|----------|
| <b>Author</b>   | <b>1</b>   | <b>2</b> | <b>3</b> | <b>4</b> |
| Crystals and a Biodegradable Release Matrix             | x  |          |          |          |
| Lysozyme Crystallization and Crystal Size Determination | x  |          |          |          |
| FITC Labeling of Lysozyme                               | x  |          |          |          |
| PCL Electrospinning                                     | x  | x        |          |          |
| In Vitro Release  | x  |          |          |          |
| Relative Bioactivity of Lysozyme                        | x  |          |          |          |
| Morphology and Fiber Diameter                           | x  | x        |          |          |
| Wettability of the Non-Wovens                           | x  |          |          |          |
| Statistical Analysis                                    | x  |          |          |          |
| Study design/concept development                        | x  |          | x        | x        |
| Data analysis and interpretation                        | x  | x        |          | x        |
| Manuscript planning                                     | x  |          | x        | x        |
| Manuscript writing                                      | x  |          |          | x        |
| Correction of manuscript                                |  | x        | x        | x        |
| Supervision of Sebastian Puhl                           |  |          | x        | x        |

| <b>P2</b>   | <b>Sebastian Puhl, David Ilko, Linhao Li, Ulrike Holzgrabe, Lorenz Meinel, Oliver Germershaus (2014); Protein release from electrospun nonwovens: Improving the release characteristics through rational combination of polyester blend matrices with polidocanol. International Journal of Pharmaceutics 477 (2014)</b> |          |          |          |          |          |          |
|---|--|----------|----------|----------|----------|----------|----------|
| <b>Author</b>   |  | <b>1</b> | <b>2</b> | <b>3</b> | <b>4</b> | <b>5</b> | <b>6</b> |
| Lysozyme crystallization and crystal size determination |  | x        |          |          |          |          |          |
| PCL electrospinning                                     |  | x        |          | x        |          |          |          |
| Morphology and fiber diameter                           |  | x        |          | x        |          |          |          |
| Wettability and sorption rate of the nonwovens          |  | x        |          |          |          |          |          |
| Differential scanning calorimetry                       |  | x        |          |          |          |          |          |
| Relative bioactivity of lysozyme                        |  | x        |          |          |          |          |          |
| Statistical analysis                                    |  | x        |          |          |          |          |          |
| Contact angle, sorption rate and swelling behavior      |  | x        |          |          |          |          |          |
| Polidocanol release                                     |  | x        | x        |          |          |          |          |
| Lysozyme release  |  | x        |          |          |          |          |          |
| Study design/concept development                        |  | x        |          |          | x        | x        | x        |
| Data analysis and interpretation                        |  | x        | x        | x        |          |          | x        |
| Manuscript planning                                     |  | x        |          |          |          | x        | x        |
| Manuscript writing                                      |  | x        | x        |          |          |          | x        |
| Correction of manuscript                                |  |          | x        |          | x        | x        | x        |
| Supervision of Sebastian Puhl                           |  |          |          |          |          | x        | x        |

| <b>M2</b>   | <b>Sebastian Puhl, Lorenz Meinel, Oliver Germershaus; Silk fibroin coating of protein crystals for controlled delivery. Unpublished manuscript</b> |          |          |          |
|---|--|----------|----------|----------|
| <b>Author</b>   |  | <b>1</b> | <b>2</b> | <b>3</b> |
| Preparation of Lysozyme Crystals and Optimization of Crystallization by Design of Experiments |  | x        |          |          |
| Silk fibroin extraction   |  | x        |          |          |
| Labeling of lysozyme with FITC and silk fibroin with Rhodamine-X                              |  | x        |          |          |
| Coating of protein crystals with silk fibroin and purification                                |  | x        |          |          |
| Microscopic characterization  |  | x        |          |          |
| Release studies   |  | x        |          |          |
| Relative Bioactivity  |  | x        |          |          |
| FTIR  |  | x        |          |          |
| CLSM analysis   |  | x        |          |          |
| Study design/concept development  |  | x        | x        | x        |
| Data analysis and interpretation  |  | x        |          | x        |
| Manuscript planning   |  | x        | x        | x        |
| Manuscript writing  |  | x        |          | x        |
| Correction of manuscript  |  |          | x        | x        |
| Supervision of Sebastian Puhl   |  |          | x        | x        |

## **11 Erklärung zu den Eigenanteilen des Doktoranden sowie der weiteren Doktoranden als Koautoren an Publikationen und Zweitpublikationsrechten bei einer kumulativen Dissertation**

Für alle in dieser kumulativen Dissertation verwendeten Manuskripte liegen die notwendigen Genehmigungen der Verlage („reprint permission“) für die Zweitpublikation vor, außer das betreffende Kapitel ist noch gar nicht publiziert. Dieser Umstand wird einerseits durch die genaue Angabe der Literaturstelle der Erstpublikation auf der ersten Seite des betreffenden Kapitels deutlich gemacht oder die bisherige Nichtveröffentlichung durch den Vermerk „unpublished“ oder „nicht veröffentlicht“ gekennzeichnet.

Die Mitautoren der in dieser kumulativen Dissertation verwendeten Manuskripte sind sowohl über die Nutzung als auch über die oben angegebenen Eigenanteile informiert.

Die Beiträge der Mitautoren an den Publikationen sind in den vorausgehenden Tabellen aufgeführt.

---

Datum, Unterschrift  
Prof. Dr. Oliver Germershaus

---

Datum, Unterschrift  
Sebastian Puhl